

Electronic Supplementary Information

Donor–acceptor–acceptor-type near-infrared fluorophores that contain dithienophosphole oxide and boryl groups: Effect of the boryl group on the nonradiative decay

Yoshiaki Sugihara,^a Naoto Inai,^a Masayasu Taki,^b Thomas Baumgartner,^c Ryosuke Kawakami,^d Takashi Saitou,^d Takeshi Imamura,^d Takeshi Yanai^{*,a,b} and Shigehiro Yamaguchi^{*,a,b}

^aDepartment of Chemistry, Graduate School of Science, and Integrated Research Consortium on Chemical Sciences (IRCCS), Nagoya University, Furo, Chikusa, Nagoya, 464-8602, Japan

^bInstitute of Transformative Bio-Molecules (WPI-ITbM), Nagoya University, Furo, Chikusa, Nagoya, 464-8602, Japan

^cDepartment of Chemistry, York University, 4700 Keele St., Toronto, ON M3J 1P3, Canada

^dDepartment of Molecular Medicine for Pathogenesis, Graduate School of Medicine, Ehime University, Shitsukawa, Toon-city, Ehime, 791-0295, Japan

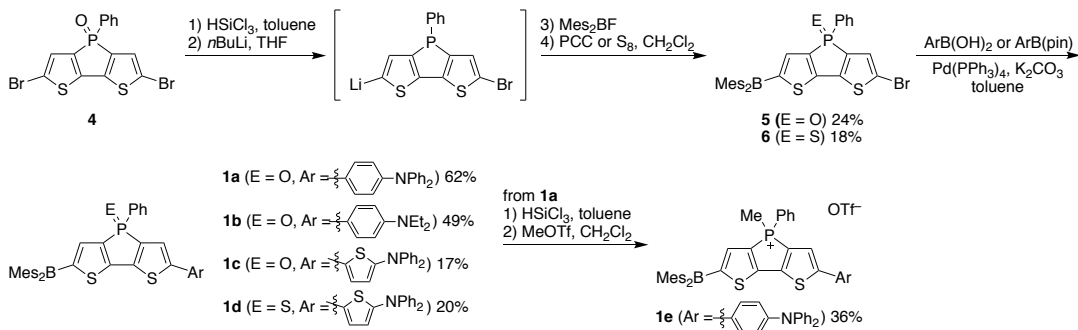
E-mail: yanait@chem.nagoya-u.ac.jp, yamaguchi@chem.nagoya-u.ac.jp

Contents

1. Experimental Details	S2
2. Photophysical Properties	S12
3. Evaluation of Photostability	S17
4. Theoretical Calculations	S20
5. <i>In vivo</i> Imaging	S29
6. References	S32
7. NMR Spectra for New Compounds	S34

1. Experimental Details

General. Melting points (mp) or decomposition temperatures were determined with a Yanaco MP-J3 instrument. ^1H , $^{13}\text{C}\{\text{H}\}$, $^{11}\text{B}\{\text{H}\}$, and $^{31}\text{P}\{\text{H}\}$ NMR spectra were recorded with a JEOL JNM-ECS400 spectrometer (400 MHz for ^1H and 100 MHz for ^{13}C) or a JEOL AL-400 spectrometer (400 MHz for ^1H , 128 MHz for ^{11}B , and 162 MHz for ^{31}P) in CDCl_3 , acetone- d_6 , or CD_2Cl_2 . The chemical shifts in ^1H NMR spectra are reported in δ ppm using the residual protons of the solvents as an internal standard ($\text{CHCl}_3 \delta$ 7.26, acetone δ 2.05, and $\text{CH}_2\text{Cl}_2 \delta$ 5.32), and those in ^{13}C NMR spectra are reported using the solvent signals as an internal standard ($\text{CDCl}_3 \delta$ 77.16, acetone δ 206.26, and $\text{CD}_2\text{Cl}_2 \delta$ 53.84). The chemical shifts in ^{31}P and ^{11}B NMR spectra are reported using H_3PO_4 (δ 0.00) and $\text{BF}_3\cdot\text{OEt}_2$ (δ 0.00) as an external standard, respectively. Mass spectra were measured with a Thermo Fischer Scientific Exactive spectrometer with the ionization method of ESI using methanol. Thin layer chromatography (TLC) was performed on glass plates coated with 0.25 mm thickness of silica gel 60 F₂₅₄ (Merck). Column chromatography was performed using silica gel PSQ100B or PSQ60B (Fuji Silysia Chemical). Preparative HPLC was performed using LC-918 (Japan Analytical Industry) equipped with silica gel column (Wakosil-II 5-Prep, Wako). Recycling preparative gel permeation chromatography (GPC) was performed using LC-918 (Japan Analytical Industry) equipped with polystyrene gel columns (JAIGEL 1H and 2H, Japan Analytical Industry) using CHCl_3 as eluent. Anhydrous toluene, THF, and CH_2Cl_2 were purchased from Kanto Chemicals and further purified by Glass Contour Solvent Systems. 2,6-Dibromodithieno[3,2-*b*:2',3'-*d*]phosphole *P*-oxide **4**,¹ fluorodimesitylborane (Mes_2BF),² 5-(4,4,5,5-tetramethyl-1,3,2-dioxaborolan-2-yl)-2-diphenylaminothiophene,³ [2,4,6-tri-(*tert*-butyl)phenyl]phenyl(thiophen-2-yl)borane **11**,⁴ and compound **10**⁵ were prepared according to the literature methods. All reactions were carried out under a nitrogen atmosphere unless stated otherwise.



2-Bromo-6-dimesitylboryldithieno[3,2-*b*:2',3'-*d*]phosphole *P*-oxide (5). To a suspension of 2,6-dibromodithieno[3,2-*b*:2',3'-*d*]phosphole *P*-oxide (2.00 g, 4.49 mmol) in anhydrous toluene (20 mL) was added HSiCl_3 (2.95 g, 21.8 mmol) in one portion. After stirring at room temperature for 30 min, all volatiles were removed under reduced pressure. The resulting mixture was passed through a silica gel column using toluene as eluent. After concentration under reduced pressure, the resulting yellow solid was dissolved in anhydrous THF (53 mL). *n*-BuLi in hexane (1.6 M, 2.20 mL, 3.52 mmol) was added to the solution at -78°C . After stirring at the same temperature for 1 h, a THF solution (4 mL) of Mes_2BF (907 mg, 3.38 mmol) was added, and the mixture was allowed to warm to room temperature and stirred for 16 h. After removal of volatiles under reduced pressure, CH_2Cl_2 (50 mL) was added. PCC (684 mg, 3.17 mmol) was then added to the mixture followed by stirring for 1 h. After concentration of the mixture under reduced pressure, the mixture was passed through a silica gel column with EtOAc as eluent. The resulting crude product was subjected to silica gel column chromatography (19/1 CHCl_3 /EtOAc, $R_f = 0.71$) to afford 662 mg (1.08 mmol, 24%) of 5 as yellow solids. Mp. 260.0°C (dec.). ^1H NMR (400 MHz, CDCl_3): δ 7.69 (dd, $J = 13.6, 6.8$ Hz, 2H), 7.56 (t, $J = 6.8$ Hz, 1H), 7.47–7.41 (m, 3H), 7.14 (d, $J = 2.4$ Hz, 1H), 6.82 (s, 4H), 2.29 (s, 6H) 2.11 (s, 12H). $^{13}\text{C}\{\text{H}\}$ NMR (100 MHz, CDCl_3): δ 156.3 (d, $J = 24.8$ Hz, C), 155.5 (d, $J = 9.6$ Hz, C), 145.8 (d, $J = 22.0$ Hz, C), 140.94 (d, $J = 106.9$ Hz, C), 140.87 (s, C), 140.1 (d, $J = 109.8$ Hz, C), 139.3 (s, C), 138.6 (d, $J = 13.3$ Hz, CH), 133.0 (s, CH), 130.9 (d, $J = 11.5$ Hz, CH), 129.4 (d, $J = 12.4$ Hz, CH), 129.0 (d, $J = 96.4$ Hz, C), 128.8 (d, $J = 13.3$ Hz, CH), 128.5 (s, CH), 117.2 (d, $J = 18.2$ Hz, C), 23.6 (s, CH_3), 21.4 (s, CH_3). One signal for the carbon atom bound to the boron atom was not observed due to the quadrupolar relaxation, and one of the doublet signals of a quaternary carbon atom paired with the signal at 129.47 ppm was overlapped. $^{11}\text{B}\{\text{H}\}$ NMR (128 MHz, CDCl_3): δ 66.3. $^{31}\text{P}\{\text{H}\}$ NMR (162 MHz, CDCl_3): δ 19.1. HRMS (ESI): m/z calcd. for $\text{C}_{32}\text{H}_{29}\text{BBrNaOPS}_2$: 637.0566 ($[\text{M}+\text{Na}]^+$); found. 637.0570.

2-Bromo-6-dimesitylboryldithieno[3,2-*b*:2',3'-*d*]phosphole *P*-sulfide (6**).** To a suspension of 2,6-dibromodithieno[3,2-*b*:2',3'-*d*]phosphole *P*-oxide (1.01 g, 2.26 mmol) in anhydrous toluene (10 mL) was added HSiCl₃ (1.47 g, 10.9 mmol) in one portion. After stirring at room temperature for 30 min, all volatiles were removed under reduced pressure. The resulting mixture was passed through a silica gel column using toluene as eluent. After concentration under reduced pressure, the resulting yellow solid was dissolved in anhydrous THF (13 mL). A hexane solution of *n*-BuLi (1.6 M, 0.64 mL, 1.02 mmol) was added to the solution at -78 °C. After stirring at the same temperature for 1 h, a THF solution (1 mL) of Mes₂BF (250 mg, 0.931 mmol) was added, and the mixture was allowed to warm to room temperature and stirred for 14 h. After removal of volatiles under reduced pressure, anhydrous CH₂Cl₂ (10 mL) was added. Sulfur (151 mg, 4.72 mmol) was then added to the mixture followed by stirring for 25 h. After concentration under reduced pressure, the resulting mixture was subjected to silica gel column chromatography (hexane to 4/1 hexane/CH₂Cl₂, *R*_f = 0.54 in 4/1 hexane/CH₂Cl₂) to afford 254 mg (0.402 mmol, 18%) of **6** as yellow solids. Mp. 250.4–250.8 °C. ¹H NMR (400 MHz, acetone-*d*₆): δ 7.85–7.77 (m, 2H), 7.64–7.59 (m, 1H), 7.51 (td, *J* = 8.0, 3.6 Hz, 2H), 7.44 (d, *J* = 2.8 Hz, 1H), 7.43 (d, *J* = 2.8 Hz, 1H), 6.86 (s, 4H), 2.27 (s, 6H), 2.12 (s, 12H). ¹³C{¹H} NMR (100 MHz, CD₂Cl₂): δ 155.6 (s, C), 155.1 (d, *J* = 21.0 Hz, C), 144.3 (d, *J* = 17.2 Hz, C), 143.9 (d, *J* = 88.8 Hz, C), 143.4 (d, *J* = 91.6 Hz, C), 141.1 (s, C), 140.7 (s, C), 139.6 (s, C), 138.4 (d, *J* = 14.3 Hz, CH), 132.8 (d, *J* = 2.9 Hz, CH), 130.9 (d, *J* = 12.4 Hz, CH), 129.7 (d, *J* = 85.0 Hz, C), 129.2 (d, *J* = 13.4 Hz, CH), 128.7 (s, CH), 128.3 (d, *J* = 15.3 Hz, CH), 117.8 (d, *J* = 18.1 Hz, C), 23.6 (s, CH₃), 21.3 (s, CH₃). ¹¹B{¹H} NMR (128 MHz, CD₂Cl₂): δ 65.9. ³¹P{¹H} NMR (162 MHz, CDCl₃): δ 27.0. HRMS (ESI): *m/z* calcd. for C₃₂H₂₉BBrNaPS₃: 653.0343 ([M+Na]⁺); found. 653.0337.

General Procedure for Synthesis of Compounds **1a–1d**.

A mixture of **5** or **6**, corresponding arylboronic acid or boronic ester, and K₂CO₃ in anhydrous toluene (10 mL) was bubbled with nitrogen gas for 1 h. To this solution, Pd(PPh₃)₄ was added and the mixture was stirred at 110 °C for 24 h. The resulting mixture was filtered through a plug of celite® and concentrated under reduced pressure. The mixture was subjected to silica gel column chromatography followed by preparative GPC (eluent: CHCl₃) to afford **1a–1d**.

Compound 1a. This compound was synthesized according to the General Procedure using **5** (110 mg, 0.178 mmol), 4-(diphenylamino)phenylboronic acid (106 mg, 0.366 mmol), K₂CO₃ (97.8 mg, 0.708 mmol), and Pd(PPh₃)₄ (26.8 mg, 0.0232 mmol). The crude product was purified by silica gel column chromatography (CHCl₃ to 9/1 CHCl₃/EtOAc, *R*_f = 0.51 in 9/1 CHCl₃/EtOAc) followed by preparative

GPC to afford 86.6 mg (0.111 mmol, 62%) of **1a** as orange solids. Mp. 175.5–176.4 °C. ^1H NMR (400 MHz, acetone- d_6): δ 7.81–7.73 (m, 2H), 7.67–7.59 (m, 1H), 7.63 (d, J = 8.8 Hz, 2H), 7.60 (d, J = 3.2 Hz, 1H), 7.54–7.48 (m, 2H), 7.45 (d, J = 2.8 Hz, 1H), 7.34 (t, J = 8.0 Hz, 4H), 7.17–7.09 (m, 6H), 7.03 (d, J = 8.8 Hz, 2H), 6.86 (s, 4H), 2.27 (s, 6H), 2.14 (s, 12H). $^{13}\text{C}\{\text{H}\}$ NMR (100 MHz, CDCl_3): δ 157.7 (d, J = 23.8 Hz, C), 154.6 (d, J = 10.5 Hz, C), 150.9 (d, J = 14.3 Hz, C), 148.6 (s, C), 147.2 (s, C), 142.9 (d, J = 21.9 Hz, C), 142.3 (d, J = 109.8 Hz, C), 140.9 (s, C), 140.3 (d, J = 109.7 Hz, C), 139.1 (s, C), 138.9 (d, J = 12.4 Hz, CH), 132.7 (s, C) 131.0 (d, J = 11.4 Hz, CH), 129.7 (d, J = 106.0 Hz, C), 129.6 (s, CH), 129.1 (d, J = 13.3 Hz, CH), 128.5 (s, CH), 126.8 (s, CH), 126.6 (s, C), 125.1 (s, CH), 123.8 (s, C), 123.0 (s, C), 120.7 (d, J = 13.4 Hz, CH), 23.6 (s, CH_3), 21.4 (s, CH_3). One signal for the carbon atom bound to the boron atom was not observed due to the quadrupolar relaxation, and one of the doublet signals of a quaternary carbon atom paired with the signal at 139.76 ppm and one of the doublet signals of a quaternary carbon atom paired with the signal at 130.19 ppm were overlapped. $^{11}\text{B}\{\text{H}\}$ NMR (128 MHz, CDCl_3): δ 65.7. $^{31}\text{P}\{\text{H}\}$ NMR (162 MHz, CDCl_3): δ 19.3. HRMS (ESI): m/z calcd. for $\text{C}_{50}\text{H}_{43}\text{BNNaOPS}_2$: 802.2509 ($[M+\text{Na}]^+$); found. 802.2506.

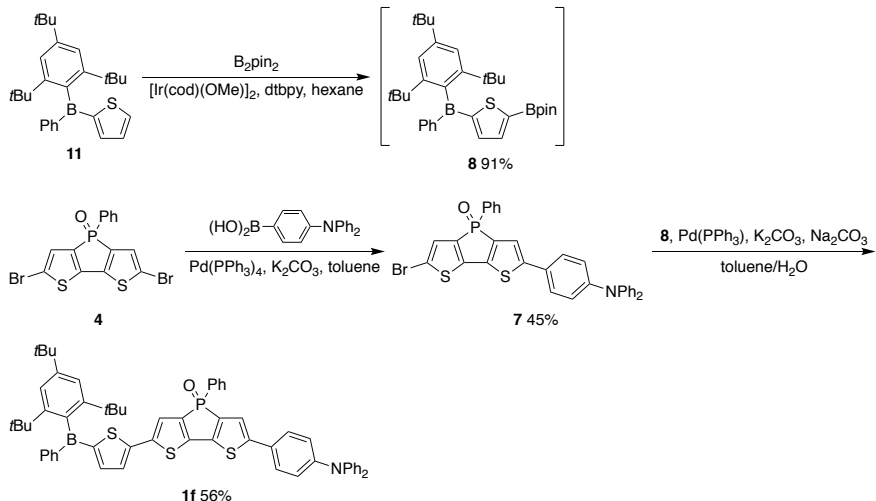
Compound 1b. This compound was synthesized according to the General Procedure using **5** (110 mg, 0.179 mmol), 4-(diethylamino)phenylboronic acid (52.0 mg, 0.269 mmol), K_2CO_3 (75.6 mg, 0.547 mmol), and $\text{Pd}(\text{PPh}_3)_4$ (20.2 mg, 0.0175 mmol). The crude product was purified by silica gel column chromatography (19/1 $\text{CHCl}_3/\text{EtOAc}$, R_f = 0.72) followed by preparative GPC to afford 60.5 mg (0.0885 mmol, 49%) of **1b** as red solids. Mp. 164.6–165.3 °C. ^1H NMR (400 MHz, CDCl_3): δ 7.75 (dd, J = 13.6 Hz, 7.2 Hz, 2H), 7.53 (t, 7.2 Hz, 1H), 7.46–7.36 (m, 3H), 7.38 (d, J = 9.2 Hz, 2H), 7.16 (d, J = 2.8 Hz, 1H), 6.82 (s, 4H), 6.63 (d, J = 9.2 Hz, 2H), 3.38 (q, J = 7.2 Hz, 4H), 2.29 (s, 6H), 2.13 (s, 12H), 1.17 (t, J = 7.2 Hz, 6H). $^{13}\text{C}\{\text{H}\}$ NMR (100 MHz, CDCl_3): δ 158.3 (d, J = 24.9 Hz, C), 153.9 (s, C), 152.6 (d, J = 15.2 Hz, C), 148.1 (s, C), 142.3 (d, J = 109.8 Hz, C), 141.3 (d, J = 21.9 Hz, C), 140.9 (s, C), 139.8 (d, J = 110.8 Hz, C), 139.1 (s, C), 139.0 (d, J = 7.7 Hz, CH), 132.6 (s, CH), 131.1 (d, J = 11.4 Hz, CH), 129.9 (d, J = 107.9 Hz, C), 129.0 (d, J = 12.5 Hz, CH), 128.4 (s, CH), 127.3 (s, CH), 120.3 (s, C), 118.9 (d, J = 14.3 Hz, CH), 111.7 (s, CH), 44.6 (s, CH_2), 23.6 (s, CH_3), 21.4 (s, CH_3), 12.7 (s, CH_3). One signal for the carbon atom bound to the boron atom was not observed due to the quadrupolar relaxation. $^{11}\text{B}\{\text{H}\}$ NMR (128 MHz, CDCl_3): δ 65.1. $^{31}\text{P}\{\text{H}\}$ NMR (162 MHz, CDCl_3): δ 19.5. HRMS (ESI): m/z calcd. for $\text{C}_{42}\text{H}_{43}\text{BNNaOPS}_2$: 706.2509 ($[M+\text{Na}]^+$); found. 706.2522.

Compound 1c. This compound was synthesized according to the General Procedure using **5** (110 mg, 0.179 mmol), 5-(4,4,5,5-tetramethyl-1,3,2-dioxaborolan-2-yl)-2-diphenylaminothiophene (136 mg,

0.359 mmol), K₂CO₃ (75.4 mg, 0.546 mmol), and Pd(PPh₃)₄ (20.7 mg, 0.0179 mmol). The crude mixture was purified by silica gel column chromatography (CH₂Cl₂ to 95/5 CH₂Cl₂/EtOAc, *R_f* = 0.83 in 95/5 CH₂Cl₂/EtOAc) followed by preparative GPC to afford 23.8 mg (0.0303 mmol, 17%) of **1c** as red solids. Mp. 155.7 °C (dec.). ¹H NMR (400 MHz, acetone-*d*₆): δ 7.80–7.71 (m, 2H), 7.64–7.58 (m, 1H), 7.50 (td, *J* = 7.6 Hz, 3.2 Hz, 2H), 7.45 (d, *J* = 2.4 Hz, 1H), 7.39–7.31 (m, 5H), 7.25 (d, *J* = 4.0 Hz, 1H), 7.20–7.09 (m, 6H), 6.85 (s, 4H), 6.61 (d, *J* = 4.0 Hz, 1H), 2.27 (s, 6H), 2.13 (s, 12H). ¹³C{¹H} NMR (100 MHz, acetone-*d*₆): δ 157.7 (d, *J* = 23.9 Hz, C), 155.5 (s, C), 153.7 (s, C), 148.3 (s, C), 145.2 (d, *J* = 15.3 Hz, C), 144.3 (d, *J* = 106.0 Hz, C), 142.33 (d, *J* = 107.9 Hz, C), 142.32 (d, *J* = 21.0 Hz, C), 141.5 (s, C), 139.9 (s, C), 139.5 (d, *J* = 13.3 Hz, CH), 133.5 (s, CH), 131.7 (d, *J* = 10.5 Hz, CH), 131.5 (d, *J* = 106.9 Hz, C), 130.5 (s, C), 130.2 (d, *J* = 12.4 Hz, CH), 129.3 (s, CH), 129.1 (s, C), 125.4 (s, CH), 125.0 (s, CH), 124.2 (s, CH), 121.8 (d, *J* = 13.3 Hz, CH), 120.9 (s, CH), 23.8 (s, CH₃), 21.3 (s, CH₃). One signal for the carbon atom bound to the boron atom was not observed due to the quadrupolar relaxation. ¹¹B{¹H} NMR (128 MHz, acetone-*d*₆): δ 66.2. ³¹P{¹H} NMR (162 MHz, CDCl₃): δ 19.0. HRMS (ESI): *m/z* calcd. for C₄₈H₄₁BNNaOPS₃: 808.2079 ([M+Na]⁺); found. 808.2076.

Compound 1d. This compound was synthesized according to the General Procedure using **6** (111 mg, 0.176 mmol), 5-(4,4,5,5-tetramethyl-1,3,2-dioxaborolan-2-yl)-2-diphenylaminothiophene (88.7 mg, 0.235 mmol), K₂CO₃ (72.5 mg, 0.535 mmol), and Pd(PPh₃)₄ (27.3 mg, 0.0236 mmol). The crude product was purified by silica gel column chromatography (hexane to 4/1 hexane/CH₂Cl₂, *R_f* = 0.21 in 4/1 hexane/CH₂Cl₂) followed by preparative GPC to afford 28.7 mg (0.0358 mmol, 20%) of **1d** as red solids. Mp. 155.7 °C (dec.). ¹H NMR (400 MHz, acetone-*d*₆): δ 7.89–7.78 (m, 2H), 7.64–7.56 (m, 1H), 7.50 (td, *J* = 8.0, 3.6 Hz, 2H), 7.42 (d, *J* = 2.8 Hz, 1H), 7.39–7.33 (m, 5H), 7.27 (d, *J* = 4.0 Hz, 1H), 7.23–7.07 (m, 6H), 6.86 (s, 4H), 6.61 (d, *J* = 4.0 Hz, 1H), 2.27 (s, 6H), 2.13 (s, 12H). ¹³C{¹H} NMR (100 MHz, acetone-*d*₆): δ 156.3 (d, *J* = 20.0 Hz, C), 155.6 (s, C), 153.9 (s, C), 148.3 (s, C), 146.6 (d, *J* = 90.7 Hz, C), 145.5 (d, *J* = 15.2 Hz, C), 144.8 (d, *J* = 91.7 Hz, C), 141.5 (s, C), 140.8 (d, *J* = 18.1 Hz, C), 140.0 (s, C), 138.9 (d, *J* = 13.4 Hz, CH), 133.4 (s, CH), 131.4 (d, *J* = 12.4 Hz, CH), 131.1 (d, *J* = 85.0 Hz, C), 130.5 (s, C), 130.0 (d, *J* = 13.4 Hz, CH), 129.3 (s, CH), 128.9 (s, C), 125.6 (s, CH), 125.0 (s, CH), 124.2 (s, CH), 121.0 (d, *J* = 15.3 Hz, CH), 120.8 (s, CH), 23.8 (s, CH₃), 21.3 (s, CH₃). One signal for the carbon atom bound to the boron atom was not observed due to the quadrupolar relaxation. ¹¹B{¹H} NMR (128 MHz, acetone-*d*₆): δ 65.4. ³¹P{¹H} NMR (162 MHz, CDCl₃): δ 26.3. HRMS (ESI): *m/z* calcd. for C₄₈H₄₁BNNaPS₄: 824.1850 ([M+Na]⁺); found. 824.1848.

Compound 1e. To a suspension of **1a** (72.7 mg, 0.0932 mmol) in anhydrous toluene (2 mL) was added HSiCl₃ (67.0 mg, 0.495 mmol) in one portion. After stirring at room temperature for 1 h, all volatiles were removed under reduced pressure. The resulting mixture was passed through a silica gel column using toluene as eluent. After concentration under reduced pressure, the resulting solid was dissolved in anhydrous CH₂Cl₂ (2 mL). MeOTf (12.8 mg, 0.0717 mmol) was added to the resulting solution at room temperature followed by stirring for 16 h. After concentration of the resulting mixture, the crude product was purified by recrystallization from a hexane/CHCl₃ mixed solvent to afford 30.9 mg (0.0333 mmol, 36%) of **1e** as dark red solids. Mp. 162.0–162.8 °C. ¹H NMR (400 MHz, CD₂Cl₂): δ 7.95–7.85 (m, 3H), 7.84–7.78 (m, 1H), 7.70–7.63 (m, 2H), 7.62 (d, *J* = 2.2 Hz, 1H), 7.52 (d, *J* = 8.8 Hz, 2H), 7.31 (t, *J* = 7.9 Hz, 4H), 7.15–7.08 (m, 6H), 7.04 (d, *J* = 8.0 Hz, 2H), 6.89 (s, 4H), 2.74 (d, *J* = 15.0 Hz, 3H), 2.31 (s, 6H), 2.15 (s, 12H). ¹³C{¹H} NMR (100 MHz, CDCl₃): δ 160.4 (d, *J* = 21.1 Hz, C), 157.0 (d, *J* = 8.6 Hz, C), 154.2 (d, *J* = 16.3 Hz, C), 149.4 (s, C), 146.9 (s, C), 144.1 (d, *J* = 19.1 Hz, C), 140.9 (s, C), 140.0 (s, C), 138.0 (d, *J* = 12.4 Hz, CH), 135.7 (s, CH), 132.6 (d, *J* = 12.4 Hz, CH), 131.4 (d, *J* = 98.3 Hz, C), 130.6 (d, *J* = 13.4 Hz, CH), 129.6 (s, CH), 128.8 (s, CH), 127.9 (d, *J* = 96.4 Hz, C), 127.2 (s, CH), 125.4 (s, CH), 125.1 (s, C), 124.1 (s, CH), 123.2 (d, *J* = 15.3 Hz, CH), 122.3 (s, CH), 120.8 (q, *J* = 318.9 Hz, C), 116.4 (d, *J* = 88.8 Hz, C), 23.7 (s, CH₃), 21.4 (s, CH₃), 8.1 (d, *J* = 53.5 Hz, CH₃). One signal for the carbon atom bound to the boron atom was not observed due to the quadrupolar relaxation. ¹¹B{¹H} NMR (128 MHz, CDCl₃): δ 62.9. ³¹P{¹H} NMR (162 MHz, CDCl₃): δ 13.3. HRMS (ESI): *m/z* calcd. for C₅₈H₄₆BNPS₂: 778.2897 ([M]⁺); found. 778.2882.



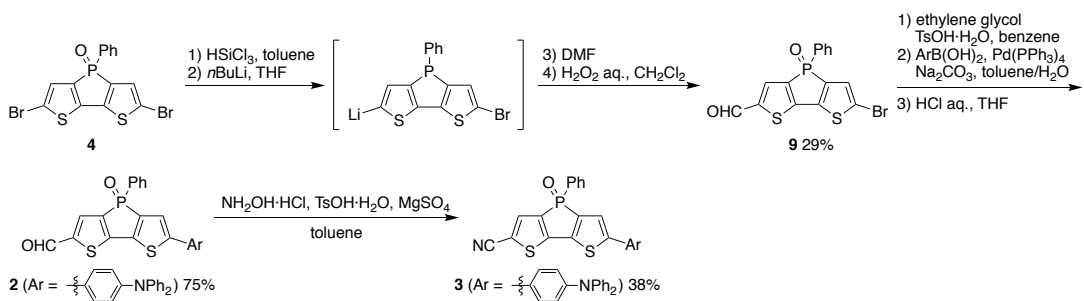
Compound 7. To a mixture of 2,6-diboromodithienophosphole *P*-oxide **4** (149 mg, 0.334 mmol), 4-(diphenylamino)phenylboronic acid (96.4 mg, 0.333 mmol), and K₂CO₃ (139 mg, 1.01 mmol) in

anhydrous toluene (10 mL) was added Pd(PPh₃)₄ (40.0 mg, 0.0346 mmol). The mixture was stirred at 110 °C for 22 h. The resulting mixture was filtered through a plug of celite® and concentrated under reduced pressure. The crude mixture was subjected to silica gel column chromatography (CH₂Cl₂ to 19/1 CH₂Cl₂/EtOAc, R_f = 0.35 in 19/1 CH₂Cl₂/EtOAc) followed by HPLC (19/1 CHCl₃/EtOAc) to afford 93.6 mg (0.153 mmol, 45%) of **7** as orange solids. Mp. 127.9–128.8 °C. ¹H NMR (400 MHz, acetone-*d*₆): δ 7.81–7.73 (m, 2H), 7.66–7.59 (m, 3H), 7.55 (d, *J* = 2.8 Hz, 1H), 7.52 (td, *J* = 7.6, 3.2 Hz, 2H), 7.42 (d, *J* = 2.4 Hz, 1H), 7.34 (t, *J* = 7.6 Hz, 4H), 7.15–7.08 (m, 6H), 7.03 (d, *J* = 8.8 Hz, 2H). ¹³C{¹H} NMR (100 MHz, CDCl₃): δ 149.2 (d, *J* = 14.3 Hz, C), 148.4 (s, C), 147.2 (s, C), 146.5 (d, *J* = 21.9 Hz, C), 142.6 (d, *J* = 22.9 Hz, C), 138.9 (d, *J* = 111.7 Hz, C), 137.7 (d, *J* = 109.8 Hz, C), 132.9 (s, CH), 131.0 (d, *J* = 11.5 Hz, CH), 129.6 (s, CH), 129.19 (d, *J* = 13.3 Hz, CH), 129.18 (d, *J* = 107.0 Hz, C), 128.4 (d, *J* = 14.3 Hz, CH), 126.7 (s, CH), 125.0 (s, CH), 123.7 (s, CH), 123.1 (s, CH), 120.4 (d, *J* = 14.3 Hz, CH), 114.5 (d, *J* = 17.2 Hz, C). One signal of a quaternary carbon was overlapped. ³¹P{¹H} NMR (162 MHz, CDCl₃): δ 20.9. HRMS (ESI): *m/z* calcd. for C₃₂H₂₁BrNNaOPS₂: 631.9878 ([M+Na]⁺); found. 631.9849.

Compound 8. A mixture of [Ir(cod)(OMe)]₂ (2.4 mg, 3.62 μmol), dtbpy (3.5 mg, 0.0130 mmol), and (Bpin)₂ (5.1 mg, 0.0201 mmol) in anhydrous hexane (0.5 mL) was stirred until the solution turned brown. To this solution was added **11** (99.0 mg, 0.238 mmol), B₂pin₂ (61.7 mg, 0.243 mmol), and anhydrous hexane (1.5 mL) followed by stirring at 80 °C for 19 h. The resulting mixture was filtered through a plug of silica gel to afford 117 mg (0.216 mmol, 91%) of **8** and used for the synthesis of **1f** without further purification.

Compound 1f. To a mixture of **7** (93.6 mg, 0.153 mmol) and **8** (117 mg, 0.216 mmol) in toluene (5 mL) was added Pd(PPh₃)₄ (12.2 mg, 0.0106 mmol) and a 2 M aqueous solution of Na₂CO₃ (0.73 mL). The mixture was stirred at 110 °C for 18 h. After addition of a saturated aqueous solution of NH₄Cl, the mixture was extracted with CHCl₃. The combined organic layer was washed with brine, dried over Na₂SO₄, and filtered. The crude mixture was subjected to silica gel column chromatography (CH₂Cl₂ to 19/1 CH₂Cl₂/EtOAc, R_f = 0.53 in 19/1 CH₂Cl₂/EtOAc) followed by preparative GPC (CHCl₃) to afford 81.0 mg (0.0856 mmol, 56%) of **1f** as red solids. Mp. 185.3–186.1 °C. ¹H NMR (400 MHz, acetone-*d*₆): δ 8.11–8.02 (m, 2H), 7.87–7.78 (m, 2H), 7.69–7.44 (m, 14H), 7.34 (t, *J* = 7.2 Hz, 4H), 7.17–7.08 (m, 6H), 7.03 (d, *J* = 8.0 Hz, 2H), 1.40 (s, 9H), 1.16 (s, 18H). ¹³C{¹H} NMR (100 MHz, CDCl₃): δ 151.74 (s, C), 151.70 (s, C), 149.3 (d, *J* = 14.3 Hz, C), 148.8 (s, C), 148.3 (s, C), 147.3 (s, C), 145.9 (s, C), 145.0 (d, *J* = 22.9 Hz, C), 143.4 (s, C), 143.1 (d, *J* = 22.9 Hz, C), 142.9 (s, CH), 140.9 (d, *J* = 15.3 Hz, C), 139.7 (d, *J* = 111.7 Hz, C), 139.2 (d, *J* = 110.8 Hz, C), 138.0 (s, CH), 135.7 (s, C), 132.8 (s, CH), 131.12 (s, CH),

131.06 (d, J = 11.5 Hz, CH), 129.6 (s, CH), 129.5 (d, J = 107.8 Hz, C), 129.2 (d, J = 13.4 Hz, CH), 127.9 (s, CH), 126.9 (s, C), 126.7 (s, CH), 125.4 (s, CH), 125.0 (s, CH), 123.7 (s, CH), 123.1 (s, CH), 122.9 (d, J = 14.3 Hz, CH), 122.6 (d, J = 11.5 Hz, CH), 120.6 (d, J = 14.4 Hz, CH), 38.6 (s, C), 35.1 (s, CH₃), 34.9 (s, C), 31.6 (s, CH₃). One singlet signal of a quaternary carbon atom was overlapped and. In addition, one of the doublet signals of a CH carbon atom paired with the signal at 131.00 ppm was overlapped. $^{11}\text{B}\{\text{H}\}$ NMR (128 MHz, CDCl₃): δ 65.9. $^{31}\text{P}\{\text{H}\}$ NMR (162 MHz, CDCl₃): δ 20.6. HRMS (ESI): *m/z* calcd. for C₆₀H₅₇BNNaOPS₃: 968.3325 ([M+Na]⁺); found. 968.3323.



6-Bromo-2-formyldithieno[3,2-*b*:2',3'-*d*]phosphole *P*-oxide (9**).** To a suspension of 2,6-dibromodithieno[3,2-*b*:2',3'-*d*]phosphole *P*-oxide **4** (1.02 g, 2.29 mmol) in anhydrous toluene (8 mL) was added HSiCl₃ (1.54 g, 11.4 mmol) in one portion. After stirring at room temperature for 30 min, all volatiles were removed under reduced pressure. The resulting mixture was passed through a short silica gel column using toluene as eluent and then concentrated under reduced pressure. The resulting yellow solid was dissolved in anhydrous THF (20 mL) and a hexane solution of *n*-BuLi (1.6 M, 1.05 mL, 1.68 mmol) was added at -78 °C followed by stirring at the same temperature for 2 h. A THF solution (10 mL) of DMF (551 mg, 7.54 mmol) was added at -78 °C, and the mixture was allowed to warm to room temperature and stirred for 18 h. Water was added to the mixture and neutralized with a 2 M aqueous solution of HCl. The organic layer was separated and the aqueous layer was extracted with CH₂Cl₂. The combined organic layer was washed with brine, dried over Na₂SO₄, and filtered. After concentration of the filtrate under reduced pressure, the resulting solid was dissolved in CH₂Cl₂ (40 mL), and an aqueous solution of H₂O₂ (6 mL, 30%) was added. After stirring for 5 h, a saturated aqueous solution of Na₂SO₃ was added and the mixture was extracted with CH₂Cl₂. The organic layer was dried over Na₂SO₄, and filtered. The mixture was subjected to silica gel column chromatography (CH₂Cl₂ to 4/1 CH₂Cl₂/EtOAc, *R*_f = 0.20 in 4/1 CH₂Cl₂/EtOAc) to afford 173 mg (0.438 mmol, 29%) of **9** as yellow solids. Mp. 236.1 °C (dec.). ^1H NMR (400 MHz, CDCl₃): δ 9.84 (s, 1H), 7.76 (d, J = 2.8 Hz, 1H), 7.72 (dd, J = 14.0, 7.2 Hz, 2H), 7.63–7.57 (m, 1H), 7.48 (td, J = 8.0, 3.6 Hz, 2H), 7.21 (d, J = 2.8 Hz, 1H). $^{13}\text{C}\{\text{H}\}$ NMR (100 MHz,

CDCl_3): δ 182.4 (s, CH), 152.8 (d, J = 23.9 Hz, C), 147.0 (d, J = 12.4 Hz, CH), 144.6 (d, J = 21.0 Hz, C), 142.0 (d, J = 107.8 Hz, C), 138.5 (d, J = 111.7 Hz, C), 134.5 (d, J = 13.4 Hz, CH), 133.4 (s, CH), 130.9 (d, J = 11.5 Hz, CH), 129.4 (d, J = 13.3 Hz, CH), 129.1 (d, J = 14.3 Hz, CH), 127.8 (d, J = 109.8 Hz, C), 119.2 (d, J = 18.2 Hz, C). $^{31}\text{P}\{\text{H}\}$ NMR (162 MHz, CDCl_3): δ 19.1. HRMS (ESI): m/z calcd. for $\text{C}_{15}\text{H}_8\text{BrNaO}_2\text{PS}_2$: 416.8779 ($[M+\text{Na}]^+$); found. 416.8778.

Compound 2. A mixture of **10** (150 mg, 0.378 mmol), ethylene glycol (72.2 mg, 1.16 mmol), and $\text{TsOH}\cdot\text{H}_2\text{O}$ (12.2 mg, 0.0641 mmol) in benzene (4 mL) was stirred at 100 °C for 18 h. After addition of an aqueous solution of NaHCO_3 , the mixture was extracted with ether. The organic layer was washed with brine, dried over Na_2SO_4 , and filtered. After concentration of the filtrate under reduced pressure, the resulting solid was dissolved in anhydrous toluene. 4-(Diphenylamino)phenylboronic acid (97.6 mg, 0.338 mmol), a 2 M aqueous solution of Na_2CO_3 (1.6 mL, 3.23 mmol) and $\text{Pd}(\text{PPh}_3)_4$ (29.2 mg, 0.0253 mmol) were added to the mixture followed by stirring at 110 °C for 16 h. After addition of a saturated aqueous solution of NH_4Cl , the mixture was extracted with CHCl_3 . The organic layer was washed with brine, dried over Na_2SO_4 , and filtered. After concentration of the filtrate under reduced pressure, the resulting solid was dissolved in THF (8 mL). A 2 M aqueous HCl solution (3 mL) was added to the solution and the mixture was stirred at room temperature for 1 h. The mixture was extracted with CHCl_3 and the organic layer was washed with brine, dried over Na_2SO_4 , and filtered. The resulting mixture was subjected to silica gel column chromatography (CH_2Cl_2 to 4/1 $\text{CH}_2\text{Cl}_2/\text{EtOAc}$, R_f = 0.28 in 4/1 $\text{CH}_2\text{Cl}_2/\text{EtOAc}$) followed by preparative GPC (CHCl_3) to afford 136 mg (0.243 mmol, 75%) of **2** as red solids. Mp. 143.2 °C (dec.). ^1H NMR (400 MHz, acetone- d_6): δ 9.93 (s, 1H), 8.12 (d, J = 2.8 Hz, 1H), 7.84–7.76 (m, 2H), 7.69–7.61 (m, 4H), 7.53 (td, J = 7.8, 3.2 Hz, 2H), 7.35 (t, J = 8.0 Hz, 4H), 7.16–7.10 (m, 6H), 7.03 (d, J = 8.8 Hz, 2H). $^{13}\text{C}\{\text{H}\}$ NMR (100 MHz, CDCl_3): δ 182.3 (s, CH), 154.3 (d, J = 23.9 Hz, C), 152.8 (d, J = 15.3 Hz, C), 149.0 (s, C), 147.1 (s, C), 146.2 (d, J = 13.7 Hz, C), 143.3 (d, J = 109.8 Hz, C), 141.4 (d, J = 21.0 Hz, C), 138.5 (d, J = 110.7 Hz, C), 134.7 (d, J = 13.4 Hz, CH), 133.2 (s, CH), 131.0 (d, J = 11.5 Hz, CH), 129.6 (s, CH), 129.3 (d, J = 13.4 Hz, CH), 128.6 (d, J = 109.8 Hz, C), 126.9 (s, CH), 126.0 (s, C), 125.3 (s, CH), 124.0 (s, CH), 122.7 (s, CH), 120.8 (d, J = 13.3 Hz, CH). $^{31}\text{P}\{\text{H}\}$ NMR (162 MHz, CDCl_3): δ 19.4. HRMS (ESI): m/z calcd. for $\text{C}_{33}\text{H}_{22}\text{NNaO}_2\text{PS}_2$: 582.0722 ($[M+\text{Na}]^+$); found. 582.0724.

Compound 3. A mixture of **2** (60.7 mg, 0.108 mmol), hydroxylamine hydrochloride (15.7 mg, 0.226 mmol), $\text{TsOH}\cdot\text{H}_2\text{O}$ (47.8 mg, 0.251 mmol), and MgSO_4 (257 mg, 2.14 mmol) in anhydrous toluene (3 mL) was stirred at 120 °C for 20 h. The mixture was filtered through a plug of celite® and concentrated

under reduced pressure. The crude mixture was subjected to silica gel column chromatography (CH_2Cl_2 to 92/8 $\text{CH}_2\text{Cl}_2/\text{EtOAc}$, $R_f = 0.54$ in 92/8 $\text{CH}_2\text{Cl}_2/\text{EtOAc}$) followed by preparative GPC (CHCl_3) to afford 22.6 mg (0.0406 mmol, 38%) of **3** as red solids. Mp. 262.3–263.1 °C. ^1H NMR (400 MHz, acetone- d_6): δ 8.04 (d, $J = 2.8$ Hz, 1H), 7.84–7.75 (m, 2H), 7.68–7.61 (m, 4H), 7.53 (td, $J = 7.6, 3.6$ Hz, 2H), 7.35 (t, $J = 6.0$ Hz, 4H), 7.16–7.09 (m, 6H), 7.03 (d, $J = 8.8$ Hz, 2H). $^{13}\text{C}\{\text{H}\}$ NMR (100 MHz, CDCl_3): δ 152.4 (d, $J = 14.3$ Hz, C), 151.8 (d, $J = 22.9$ Hz, C), 149.0 (s, C), 147.1 (s, C), 142.9 (d, $J = 110.7$ Hz, C), 140.5 (d, $J = 21.9$ Hz, C), 138.0 (d, $J = 109.8$ Hz, C), 136.0 (d, $J = 14.3$ Hz, CH), 133.3 (s, CH), 131.0 (d, $J = 11.5$ Hz, CH), 129.6 (s, CH), 129.4 (d, $J = 13.3$ Hz, CH), 128.1 (d, $J = 109.8$ Hz, C), 126.9 (s, CH), 125.8 (s, C), 125.3 (s, CH), 124.0 (s, CH), 122.6 (s, CH), 120.7 (d, $J = 14.3$ Hz, CH), 113.6 (s, C), 110.9 (d, $J = 16.2$ Hz, C). $^{31}\text{P}\{\text{H}\}$ NMR (162 MHz, CDCl_3): δ 19.6. HRMS (ESI): m/z calcd. for $\text{C}_{33}\text{H}_{21}\text{N}_2\text{NaOPS}_2$: 579.0725 ($[M+\text{Na}]^+$); found. 579.0720.

2. Photophysical Properties

Measurements. UV-vis absorption spectra were recorded on a Shimadzu UV-3150 spectrometer with a resolution of 0.2 nm using diluted sample solutions in spectral grade solvents in a 1 cm square quartz cuvette. Emission spectra were recorded on a HORIBA SPEX Fluorolog-3 spectrofluorometer equipped with a Hamamatsu PMA R5509-73 and a cooling system C9940-01 with a resolution of 0.5 nm. Absolute fluorescence quantum yields were determined with a Hamamatsu Photonics C-9920-02 calibrated with an integrating sphere system. The absorption and emission spectra of **1b–1f**, **2**, and **3** in various solvents are given in Figures S1–S7. All photophysical properties are summarized in Table S1.

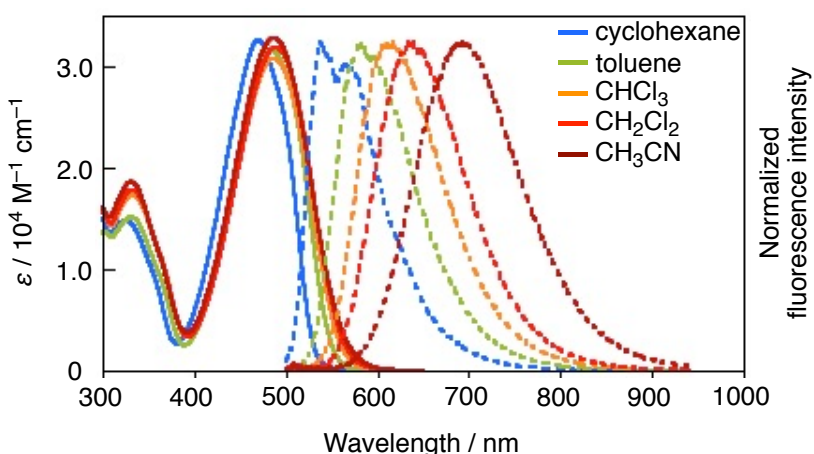


Figure S1. UV-vis absorption and emission spectra of **1b** in various solvents.

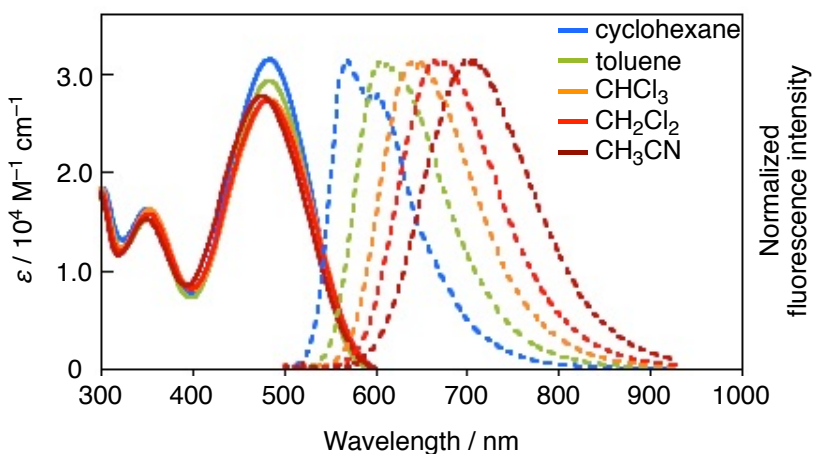


Figure S2. UV-vis absorption and emission spectra of **1c** in various solvents.

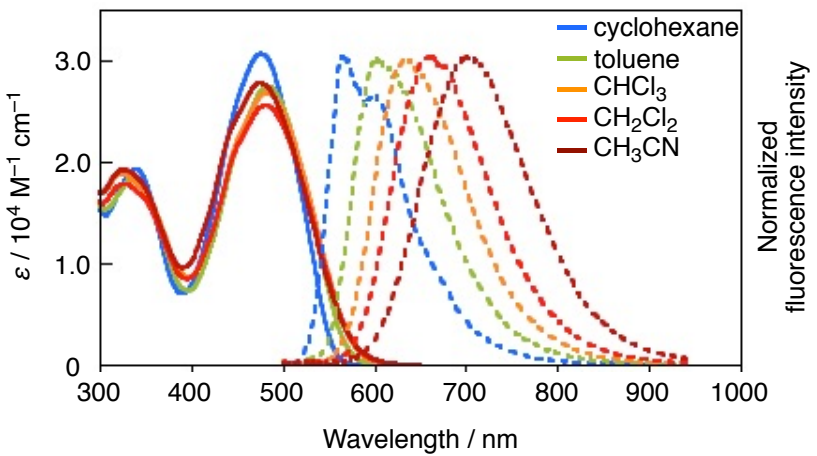


Figure S3. UV–vis absorption and emission spectra of **1d** in various solvents.

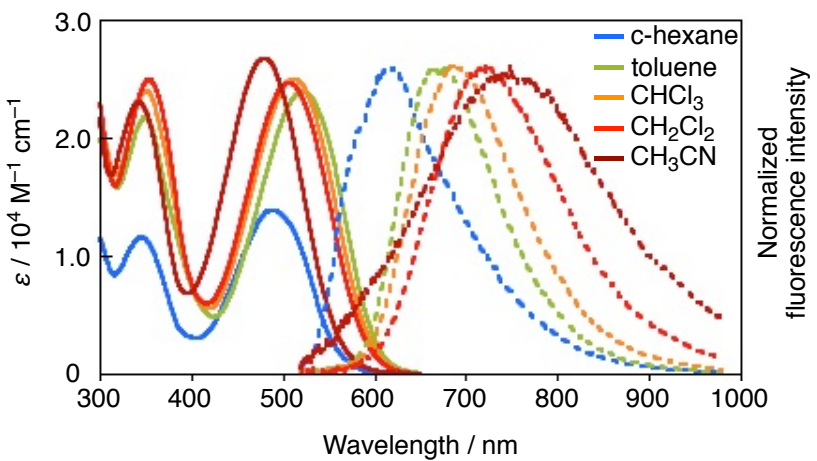


Figure S4. UV–vis absorption and emission spectra of **1e** in various solvents. The value of the molar absorption coefficient in cyclohexane is underestimated due to the low solubility of **1e**.

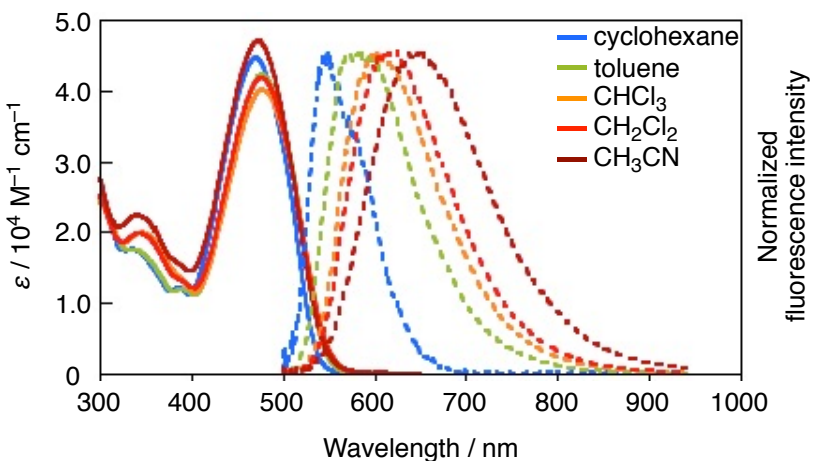


Figure S5. UV–vis absorption and emission spectra of **1f** in various solvents.

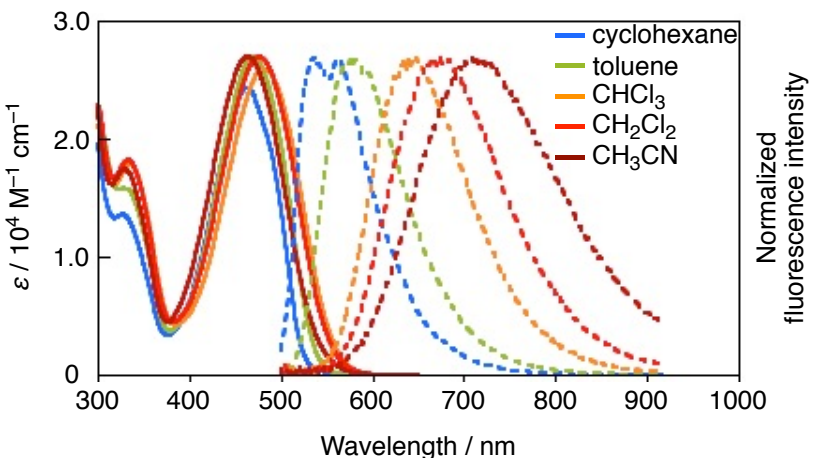


Figure S6. UV–vis absorption and emission spectra of **2** in various solvents.

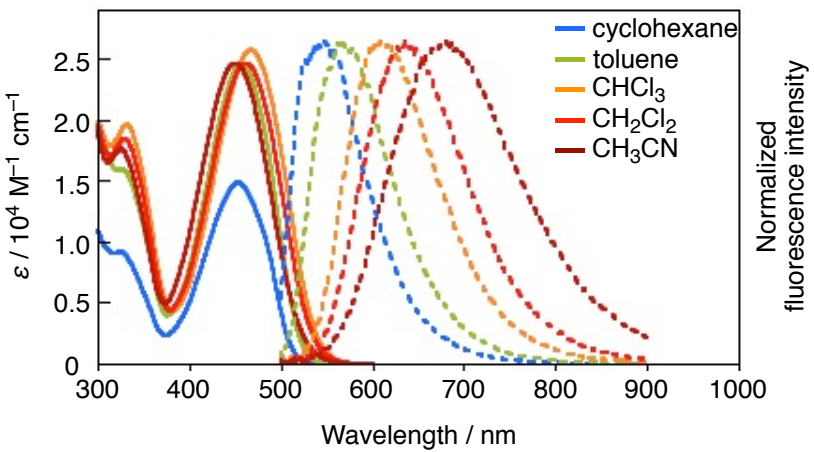


Figure S7. UV–vis absorption and emission spectra of **3** in various solvents. The value of the molar absorption coefficient in cyclohexane is underestimated due to the low solubility of **3**.

Table S1. Photophysical properties of compounds **1a–1f**, **2** and **3**

Cmpd	Solvent	λ_{abs} /nm ^[a]	ε $/10^4 \text{ M}^{-1} \text{cm}^{-1}$	λ_{em} /nm	$\Phi_F^{[b]}$	τ /ns	k_r $/10^8 \text{ s}^{-1}$	k_{nr} $/10^8 \text{ s}^{-1}$
1a	cyclohexane	458	3.56	532	0.81 (0.90)	3.07	2.6	0.62
	toluene	466	3.43	566	0.90 (0.93)	3.19	2.8	0.31
	CHCl ₃	466	3.18	597	0.90 (0.92)	3.99	2.3	0.25
	CH ₂ Cl ₂	466	3.32	626	0.88 (0.89)	4.26	2.1	0.28
	CH ₃ CN	462	3.45	665	0.59 (0.63)	3.99	1.5	1.0
1b	cyclohexane	470	3.26	540	0.81 (0.74)	3.52	2.3	0.54
	toluene	484	3.17	584	0.87 (0.93)	3.72	2.3	0.35
	CHCl ₃	487	3.08	617	0.89 (0.91)	4.51	2.0	0.24

	CH ₂ Cl ₂	488	3.19	639	0.87 (0.91)	4.58	1.9	0.28
	CH ₃ CN	487	3.28	695	0.72 (0.77)	4.78	1.5	0.59
1c	cyclohexane	486	3.14	570	0.65 (0.64)	3.52	1.9	0.99
	toluene	486	2.92	606	0.83 (0.87)	3.73	2.2	0.46
	CHCl ₃	483	2.74	648	0.81 (0.84)	4.51	1.8	0.42
	CH ₂ Cl ₂	482	2.72	665	0.78 (0.82)	4.55	1.7	0.48
	CH ₃ CN	477	2.77	704	0.67 (0.71)	4.46	1.5	0.74
1d	cyclohexane	476	3.07	567	0.86 (0.87)	3.55	2.4	0.39
	toluene	484	2.74	603	0.88 (0.92)	3.79	2.3	0.32
	CHCl ₃	482	2.68	641	0.85 (0.88)	4.38	1.9	0.34
	CH ₂ Cl ₂	483	2.56	660	0.83 (0.84)	4.59	1.8	0.37
	CH ₃ CN	475	2.77	704	0.69 (0.74)	4.66	1.5	0.67
1e	cyclohexane	488	— ^[c]	617	0.62 (0.45)	1.78 4.31	—	—
	toluene	522	2.39	664	0.71 (0.69)	4.85	1.5	0.60
	CHCl ₃	514	2.50	686	0.64 (0.67)	4.76	1.3	0.76
	CH ₂ Cl ₂	506	2.47	713	0.35 (0.33)	3.18	1.1	2.0
	CH ₃ CN	480	2.67	748	0.07 (0.06)	— ^[d]	—	—
1f	cyclohexane	470	4.47	550	0.44 (0.35)	2.16	2.0	2.6
	toluene	478	4.23	585	0.76 (0.79)	2.91	2.6	0.83
	CHCl ₃	478	4.01	601	0.82 (0.85)	3.81	2.2	0.47
	CH ₂ Cl ₂	477	4.18	625	0.83 (0.85)	3.87	2.1	0.44
	CH ₃ CN	474	4.70	651	0.71 (0.76)	4.04	1.8	0.72
2	cyclohexane	463	2.44	537	0.60 (0.50)	3.93	1.5	1.0
	toluene	470	2.70	578	0.90 (0.92)	4.12	2.2	0.24
	CHCl ₃	482	2.59	649	0.88 (0.89)	4.96	1.8	0.24
	CH ₂ Cl ₂	477	2.69	674	0.66 (0.70)	4.48	1.5	0.76
	CH ₃ CN	464	2.70	709	0.08 (0.07)	0.85	0.94	11
3	cyclohexane	453	— ^[c]	548	0.59 (0.59)	4.18	1.4	0.98
	toluene	456	2.46	567	0.89 (0.93)	4.36	2.0	0.25
	CHCl ₃	467	2.57	609	0.89 (0.91)	5.51	1.6	0.20
	CH ₂ Cl ₂	462	2.46	636	0.83 (0.84)	5.91	1.9	0.38
	CH ₃ CN	452	2.46	681	0.26 (0.27)	2.74	0.95	2.7

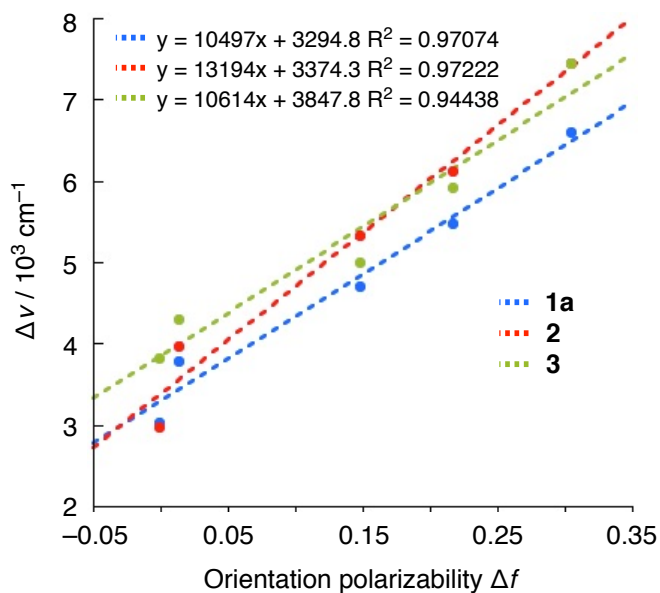
[a] Only the longest absorption maximum wavelengths are shown. [b] Absolute fluorescence quantum yields determined by a calibrated integrating sphere system within $\pm 3\%$ error. The quantum yields after N₂ purge are shown in the parentheses. [c] Not dissolved. [d] Not determined.

Table S2. Calculated dipole moments in the ground state (μ_G)^a and excited state (μ_E)

Compounds	μ_G / D	μ_E / D	$\Delta\mu$ / D ^b
1a	4.95	20.6	15.6
2	8.48	23.8	15.4
3	9.17	21.0	11.8

^aCalculated at the B3LYP/6-31G(d) level of theory. ^bCalculated by the Lippert-Mataga Equation using the calculated Onsager cavity radius a obtained at the B3LYP/6-31G(d) level of theory. $\Delta\nu$ = Stokes shift, ε_0 = dielectric constant of vacuum, $\Delta\mu$ = difference between the dipole moments in the ground state and the excited state, h = Plank constant, c = speed of light in vacuum, Δf = orientation polarizability, and a = Onsager cavity radius.

$$\Delta\nu = \frac{1}{4\pi\varepsilon_0} \frac{2\Delta\mu^2}{hca^3} \Delta f + \text{constant}$$

**Figure S8.** Lippert-Mataga plots for **1a**, **2**, and **3**.

3. Evaluation of Photostability

Photostability of the fluorophores was evaluated based on the absorption variation of each sample at 450 nm along with irradiation time upon the irradiation. The sample solution in N₂ purged CH₃CN in a quartz cuvette was irradiated at room temperature. The setup consisted of a LED lamp (CCS Inc., PFBR-150BL) equipped with a band-path filter of 450 nm (a half peak width of 10 nm). Through a glass fiber, the solution of dye in a quartz cuvette was irradiated.

The total quantum yield for photodecomposition (Φ_{dec}), which is defined as the sum of the quantum yields for all reaction to produce photo-reacted products by light irradiation, is described as^{6,7}

$$\ln \left(10^{A(t)} - 1 \right) - \ln \left(10^{A(0)} - 1 \right) = -\ln 10 \cdot \Phi_{dec} \cdot \varepsilon \cdot I_0 \cdot t$$

where $A(t)$ is absorbance of the fluorophore at time t , ε is the molar absorption coefficient of the fluorophore at the wavelength of the incident light, and I_0 is the intensity of the incident light, which was estimated by a diarylethene derivative **BT**⁸ as a chemical actinometer.

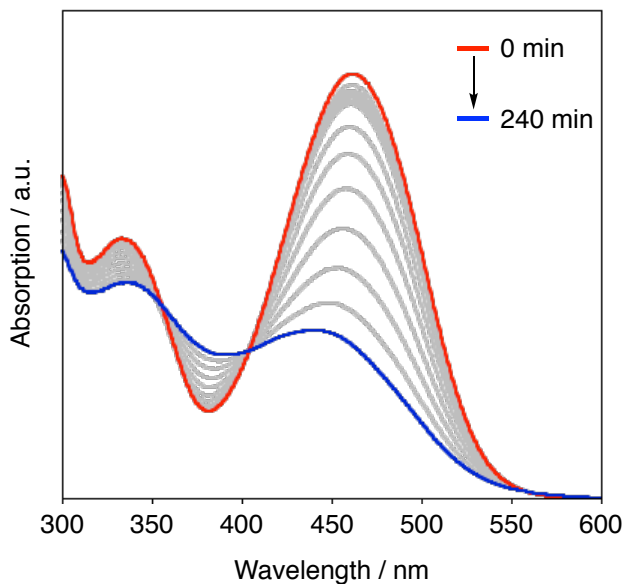


Figure S9. Absorption spectral change of **1a** upon irradiation with a LED lamp (a band-path filter of 450 nm with a half peak width of 10 nm).

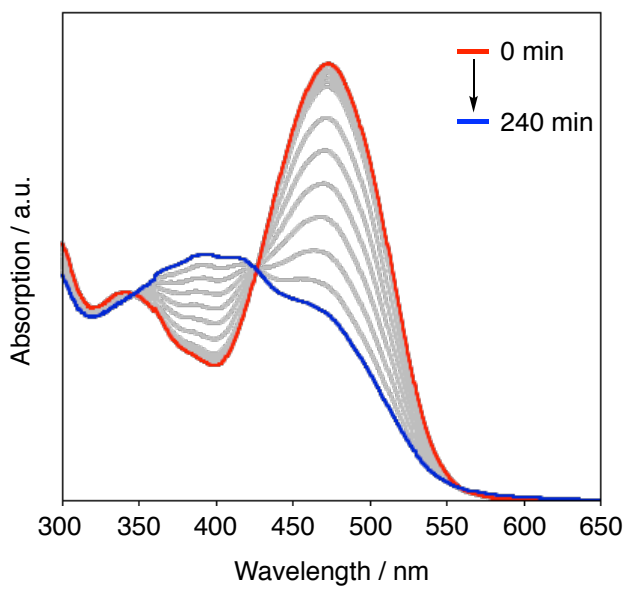


Figure S10. Absorption spectral change of **1f** upon irradiation with a LED lamp (a band-path filter of 450 nm with a half peak width of 10 nm).

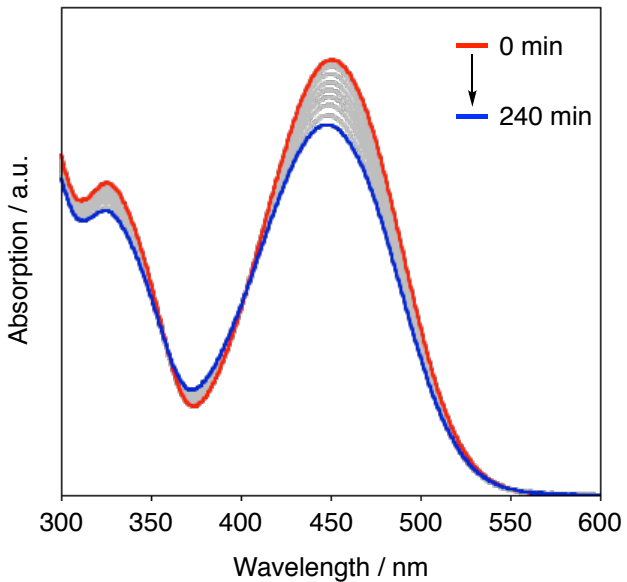


Figure S11. Absorption spectral change of **3** upon irradiation with a LED lamp (a band-path filter of 450 nm with a half peak width of 10 nm).

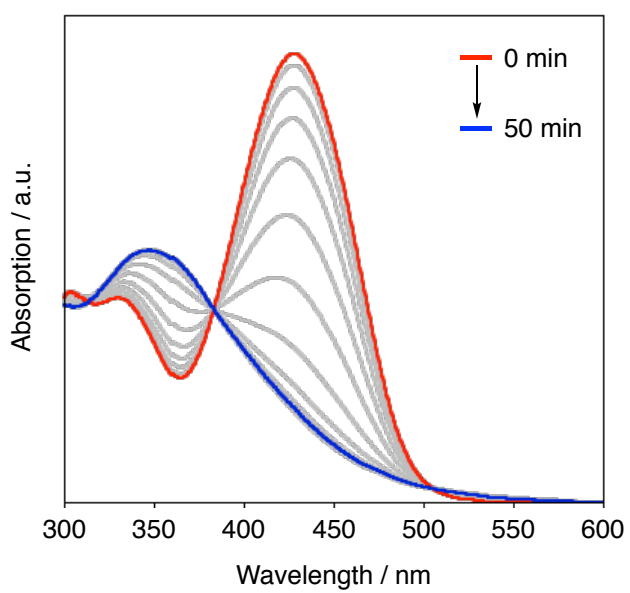


Figure S12. Absorption spectral change of **10** upon irradiation with a LED lamp (a band-path filter of 450 nm with a half peak width of 10 nm).

4. Theoretical Calculations

All quantum mechanical calculations were carried out using the Gaussian 16 Revision B.01 suite of programs with default thresholds and algorithms,⁹ except for the removal of level shift in the self-consistent field (SCF) procedure for rate constant calculations. Throughout the calculations, Density Functional Theory (DFT) with CAM-B3LYP functional¹⁰ and 6-31G(d) basis sets¹¹⁻¹⁵ were employed. Solvation effect was treated by employing the Polarizable Continuum Model (PCM) implemented in Gaussian 16.¹⁶ Rate constants on the S₁→S₀ IC process (k_{IC}) and the S₁→T₂ ISC process (k_{ISC}) were computed using MOMAP-2020A program,¹⁷ where the vibrational state at the initial state is given by the Boltzmann distribution at 300K, and integration of vibration correlation function was conducted from -1000 fs to +1000 fs with a time step of 0.01 fs. The S₁-S₀ NACs were computed at the minimum of S₁ using Gaussian 16 in accordance with the procedure in MOMAP user guide, where the keyword “td=nac” in Gaussian 16 was unused. The S₁-T₂ SOCs were computed at the minimum of T₂ using Gaussian 16 and PySOC program.¹⁸ In all rate constant calculations, the mixing of normal modes in either electronic state (Duschinsky rotation) was neglected because the computation with Duschinsky rotation was observed to give unphysical results.

There appeared to be inadequacy in our rate constant calculations to fully reproduce the intermolecular trend of the experimentally obtained nonradiative decay rate constant (k_{nr}). The errors may arise from the fact that in our calculation of k_{ISC} using MOMAP-2020A, the contribution from the coupling with intermediate electronic states and the first order derivatives of SOCs along with vibrational coordinates were neglected. The molecules of interest do not contain any heavy atoms, resulting in small direct SOCs between S₁ and T₂, which were computed to be 0.196, 0.319 and 0.357 cm⁻¹ for **1a**, **2** and **3**, respectively, in CH₃CN solution. In such cases, the first order derivatives of SOCs or terms of the spin-vibronic coupling may have an effective impact on the estimation of k_{ISC} , as indicated previously.^{19,20}

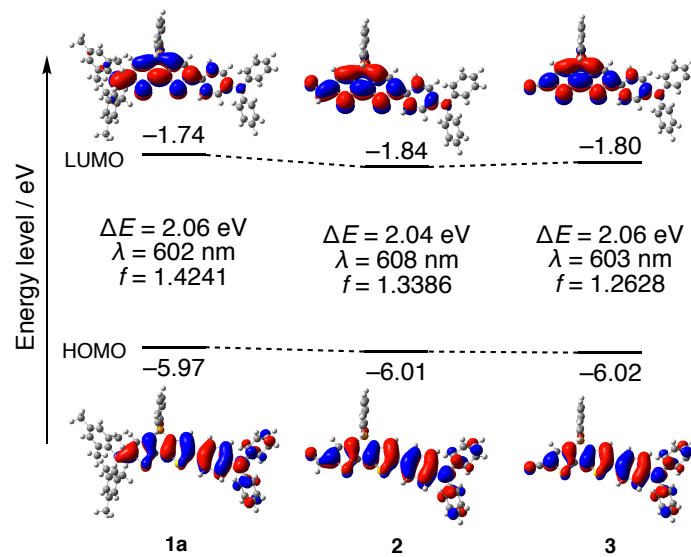


Figure S13. Energy diagrams of frontier orbitals in CH_3CN using optimized structures in the excited states. Kohn-Sham molecular orbitals, electronic transition energies (ΔE), and oscillator strength (f) calculated at the (TD-)CAM-B3LYP/6-31G(d) level of theory.

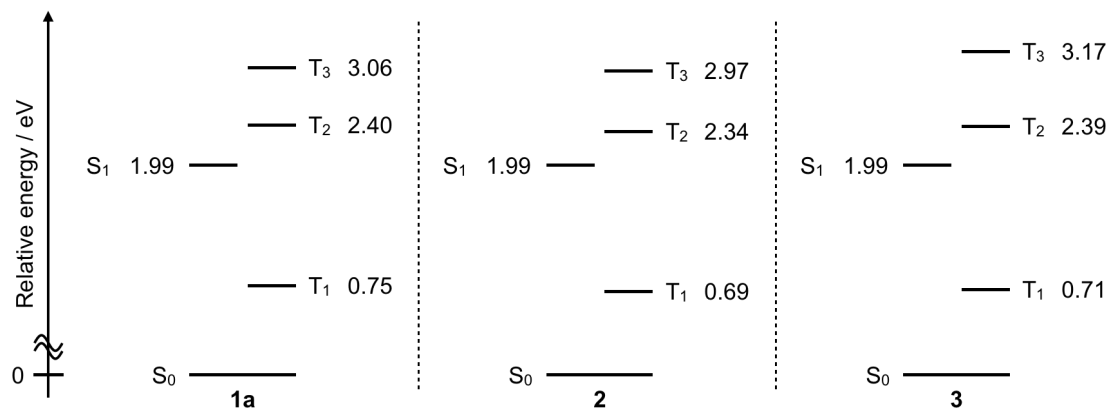


Figure S14. Energy levels of the singlet and triplet excited states in CH_3CN calculated at the TD-CAM-B3LYP/6-31G(d) level of theory including the PCM model.

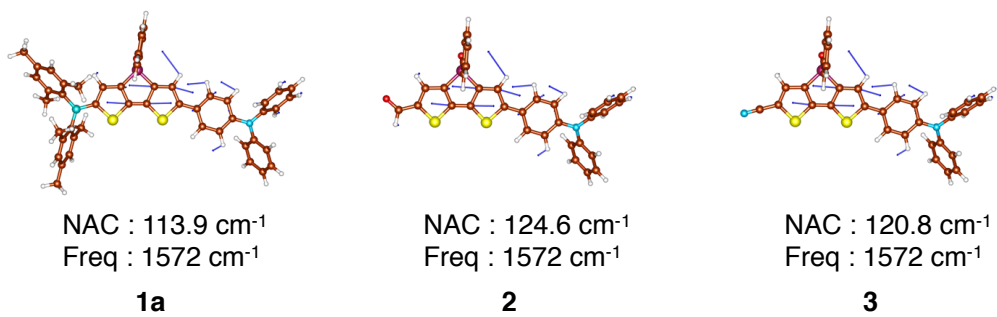


Figure S15. Representative vibrational modes at the S_1 state with the largest NAC. NAC and frequency are shown for each vibrational mode. Computations were conducted at the TD-CAM-B3LYP/6-31G(d) with PCM level of theory for CH_3CN solution.

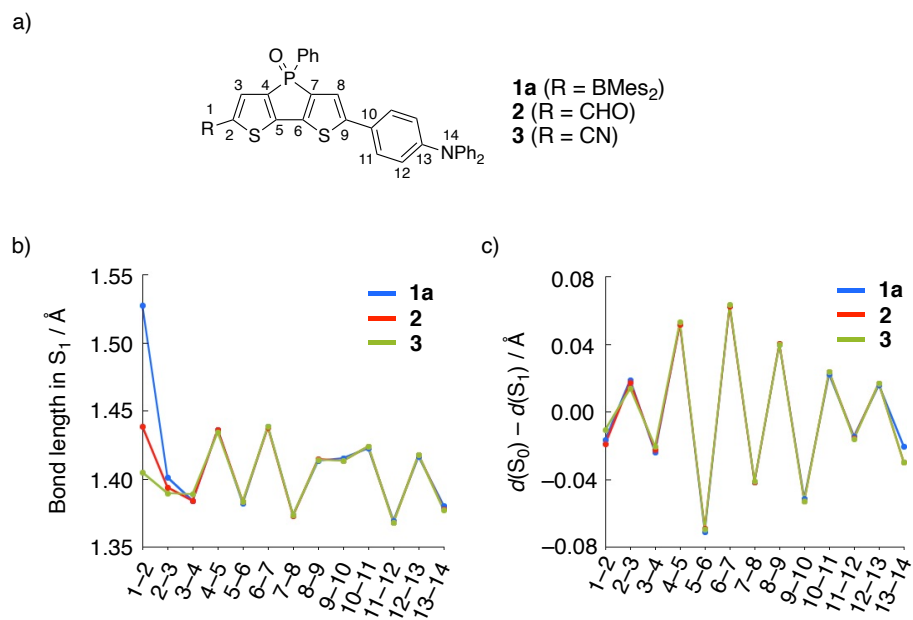


Figure S16. a) An atom-labeling scheme of compounds **1a**, **2**, and **3**, b) plots of their bond distances in the excited states in CH_3CN , and c) changes in bond length by the geometry relaxation after Franck-Condon transition. Calculations were conducted at the TD-CAM-B3LYP/6-31G(d) level of theory including the PCM model.

Table S3. Cartesian coordinates [Å] of the optimized structure for **1a** in S₀

atom	X	Y	Z	atom	X	Y	Z
C	3.97372214	0.37526069	-0.19843193	C	-10.80931231	-1.74085782	1.11560236
C	3.60513925	-0.80821942	-0.81049648	C	-9.15197569	-1.73547805	2.8549949
H	4.34114897	-1.51399458	-1.17776432	H	-7.4361039	-0.48307322	2.51770434
C	2.2120954	-0.98664249	-0.90798363	H	-10.37002884	-0.52904588	-0.60708237
C	1.50563974	0.06380132	-0.34857305	H	-11.75687541	-2.08765222	0.71504791
S	2.53863342	1.27481096	0.26729806	H	-8.80237008	-2.06834478	3.82739379
C	0.06227318	-0.10236564	-0.3881045	H	-10.97726095	-2.87564015	2.93840571
C	-0.36541609	-1.27037534	-0.9750289	C	-8.66140933	1.61767132	-0.50506168
C	-1.77498209	-1.38895468	-1.01048452	C	-9.93073129	3.7977128	-1.7164512
H	-2.30748309	-2.22174995	-1.45309071	C	-8.36832525	1.96059782	-1.82744034
C	-2.41136212	-0.30952433	-0.44741151	C	-9.59697258	2.37429326	0.20448322
S	-1.25377226	0.86551103	0.141571	C	-10.2318178	3.45045955	-0.40305144
B	5.39677009	0.90880465	0.07424138	C	-8.9930256	3.04967467	-2.42206523
C	6.59211562	-0.12085982	-0.02732185	H	-7.64975959	1.37029562	-2.38598567
C	8.73094311	-1.97888591	-0.25049854	H	-9.82432808	2.1137274	1.23264187
C	7.66178763	0.10112453	-0.92801182	H	-10.9577759	4.02815529	0.16072238
C	6.62419519	-1.29058358	0.76140546	H	-8.75412869	3.30469081	-3.44991603
C	7.69123285	-2.18437733	0.6462634	H	-10.42290476	4.64301343	-2.18630639
C	8.69442528	-0.82478229	-1.03131649	C	-3.85248447	-0.08519592	-0.29746657
H	7.70590466	-3.0672859	1.28153504	C	-6.63922282	0.30974596	-0.02509694
H	9.50014579	-0.6375957	-1.73758432	C	-4.73340483	-1.17059075	-0.21411712
C	5.57961274	2.43437971	0.44928003	C	-4.39944514	1.2014903	-0.23721203
C	5.83849932	5.17138176	1.17136992	C	-5.76245867	1.39900054	-0.09262909
C	5.19516763	3.46019609	-0.43770745	C	-6.09909054	-0.98080514	-0.09396021
C	6.10859456	2.81129499	1.70952763	H	-4.34432692	-2.18307845	-0.24061855
C	6.22129413	4.15430027	2.04702126	H	-3.75214664	2.0705355	-0.30791765
C	5.33377207	4.80063359	-0.06564284	H	-6.15429727	2.40801358	-0.03811807
H	6.61979746	4.4193694	3.02384017	H	-6.75652183	-1.84103501	-0.04379766
H	5.03956611	5.57288028	-0.77333511	C	1.21051496	-3.70044251	-0.47910003
C	5.55385795	-1.63487076	1.77624902	C	1.42843569	-5.99495444	1.08105779
H	5.99842367	-2.13877833	2.63952093	C	1.24260434	-4.95601055	-1.08413168
H	4.80709707	-2.31592671	1.35344122	C	1.28870164	-3.59572613	0.91247686
H	5.01448841	-0.76037003	2.14197472	C	1.39709812	-4.74141765	1.68892312
C	7.70799904	1.31728068	-1.82315691	C	1.35168683	-6.10226365	-0.30279408
H	7.69681498	2.24573701	-1.24604848	H	1.18626285	-5.02779859	-2.16516956
H	6.85157164	1.35232753	-2.50443373	H	1.26675645	-2.62104716	1.39141529
H	8.6128898	1.31148481	-2.43614761	H	1.45846555	-4.65814553	2.76912345
C	6.52183998	1.78396317	2.73693763	H	1.37772755	-7.07819381	-0.77667762
H	7.02182395	2.2622073	3.58307407	H	1.51435933	-6.88908566	1.69039615
H	7.20209342	1.03848045	2.31793559	P	1.0647811	-2.24213121	-1.54254761
H	5.65581252	1.24377457	3.13590056	O	1.12636415	-2.58393425	-3.0015649
C	4.69168018	3.19528857	-1.83947212	C	9.85851579	-2.96803798	-0.38603644
H	3.76788162	3.74954893	-2.03386667	H	10.82956308	-2.46402429	-0.41564148
H	4.49328315	2.14051665	-2.03111057	H	9.76756086	-3.54428859	-1.31389307

H	5.42823518	3.53079125	-2.57822575	H	9.86787942	-3.6784768	0.44471713
N	-8.02672239	0.50550657	0.11047078	C	5.97317684	6.61845383	1.56655385
C	-8.81167587	-0.40560968	0.86731228	H	5.33962223	6.85386886	2.42869311
C	-10.37216656	-2.18540888	2.35964116	H	5.68604293	7.2834496	0.74801766
C	-8.37925403	-0.84397536	2.12143228	H	7.00301318	6.85778874	1.85188156
C	-10.03294166	-0.86417347	0.36800358				

Table S4. Cartesian coordinates [Å] of the optimized structure for **2** in S₀

atom	X	Y	Z	atom	X	Y	Z
C	6.41101269	-2.18849847	-0.7935677	H	-7.45530214	-0.97014072	-1.35222899
C	6.3485547	-1.1478455	0.10500428	H	-8.89920407	-2.85427046	-0.6698383
H	7.23580418	-0.725184	0.56014029	H	-6.46522251	-3.45121059	2.81379728
C	5.02713799	-0.72846821	0.34141127	H	-8.40765772	-4.11429742	1.41408365
C	4.09859796	-1.45605187	-0.38290261	C	-1.11764798	-0.33827634	0.11543909
S	4.82492513	-2.65539493	-1.35911139	C	-3.9362116	-0.13901343	0.01489376
C	2.72018781	-1.05283902	-0.16612161	C	-1.76729152	0.87623008	0.36849333
C	2.56270103	-0.01510335	0.72308077	C	-1.91177471	-1.44894452	-0.19132273
C	1.20894647	0.34458074	0.91940967	C	-3.29180555	-1.353018	-0.25185935
H	0.87472777	1.12019348	1.59726441	C	-3.14727248	0.9742146	0.33248805
C	0.34450755	-0.42373175	0.17746058	H	-1.18363928	1.76268401	0.593887
S	1.2147709	-1.5996867	-0.78446154	H	-1.44800461	-2.41181173	-0.38381445
N	-5.33889731	-0.0384476	-0.03661176	H	-3.87857198	-2.22889632	-0.50297242
C	-5.95948628	1.15836418	-0.48602817	H	-3.62173727	1.92550003	0.54368893
C	-7.19957919	3.50372684	-1.3750838	C	4.54125166	2.14592926	0.66220085
C	-5.5019627	1.80729189	-1.63557347	C	5.12012784	4.67965728	-0.3304666
C	-7.0446426	1.69215078	0.21287955	C	4.98259308	3.14893217	1.52403
C	-7.66354206	2.85202241	-0.23650837	C	4.38913902	2.41434205	-0.70087512
C	-6.11375886	2.97713308	-2.06818392	C	4.67872732	3.67902944	-1.19405793
H	-4.66588554	1.39093196	-2.18730522	C	5.27167842	4.41554384	1.02587189
H	-7.40018727	1.19285353	1.10788119	H	5.0965995	2.93178877	2.58073561
H	-8.5067668	3.25448969	0.31625846	H	4.04425711	1.63856681	-1.37849636
H	-5.74639031	3.47110802	-2.96238792	H	4.5602329	3.88619712	-2.25258313
H	-7.68040863	4.41336653	-1.7199025	H	5.61503766	5.19468609	1.69863692
C	-6.15505342	-1.13544454	0.35062343	H	5.34566152	5.66779013	-0.71887042
C	-7.77820059	-3.28186812	1.11681474	P	4.18025968	0.51706159	1.36268868
C	-5.88547343	-1.84040829	1.52633443	O	4.39574808	0.45939811	2.84471181
C	-7.24530831	-1.51275018	-0.43670344	C	7.61625447	-2.86361909	-1.25843669
C	-8.05443884	-2.57340043	-0.0485055	H	7.46527824	-3.68173189	-1.98671242
C	-6.68762131	-2.91193853	1.89822122	O	8.73402774	-2.56200395	-0.88159213
H	-5.04565682	-1.54482479	2.14614052				

Table S5. Cartesian coordinates [Å] of the optimized structure for **3** in S₀

atom	X	Y	Z	atom	X	Y	Z
C	6.46655064	-2.19780041	-0.75454423	H	-4.99622921	-1.50064596	2.17099532
C	6.41120838	-1.15192405	0.13661292	H	-7.38852833	-0.9848096	-1.34841546
H	7.29292785	-0.72005476	0.5931946	H	-8.83920452	-2.85358401	-0.63885531
C	5.0858865	-0.73347299	0.36775442	H	-6.42257956	-3.39204139	2.86632925
C	4.15926477	-1.46436229	-0.34899073	H	-8.35982153	-4.07664148	1.46977344
S	4.88204256	-2.67395635	-1.31982515	C	-1.056621	-0.33927688	0.13199955
C	2.77986466	-1.06007621	-0.13731647	C	-3.87404317	-0.13641394	0.01906328
C	2.62286063	-0.01514791	0.74322102	C	-1.70437198	0.88066503	0.36248278
C	1.26940097	0.34769836	0.93498958	C	-1.85171378	-1.45375526	-0.15781037
H	0.93509907	1.12927562	1.60588487	C	-3.23135731	-1.35627204	-0.22415564
C	0.40530801	-0.42608166	0.19820408	C	-3.08402134	0.98062651	0.32022948
S	1.2750721	-1.61072668	-0.75277573	H	-1.11947028	1.76963395	0.57434595
N	-5.27621748	-0.03352174	-0.03971835	H	-1.38903844	-2.42058957	-0.33218972
C	-5.89179609	1.1553887	-0.51628774	H	-3.8191329	-2.2351972	-0.46187371
C	-7.12194682	3.4849305	-1.45901815	H	-3.55741819	1.93628663	0.51330012
C	-5.42672692	1.78007815	-1.67617433	C	4.6056927	2.14303813	0.66558306
C	-6.97948807	1.70535525	0.16592074	C	5.19254277	4.66610003	-0.34809814
C	-7.59340713	2.85725084	-0.31006068	C	5.05451288	3.15032798	1.5185605
C	-6.03360173	2.94225231	-2.13553304	C	4.44989538	2.40152453	-0.69900544
H	-4.58867344	1.35095841	-2.21497058	C	4.74362462	3.66107102	-1.2026567
H	-7.34094074	1.22490315	1.06884261	C	5.34754999	4.41172904	1.00971202
H	-8.43870863	3.27253236	0.22990685	H	5.17104246	2.94083463	2.57652154
H	-5.66037736	3.41732226	-3.03752626	H	4.09891527	1.6223636	-1.36955366
H	-7.59894021	4.38843864	-1.82465704	H	4.62237839	3.86080542	-2.26227163
C	-6.09650096	-1.12173749	0.36321781	H	5.6966314	5.1944251	1.67533205
C	-7.72734946	-3.25091581	1.16045752	H	5.42118257	5.65021075	-0.74476391
C	-5.83373043	-1.80584899	1.55271053	P	4.239903	0.52195723	1.37988185
C	-7.18381458	-1.51115219	-0.42226564	O	4.45703935	0.47295009	2.861437
C	-7.99678752	-2.56311622	-0.01875015	C	7.63024411	-2.86415119	-1.20900118
C	-6.63967516	-2.86898244	1.94013771	N	8.58014183	-3.41187078	-1.5837944

Table S6. Cartesian coordinates [Å] of the optimized structure for **1a** in S₁

atom	X	Y	Z	atom	X	Y	Z
C	-3.95433182	-0.36983667	-0.21860406	C	10.90468022	1.6736415	-0.54788359
C	-3.5375488	0.89219994	-0.66224836	C	9.58089205	2.59916257	1.23661831
H	-4.26231395	1.653376	-0.92920476	H	7.82994386	1.47456084	1.78967167
C	-2.16654564	1.06278567	-0.73738531	H	10.16752398	-0.15441269	-1.41528481
C	-1.44549382	-0.10781623	-0.32333502	H	11.76747271	1.72159645	-1.20434906
S	-2.53482203	-1.38418754	0.12199493	H	9.41294839	3.36522452	1.98667392
C	-0.07140885	0.03976703	-0.34664459	H	11.39128177	3.49363751	0.4926772
C	0.38158126	1.33224232	-0.78546176	C	8.54648319	-1.86315045	0.04996809
C	1.74997141	1.44895894	-0.78963797	C	9.66663824	-4.41410669	0.02561349
H	2.27900376	2.34686188	-1.08365479	C	8.19787456	-2.76940182	-0.95250433

C	2.425716	0.28232879	-0.36514551	C	9.46165445	-2.2329275	1.03566803
S	1.2643283	-1.00135076	0.04859926	C	10.02088774	-3.50417008	1.01742452
B	-5.38454419	-0.87316839	-0.03382893	C	8.75300874	-4.04264861	-0.95637385
C	-6.5575595	0.19380602	-0.07524257	H	7.49887189	-2.47108597	-1.72658051
C	-8.66187405	2.10967126	-0.1861376	H	9.72870406	-1.52381602	1.81178342
C	-7.61200554	0.07470735	-1.01483795	H	10.73074838	-3.78653445	1.7881761
C	-6.59244556	1.29348753	0.80978651	H	8.4787865	-4.7422019	-1.73937238
C	-7.63929389	2.21712179	0.74600218	H	10.10285201	-5.40754663	0.01630123
C	-8.6264604	1.02478325	-1.06119667	C	3.82050688	0.07185873	-0.25461985
H	-7.65214729	3.04389359	1.45316463	C	6.63040175	-0.34542024	-0.04317491
H	-9.41770617	0.91441185	-1.79966734	C	4.75604681	1.07492172	-0.63215311
C	-5.6331686	-2.42161052	0.20918474	C	4.36169799	-1.14766673	0.23389245
C	-6.02110606	-5.19952787	0.69785064	C	5.71330948	-1.3525824	0.33591941
C	-5.27574907	-3.38941489	-0.75203626	C	6.10703312	0.87737431	-0.52974969
C	-6.19965602	-2.88167783	1.42513952	H	4.40237076	2.01774783	-1.03241944
C	-6.3773458	-4.24188169	1.64834211	H	3.69584766	-1.94123981	0.55739633
C	-5.47607492	-4.74916475	-0.49502143	H	6.08251972	-2.29049476	0.73121929
H	-6.80496743	-4.56863639	2.59394286	H	6.78534845	1.65949265	-0.84666388
H	-5.19879803	-5.47260918	-1.25922349	C	-1.16944668	3.73612624	-0.06177728
C	-5.54453157	1.53038235	1.87705774	C	-1.35364303	5.88149037	1.70629944
H	-6.00422017	1.9584228	2.77318563	C	-1.06796279	5.0445879	-0.53451737
H	-4.78034621	2.23909714	1.5380902	C	-1.36537951	3.50642753	1.30293341
H	-5.02350424	0.61777381	2.1676857	C	-1.45731155	4.57680547	2.18324545
C	-7.65765364	-1.05630235	-2.01514847	C	-1.15949918	6.11511212	0.34912138
H	-7.68577396	-2.03210305	-1.52292482	H	-0.92597057	5.21579622	-1.59624284
H	-6.77882126	-1.05367681	-2.66797919	H	-1.4502685	2.49094883	1.67864596
H	-8.54143865	-0.97344344	-2.65324405	H	-1.61184535	4.3943939	3.24183242
C	-6.58597981	-1.92583578	2.52912998	H	-1.08217618	7.13154329	-0.02350681
H	-7.10775508	-2.45158061	3.33318829	H	-1.42705146	6.71696599	2.39544746
H	-7.23678696	-1.12607663	2.16715068	P	-1.0323765	2.36850308	-1.24488038
H	-5.70483502	-1.4474945	2.9714474	O	-1.08340165	2.86743878	-2.66213371
C	-4.72780219	-3.03114834	-2.11537605	C	-9.7706112	3.12650783	-0.2596259
H	-3.82834688	-3.61293171	-2.34101947	H	-10.75285609	2.64415689	-0.29226287
H	-4.47479895	-1.97399663	-2.20203596	H	-9.68530449	3.74011383	-1.16373943
H	-5.46241607	-3.260437	-2.89588357	H	-9.75128093	3.80017213	0.60113312
N	7.99192417	-0.54748252	0.05571517	C	-6.22466626	-6.66734472	0.96821567
C	8.89706074	0.55096121	0.16753866	H	-5.62439357	-7.00073645	1.82194017
C	10.69218697	2.66884712	0.4017242	H	-5.94316868	-7.2743186	0.10376002
C	8.68744543	1.54101513	1.12855714	H	-7.27053704	-6.88633531	1.20855764
C	10.01008136	0.61843689	-0.67071113				

Table S7. Cartesian coordinates [Å] of the optimized structure for **2** in S₁

atom	X	Y	Z	atom	X	Y	Z
C	6.40696274	-2.31497536	-0.21352407	H	-7.21523813	-0.50385721	-1.78320353
C	6.30440782	-1.04363215	0.34730397	H	-8.66492423	-2.50693578	-1.89652986
H	7.18674675	-0.48795344	0.64246707	H	-6.60956841	-4.18048178	1.4804559
C	4.99892795	-0.60247448	0.47468606	H	-8.36174398	-4.35612319	-0.26904552
C	4.04255329	-1.55922165	-0.00609697	C	-1.07487766	-0.32095485	0.17523801
S	4.82118575	-2.99715996	-0.60024607	C	-3.91472287	-0.13809865	0.04756154
C	2.72644615	-1.14529186	0.09169846	C	-1.77397744	0.82064813	0.66041112
C	2.56060925	0.166057	0.65744866	C	-1.86894817	-1.36440901	-0.37511916
C	1.24631997	0.55608058	0.73151963	C	-3.23486765	-1.28132059	-0.43581973
H	0.92103774	1.51139751	1.12396607	C	-3.13756875	0.91209355	0.59763108
C	0.33395853	-0.40738553	0.2419105	H	-1.22320118	1.638047	1.11041157
S	1.19718336	-1.85707391	-0.32713225	H	-1.38976483	-2.25026421	-0.77917898
N	-5.2879043	-0.04843312	-0.01348345	H	-3.79981514	-2.09091418	-0.88011144
C	-5.94927094	1.21737455	-0.00746632	H	-3.63173831	1.78951508	0.9950781
C	-7.27391039	3.66717621	-0.01472718	C	4.52795033	2.27517403	0.07624879
C	-5.5611943	2.21757075	-0.89988253	C	5.08717091	4.49896469	-1.50418432
C	-7.00562403	1.44127112	0.87554221	C	4.87964351	3.4862604	0.67155181
C	-7.66571031	2.66310457	0.86606082	C	4.45795253	2.18138112	-1.31642525
C	-6.21989737	3.44048572	-0.89477333	C	4.73661768	3.2909231	-2.10328679
H	-4.75115522	2.03099911	-1.59689835	C	5.15893942	4.59659079	-0.11893841
H	-7.30217777	0.6589703	1.56581262	H	4.93422159	3.54959045	1.75304104
H	-8.48518245	2.83287289	1.55687691	H	4.18723763	1.24101167	-1.78802514
H	-5.91487912	4.21415284	-1.59188001	H	4.68195927	3.21474007	-3.18444585
H	-7.79002961	4.62157172	-0.01726435	H	5.43319522	5.53717267	0.3479634
C	-6.1036811	-1.21855716	-0.08881386	H	5.30549697	5.3651625	-2.12091234
C	-7.72852519	-3.47650115	-0.21845769	P	4.16611226	0.85316628	1.14067721
C	-5.93553635	-2.25265646	0.83295792	O	4.36905672	1.1893707	2.59116638
C	-7.09003659	-1.31189142	-1.07056478	C	7.62625708	-3.0349128	-0.46790627
C	-7.9005559	-2.43817886	-1.12932617	H	7.50873607	-4.03964412	-0.91843028
C	-6.74353154	-3.38011927	0.76003136	O	8.74537303	-2.59650603	-0.21466368
H	-5.17859423	-2.16611813	1.60517592				

Table S8. Cartesian coordinates [Å] of the optimized structure for **3** in S₁

atom	X	Y	Z	atom	X	Y	Z
C	6.46682295	-2.30167556	-0.18772595	H	-5.12509343	-2.14852697	1.62484702
C	6.36999823	-1.03039252	0.36378098	H	-7.14469663	-0.5225214	-1.79123092
H	7.24585309	-0.46174356	0.65361434	H	-8.59676524	-2.52476085	-1.88779636
C	5.05812169	-0.59461209	0.49329249	H	-6.55844507	-4.16221661	1.51709766
C	4.1061431	-1.55843427	0.02298006	H	-8.30326391	-4.35551455	-0.23786358
S	4.88581178	-3.00072926	-0.56422204	C	-1.01251555	-0.323939	0.18801309
C	2.78801224	-1.15008812	0.11819742	C	-3.85166167	-0.14025494	0.04883384
C	2.62227951	0.16707212	0.67241566	C	-1.71219276	0.82386116	0.65773221
C	1.30755266	0.55755689	0.74062694	C	-1.80568677	-1.3734078	-0.35227022

H	0.9815924	1.51664208	1.12326263	C	-3.17132674	-1.28995642	-0.41830608
C	0.39602544	-0.41013225	0.25909652	C	-3.07536389	0.91572982	0.58930674
S	1.25932572	-1.86716518	-0.29398886	H	-1.1620373	1.64599913	1.09976975
N	-5.22432896	-0.04952821	-0.01851374	H	-1.32593049	-2.26436904	-0.74420365
C	-5.88385902	1.2172443	-0.03044755	H	-3.73557552	-2.10430761	-0.85470684
C	-7.20474168	3.66862492	-0.07282938	H	-3.57015375	1.79817049	0.97465867
C	-5.49083865	2.2058221	-0.93357104	C	4.58513311	2.28173361	0.08727653
C	-6.94322514	1.45341461	0.84570403	C	5.14170428	4.50368501	-1.49722727
C	-7.60141348	2.67601353	0.81871151	C	4.93803078	3.4937249	0.68017407
C	-6.14772876	3.4296515	-0.94599591	C	4.51258693	2.18644339	-1.30515673
H	-4.67845632	2.00948865	-1.62516124	C	4.78981359	3.2949371	-2.09407415
H	-7.24356657	0.68003957	1.54434476	C	5.21606353	4.60302296	-0.11221111
H	-8.42327618	2.85546011	1.5042191	H	4.99423518	3.55838029	1.76147712
H	-5.8389089	4.19425686	-1.65137594	H	4.24095716	1.24538217	-1.7748349
H	-7.71942186	4.62366406	-0.08906632	H	4.73300327	3.2173878	-3.17503625
C	-6.041515	-1.21929022	-0.08392752	H	5.49122061	5.5442057	0.35297838
C	-7.66900132	-3.47625372	-0.19465052	H	5.35895996	5.36908566	-2.11546496
C	-5.87880463	-2.24292029	0.85039591	P	4.22516099	0.85994717	1.15359222
C	-7.02375132	-1.3224761	-1.06881066	O	4.42785538	1.20392668	2.60266884
C	-7.83562299	-2.4482359	-1.11813031	C	7.64942049	-3.01470699	-0.44617932
C	-6.68812218	-3.37000962	0.78694568	N	8.62365602	-3.61176102	-0.66365879

5. *In vivo* Imaging

***In vivo* imaging of blood vessels in Japanese Medaka larvae**

Fish husbandry. Medaka fish were maintained in freshwater tanks with a water circulating system (LABREED, IWAKI Inc.) at 26–28 °C under the condition of 14 h light and 10 h dark cycle (8:30–22:30 light). Fish were fed artemia larvae and powdered diet daily. The spawned eggs were collected in the morning, and eggs were incubated at 28 °C in a dish filled with diluted artificial sea water (0.03 (w/v)%) containing methylene blue. The transparent Medaka strain See-Through II (STII) strain (StrainID: MT112) were supplied by NBRP Medaka (<https://shigen.nig.ac.jp/medaka/>). All experiments were conducted in accordance with the guidelines of the ethics committee for animal experiments of Ehime University.

Preparation of medaka embryos and larvae. For observation, we embedded fish samples into 1 (w/v)% agarose gel set in the glass bottom dish. Living larvae, 2–3 weeks after hatching, were first anesthetized by cold water, then embedded in the agarose gel.

For labeling of bloods, an appropriate amount of 1 mM DMSO solution of **1c** was injected into the peritoneal cavity using a microinjection technique. The microinjection was performed using the pneumatic microinjector (IM-11-2, Narishige Inc.) and the homemade micro-glass needles under the stereomicroscope (M205 FA, Leica Inc.).

***In vivo* deep imaging of blood vessels in mice**

Materials and methods. Young adult (4 weeks-old) ICR mouse for *in vivo* imaging were used in this study. All mice were housed with food and water *ad libitum* on a 12:12 light-dark cycle (lights on from 08:00 to 20:00) with controlled temperature and humidity. All animal experiments were approved by the Ethics Committee for Animal Experiments of Ehime University (#05-RE-4-16). The experimental procedures we employed were conducted in accordance with the approved guidelines. A sample solution for injection was prepared as follows: 3.6 mg of bovine serum albumin (BSA) was dissolved in 180 µL of phosphate-buffered saline (PBS), to which 40 µL of 5 mM DMSO solution of **1c** was added to give 0.9 mM of the dye in PBS containing 1.6% BSA (w/w) and 18% DMSO (v/v). The absence of precipitation under these conditions was confirmed by dynamic light scattering (DLS) measurements.

Cranial window for *in vivo* imaging. For high-resolution imaging of blood vessels in the cortex of living mice, the overlying opaque skull bone must be partially removed to make a cranial window, the “open-skull” glass window. In the open-skull preparation, a piece of the cranial bone (about 3 mm in diameter) is removed, leaving the dura intact, and the exposed brain is covered with a thin glass cover slip (for detailed methods, see published protocols²¹⁻²³).

Image acquisition. The fluorescence images of medaka larvae were measured using the upright confocal microscope (A1R+, Nikon), equipped with multi-immersion objective lens (10×, NA0.5, CFI Plan Apochromat 10XC Glyc, Nikon). Multi z-stack images were acquired with 3-μm Z-steps, and then individual z-stack images were stitched as a whole image. The image stitching was performed using NIS elements software (Nikon). The field of view for each image was 1.24 × 1.24 mm with 512 × 512 pixels(1.21 μ m/pixel).

In the case of mouse brain imaging, fluorescence image stacks consisting of over 46 optical sections with 3-μm Z-steps were acquired from the deep region, an area covering 500 × 500 μm (512 × 512 pixels, 0.994 μm/pixel). These images were obtained using a Two-photon laser scanning microscope customized for *in vivo* imaging (A1R MP+, confocal microscope, Nikon, with MaiTai DeepSee eHP, Spectra Physics) with a 25× water immersion objective lens (NA 1.10). Fluorescence signals with wavelengths of 500–550 and 601–657 nm were detected via the GaAsP and multi-alkali PMT, respectively.

Image processing

Three dimensional image reconstruction was performed with a volume-rendering method using Imaris software (Bitplane).

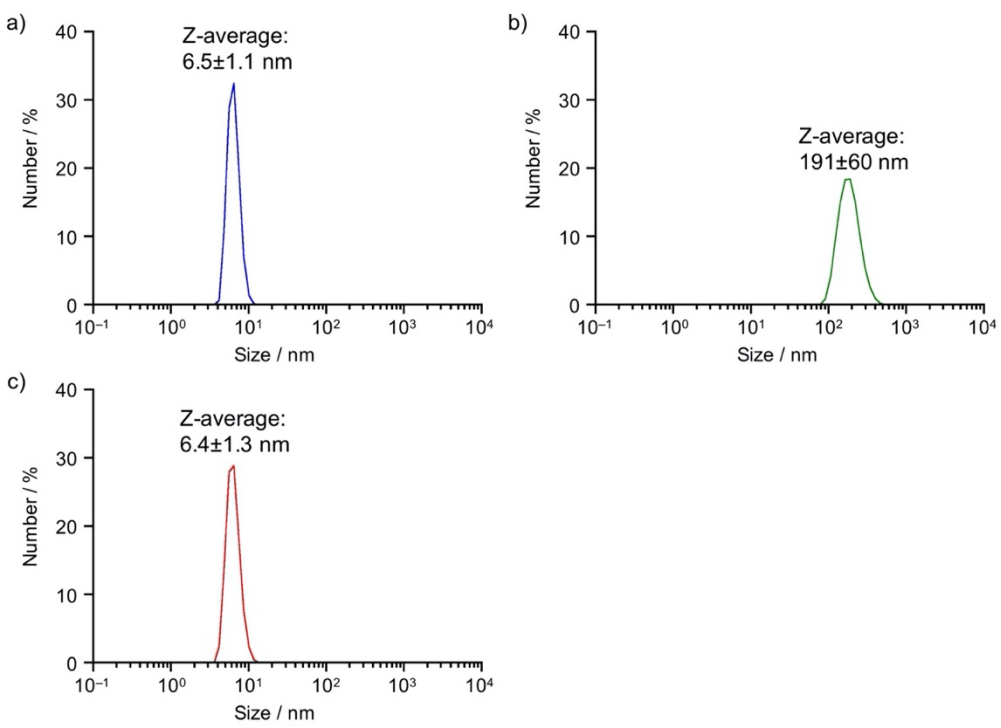


Figure S17. Dynamic light scattering (DLS) measurements of (a) bovine serum albumin (BSA, 2% w/w), (b) **1c** without BSA, and (c) **1c** with BSA in phosphate buffered saline (PBS) at pH 7.4. To 3 mL PBS with or without BSA, 15 μ M DMSO solution of **1c** (1mM) was added and gently stirred for 4 h.

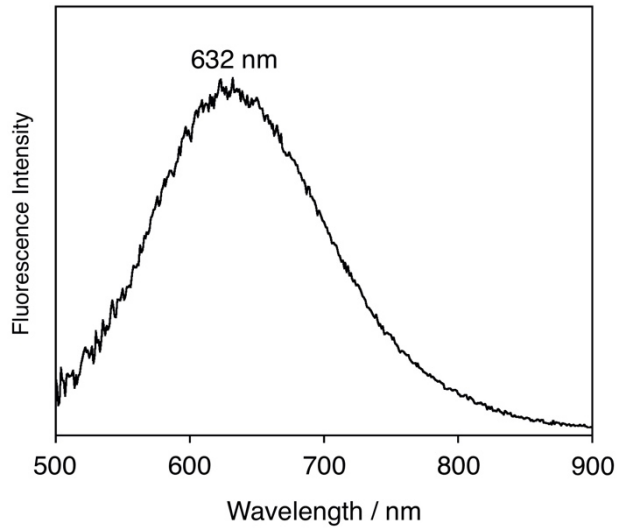


Figure S18. Emission spectrum of **1c** in PBS containing 0.5% DMSO (v/v) and 2% BSA (w/w).

6. References

1. Y. Dienes, S. Durben, T. Karpati, T. Neumann, U. Englert, L. Nyulaszi and T. Baumgartner, *Chem.–Eur. J.*, 2007, **13**, 7487–7500.
2. J. J. Eisch, B. Shafii, J. D. Odom and A. L. Rheingold, *J. Am. Chem. Soc.*, 1990, **112**, 1847–1853.
3. M. K. R. Fischer, S. Wenger, M. Wang, A. Mishra, S. M. Zakeeruddin, M. Grätzel and P. Bäuerle, *Chem. Mater.*, 2010, **22**, 1836–1845.
4. M. Ito, E. Ito, M. Hirai and S. Yamaguchi, *J. Org. Chem.*, 2018, **83**, 8449–8456.
5. Z. Zhang, R. M. Edkins, J. Nitsch, K. Fucke, A. Eichhorn, A. Steffen, Y. Wang and T. B. Marder, *Chem.–Eur. J.*, 2015, **21**, 177–190.
6. T. Sumi, Y. Takagi, A. Yagi, M. Morimoto and M. Irie, *Chem. Commun.*, 2014, **50**, 3928–3930.
7. H. Sotome, T. Nagasaka, K. Une, C. Okui, Y. Ishibashi, K. Kamada, S. Kobatake, M. Irie and H. Miyasaka, *J. Phys. Chem. Lett.*, 2017, **8**, 3272–3276.
8. M. Hanazawa, R. Sumiya, Y. Horikawa and M. Irie, *J. Chem. Soc., Chem. Commun.*, 1992, 206–207.
9. M. J. Frisch, G. W. Trucks, H. B. Schlegel, G. E. Scuseria, M. A. Robb, J. R. Cheeseman, G. Scalmani, V. Barone, G. A. Petersson, H. Nakatsuji *et al.*, *Gaussian 16, Revision B.01*, Gaussian Inc., Wallingford CT, 2016.
10. T. Yanai, D. P. Tew and N. C. Handy, *Chem. Phys. Lett.*, 2004, **393**, 51–57.
11. R. Ditchfield, W. J. Hehre and J. A. Pople, *J. Chem. Phys.*, 1971, **54**, 724–728.
12. W. J. Hehre, R. Ditchfield and J. A. Pople, *J. Chem. Phys.*, 1972, **56**, 2257–2261.
13. P. C. Hariharan and J. A. Pople, *Theor. Chim. Acta.*, 1973, **28**, 213–222.
14. J. D. Dill and J. A. Pople, *J. Chem. Phys.*, 1975, **62**, 2921–2923.
15. M. M. Franci, W. J. Pietro, W. J. Hehre, J. S. Binkley, M. S. Gordon, D. J. DeFrees and J. A. Pople, *J. Chem. Phys.*, 1982, **77**, 3654.
16. G. Scalmani and M. J. Frisch, *J. Chem. Phys.*, 2010, **132**, 114110.
17. Y. Niu, W. Li, Q. Peng, H. Geng, Y. Yi, L. Wang, G. Nan, D. Wang and Z. Shuai, *Mol. Phys.*, 2018, **116**, 1078–1090.
18. X. Gao, S. Bai, D. Fazzi, T. Niehaus, M. Barbatti and W. Thiel, *J. Chem. Theory Comput.*, 2017, **13**, 515–524.
19. Q. Peng, Y. Niu, Q. Shi, X. Gao and Z. Shuai, *J. Chem. Theory Comput.*, 2013, **9**, 1132–1143.
20. T. J. Penfold, E. Gindensperger, C. Daniel and C. M. Marian, *Chem. Rev.*, 2018, **118**, 6975–7025.
21. W. Denk, J. H. Strickler and W. W. Webb, *Science*, 1990, **248**, 73.
22. R. Mostany and C. Portera-Cailliau, *J. Vis. Exp.*, 2008, DOI: doi:10.3791/680, e680.

23. R. Kawakami, K. Sawada, A. Sato, T. Hibi, Y. Kozawa, S. Sato, H. Yokoyama and T. Nemoto, *Sci. Rep.* 2013, **3**, 1014.

7. NMR Spectra for New Compounds

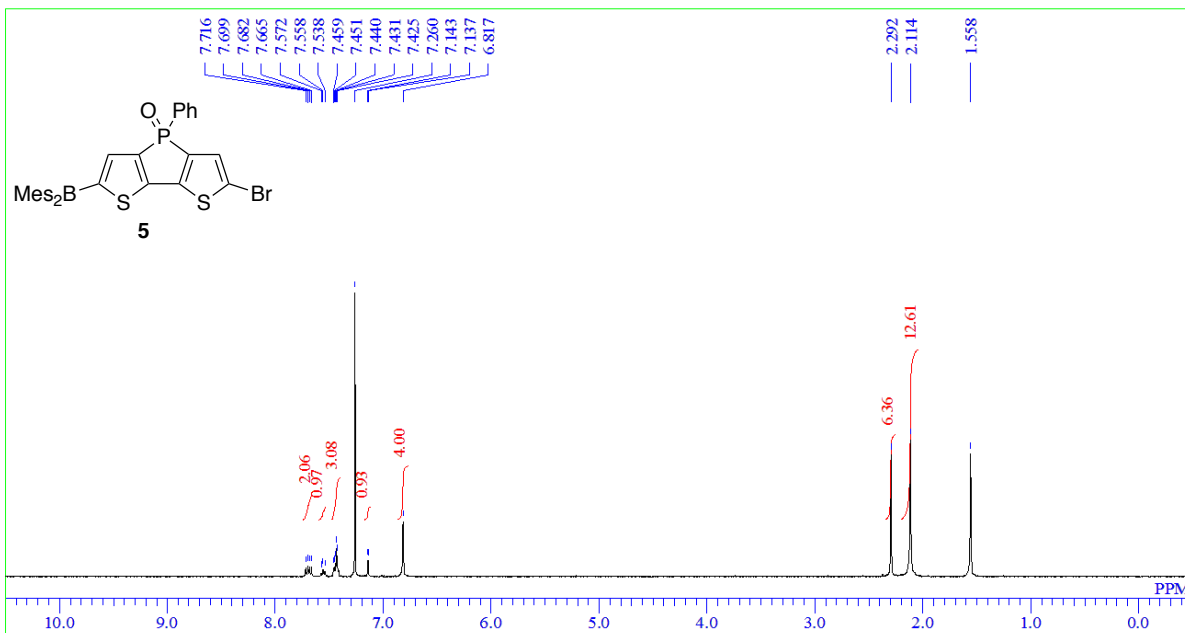


Figure S19. ^1H NMR spectrum of **5** (400 MHz, CDCl_3).

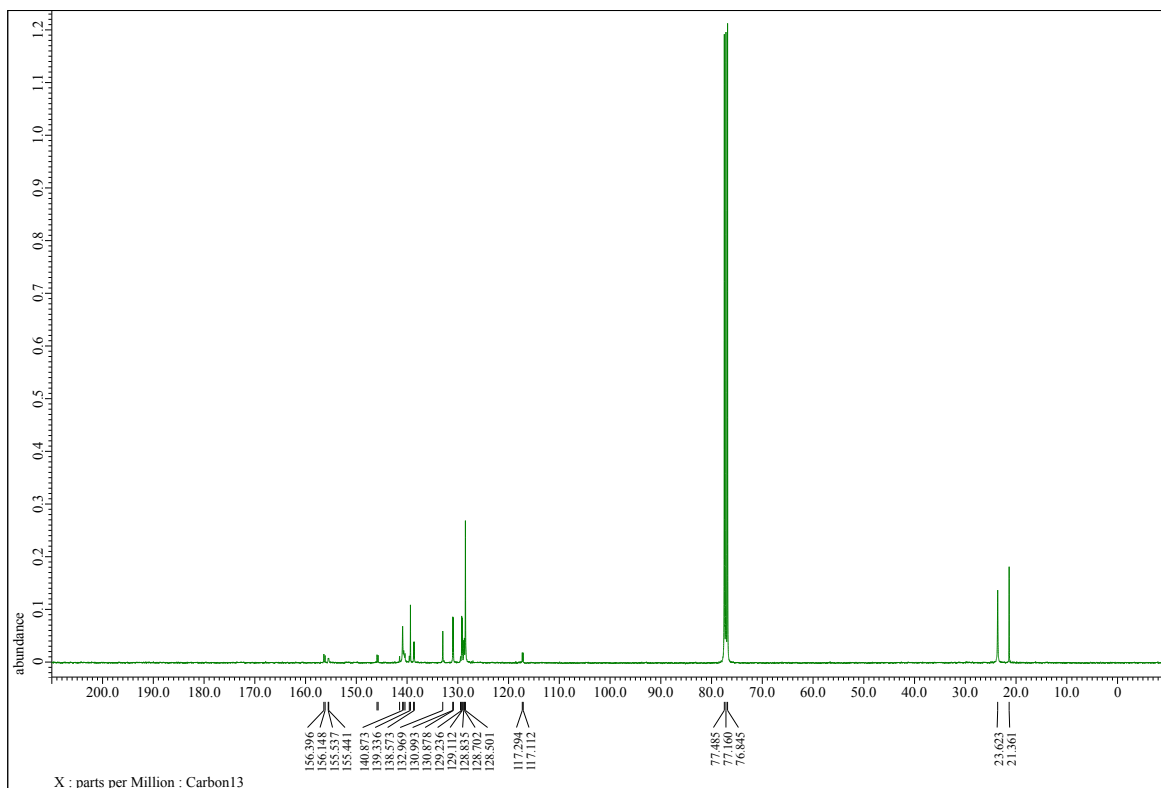


Figure S20. ^{13}C NMR spectrum of **5** (100 MHz, CDCl_3).

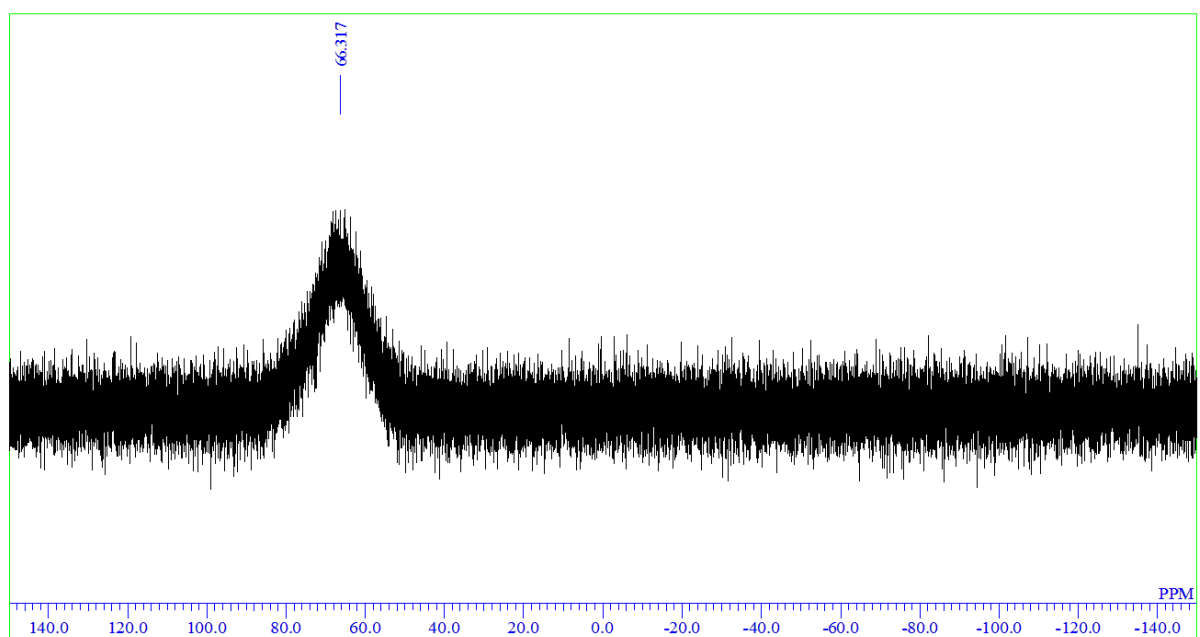


Figure S21. ^{11}B NMR spectrum of **5** (128 MHz, CDCl_3).

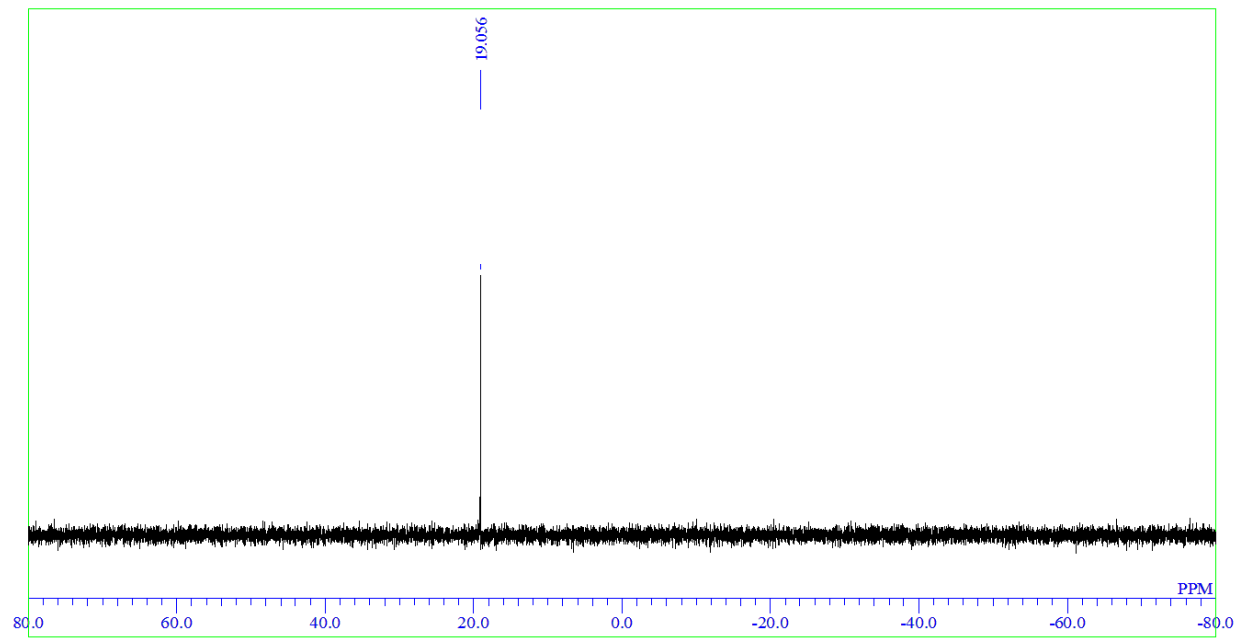


Figure S22. ^{31}P NMR spectrum of **5** (162 MHz, CDCl_3).

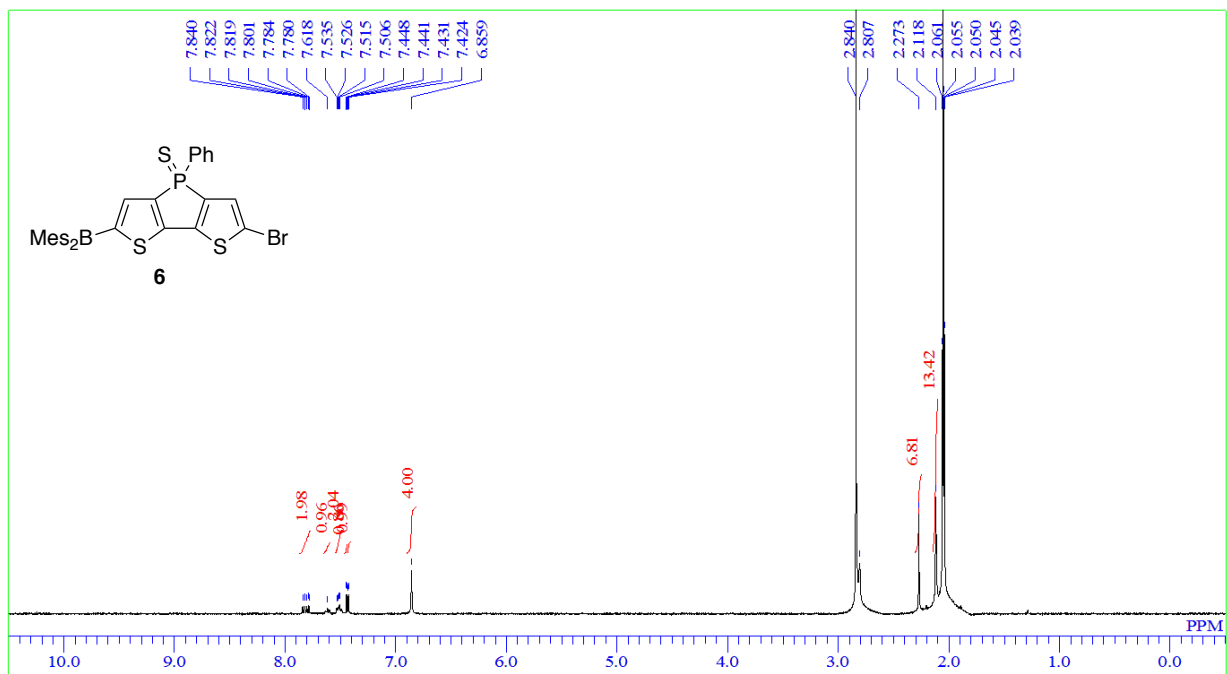


Figure S23. ^1H NMR spectrum of **6** (400 MHz, acetone- d_6).

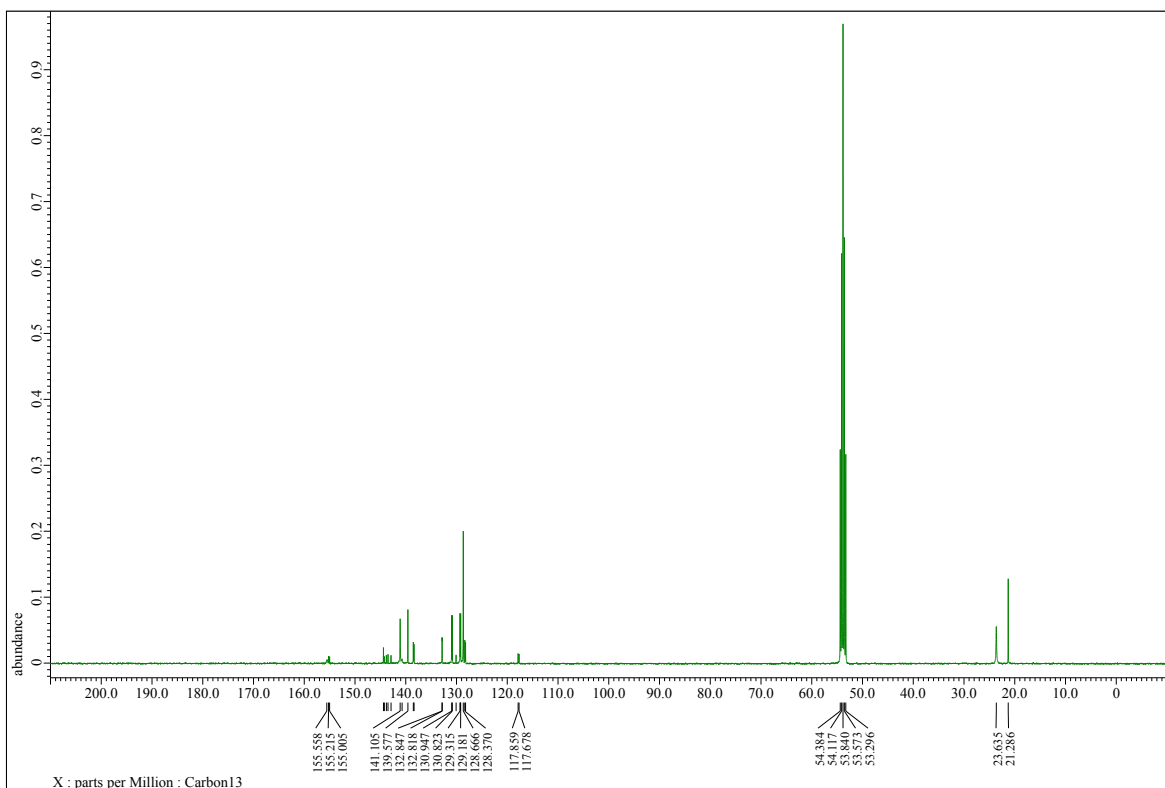


Figure S24. ^{13}C NMR spectrum of **6** (100 MHz, CD_2Cl_2).

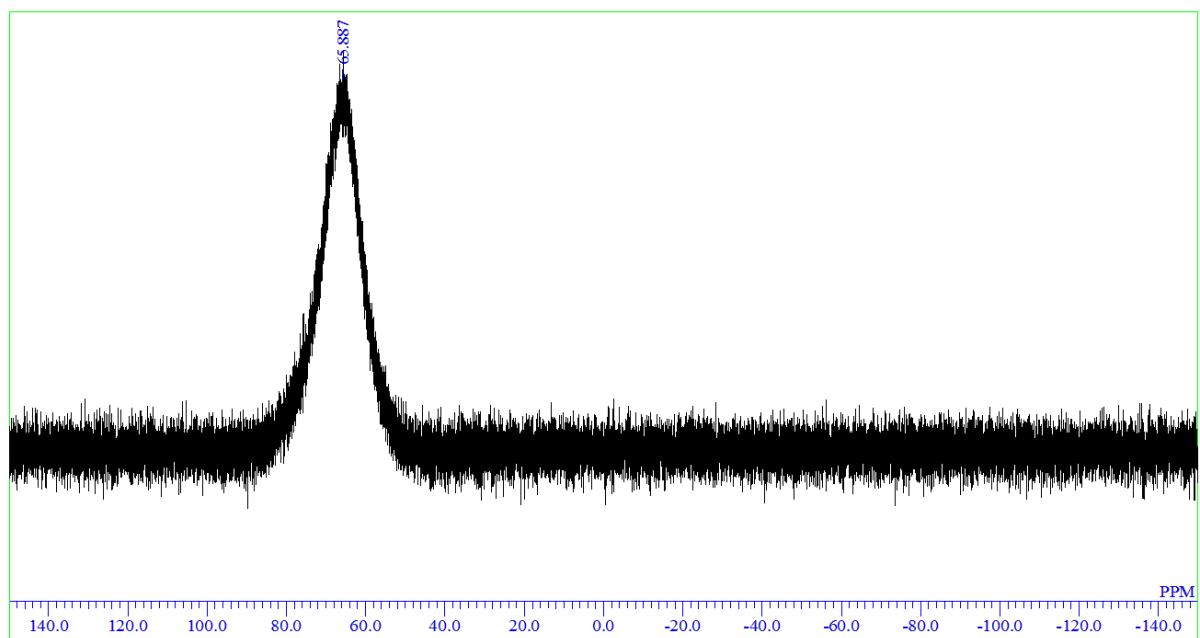


Figure S25. ^{11}B NMR spectrum of **6** (128 MHz, CD_2Cl_2).

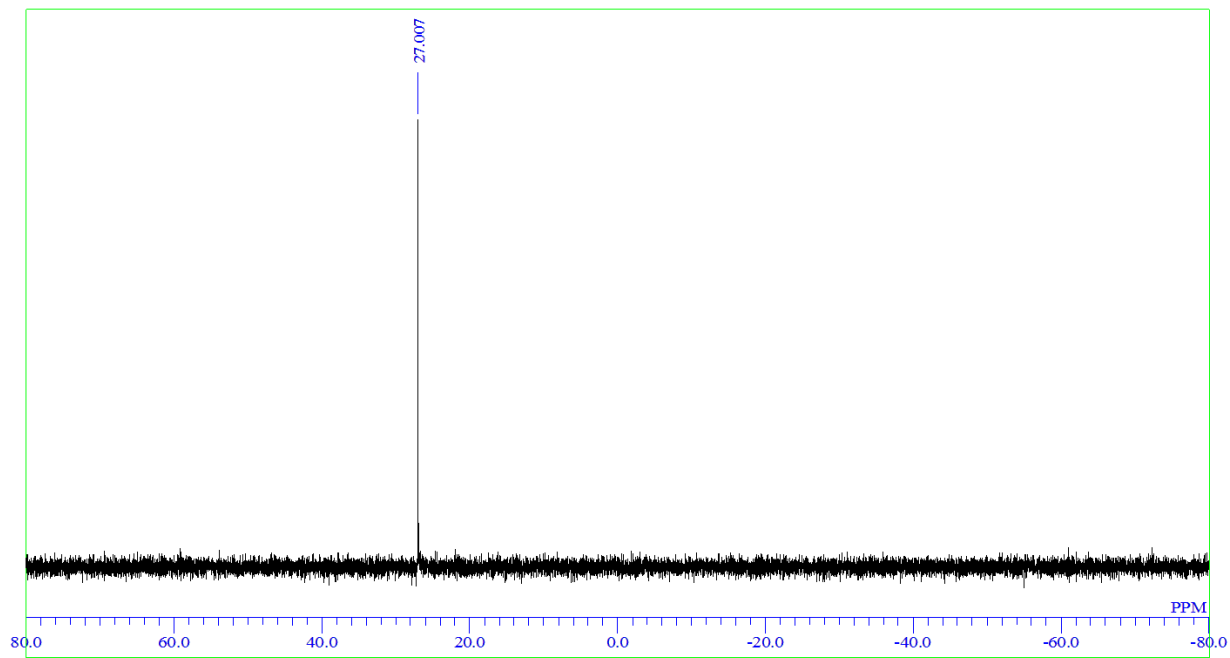


Figure S26. ^{31}P NMR spectrum of **6** (162 MHz, CDCl_3).

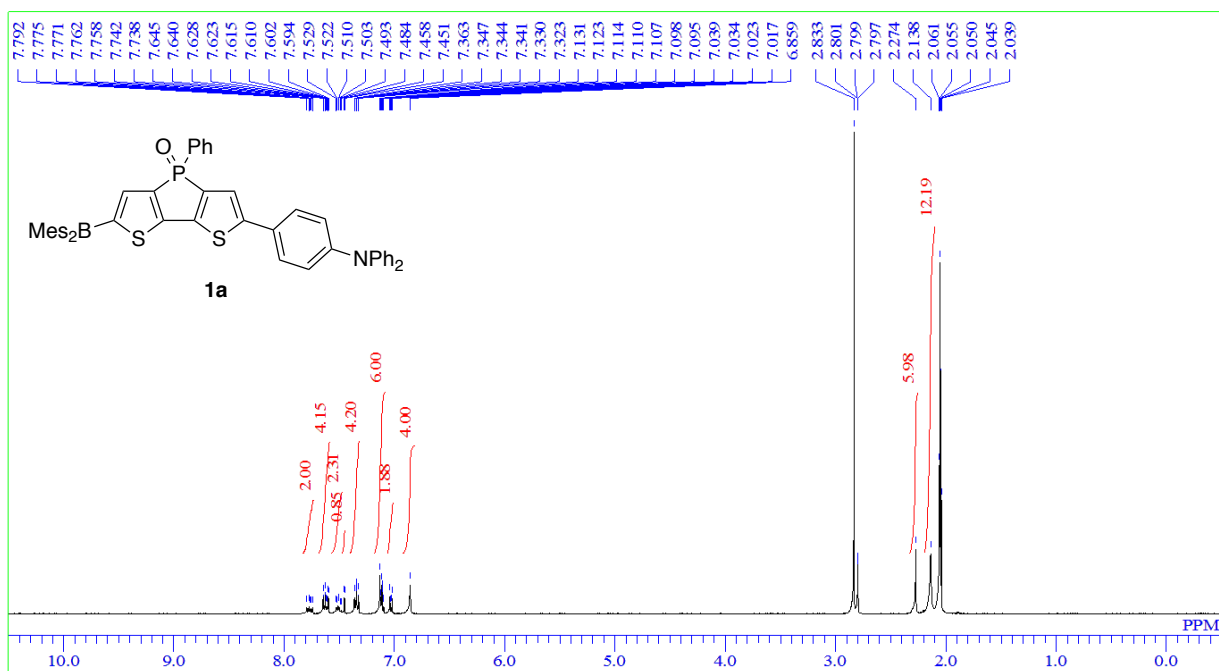


Figure S27. ^1H NMR spectrum of **1a** (400 MHz, acetone- d_6).

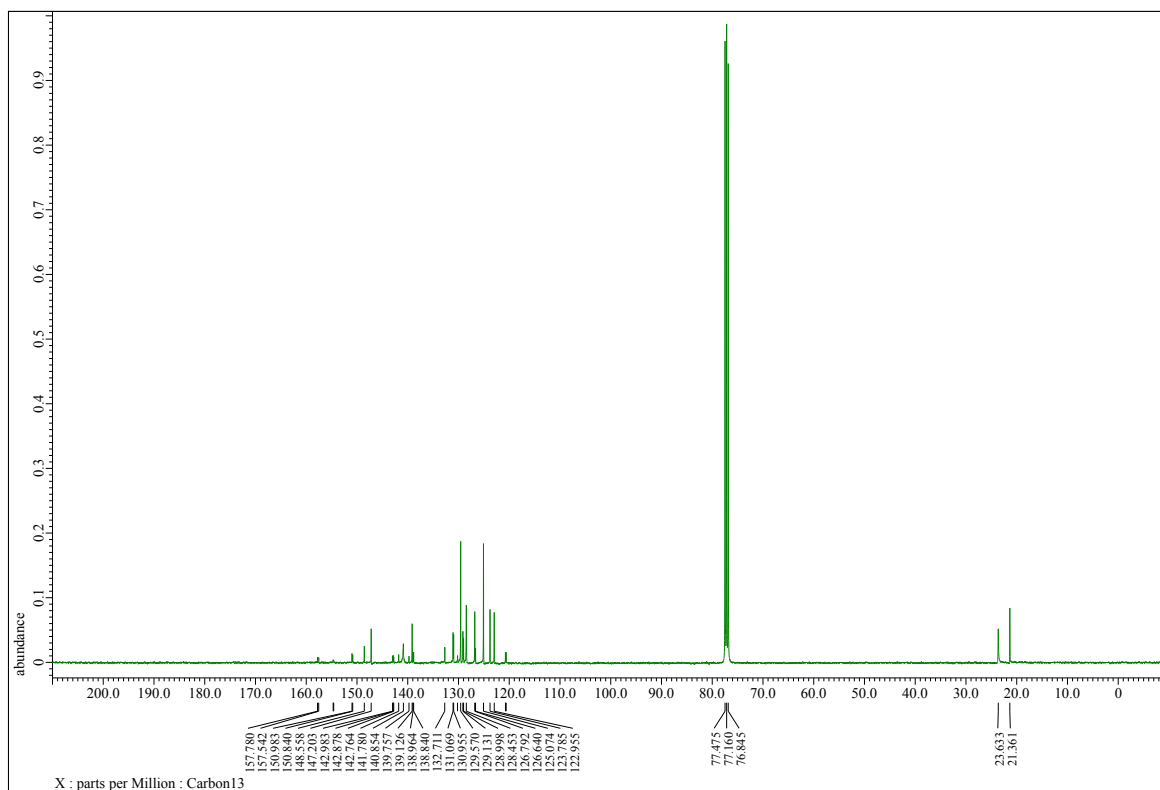


Figure S28. ^{13}C NMR spectrum of **1a** (100 MHz, CDCl_3).

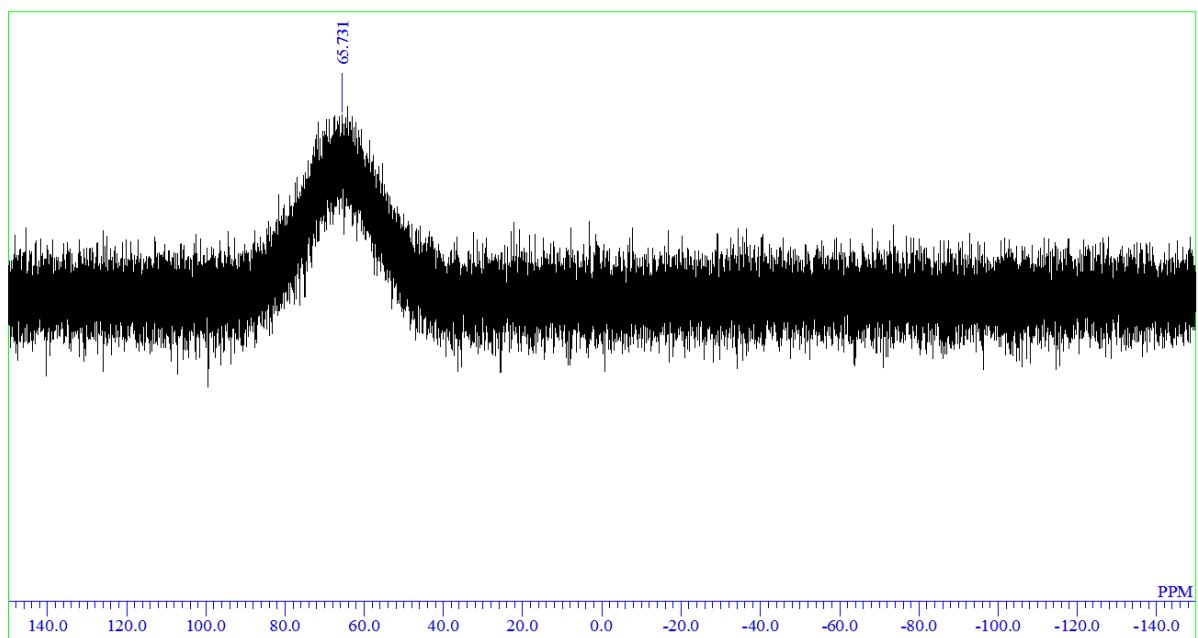


Figure S29. ^{11}B NMR spectrum of **1a** (128 MHz, CDCl_3).

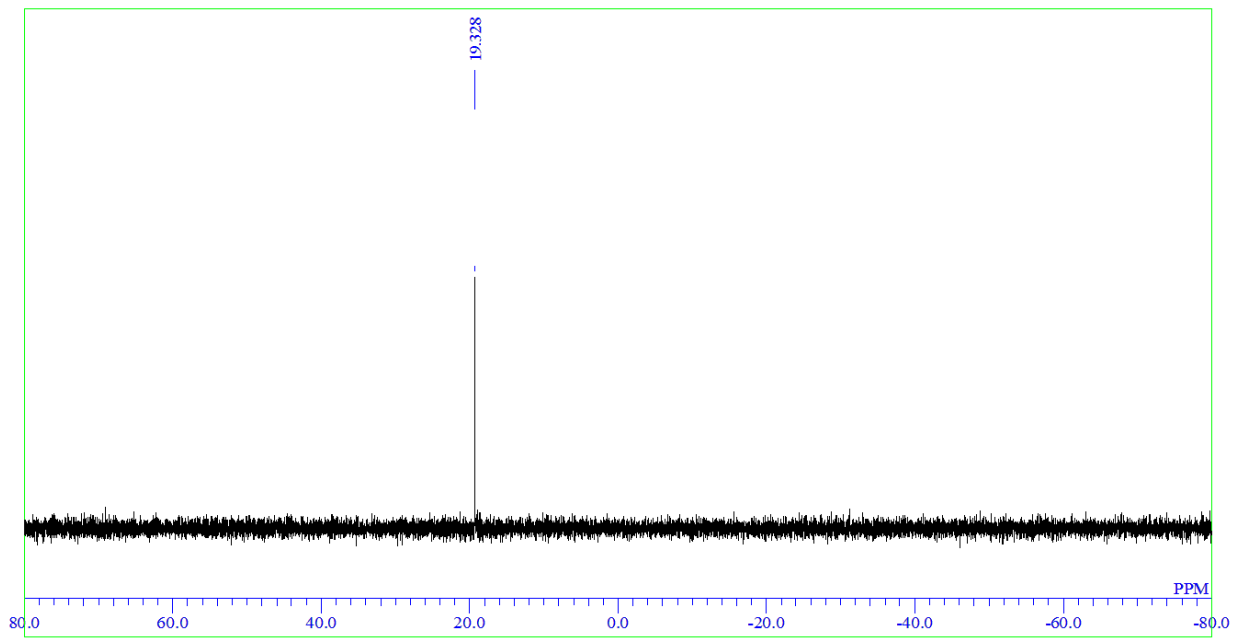


Figure S30. ^{31}P NMR spectrum of **1a** (162 MHz, CDCl_3).

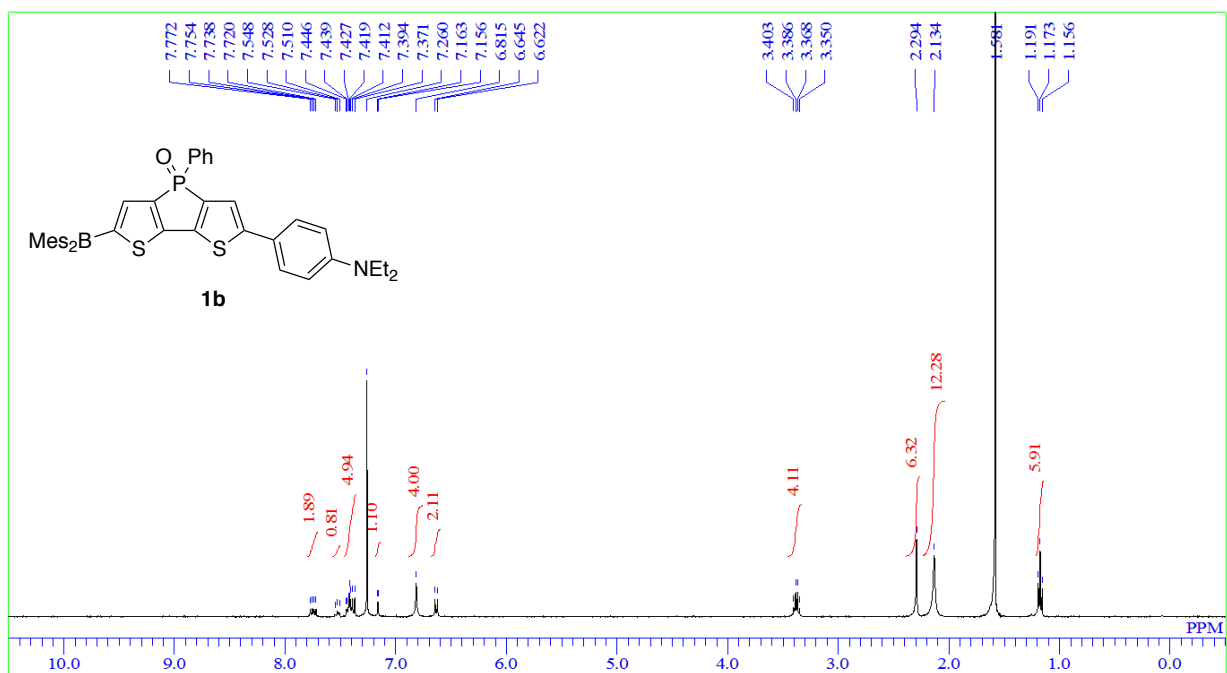


Figure S31. ^1H NMR spectrum of **1b** (400 MHz, CDCl_3).

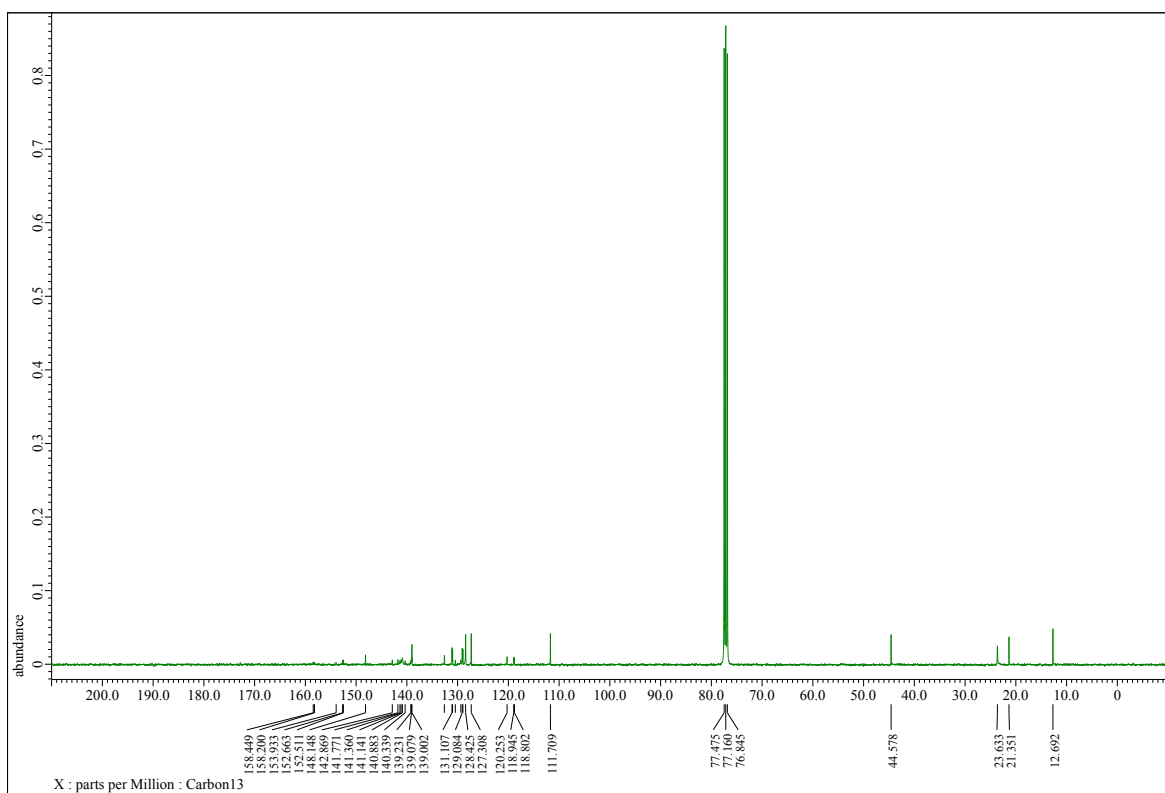


Figure S32. ^{13}C NMR spectrum of **1b** (100 MHz, CDCl_3).

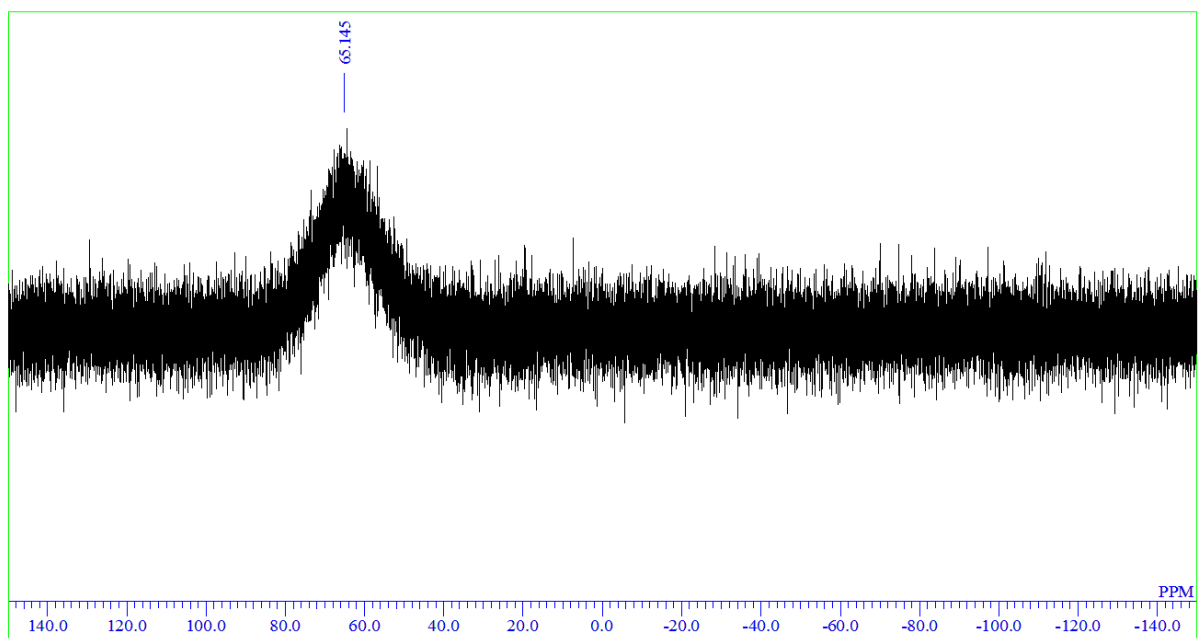


Figure S33. ^{11}B NMR spectrum of **1b** (128 MHz, CDCl_3).

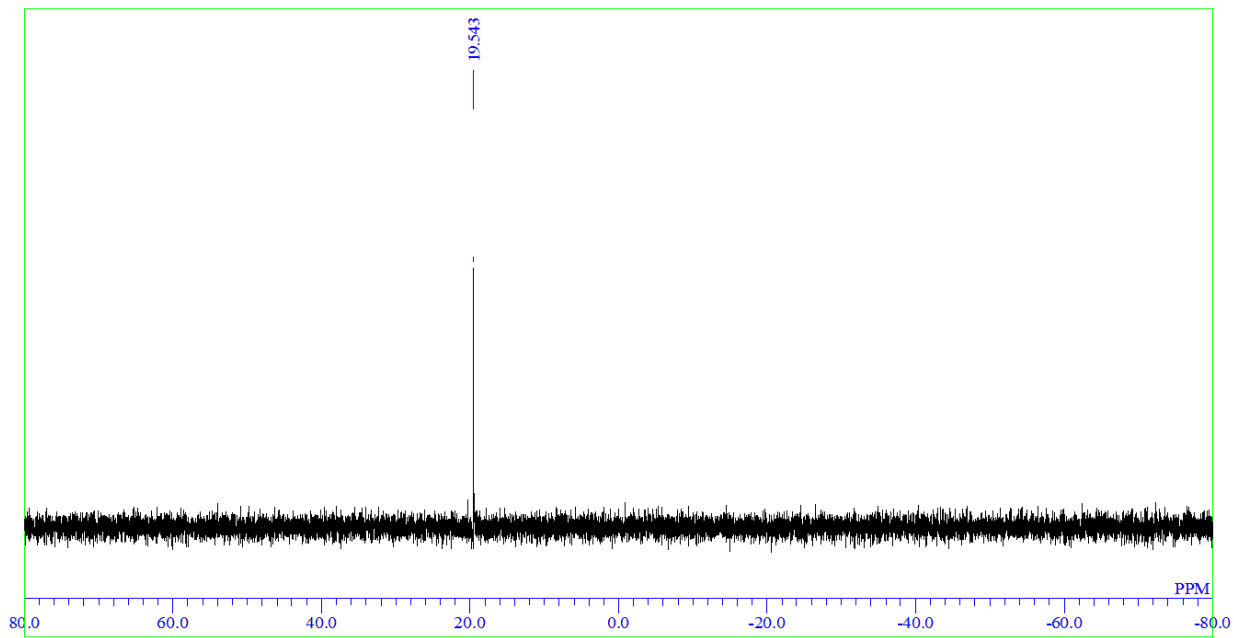


Figure S34. ^{31}P NMR spectrum of **1b** (162 MHz, CDCl_3).

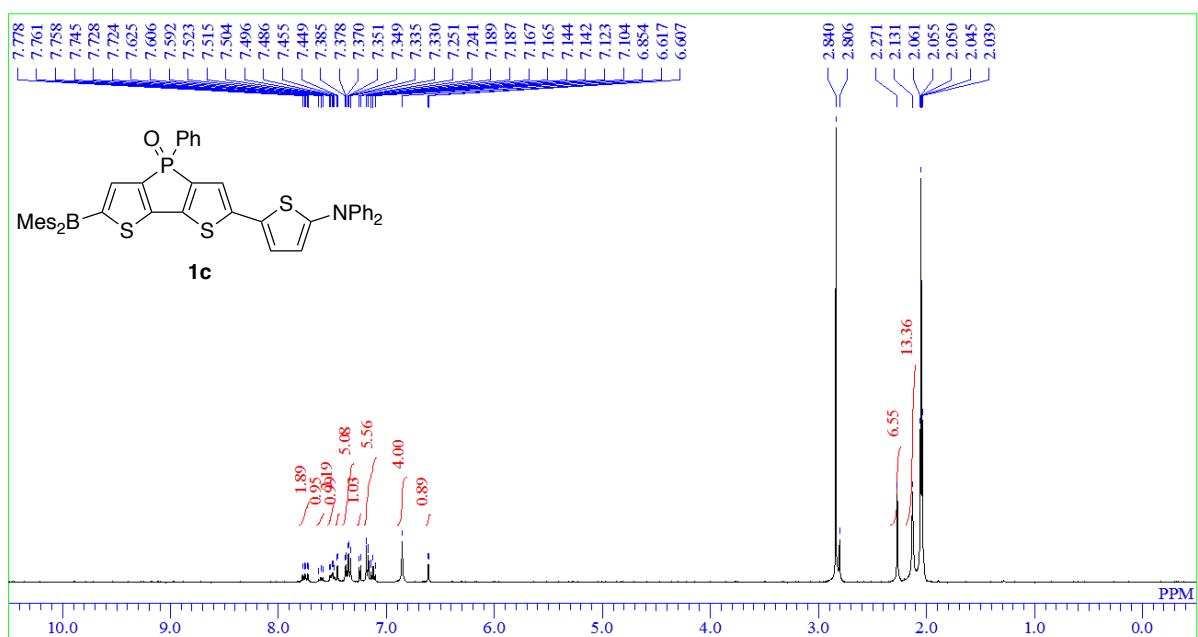


Figure S35. ^1H NMR spectrum of **1c** (400 MHz, acetone- d_6).

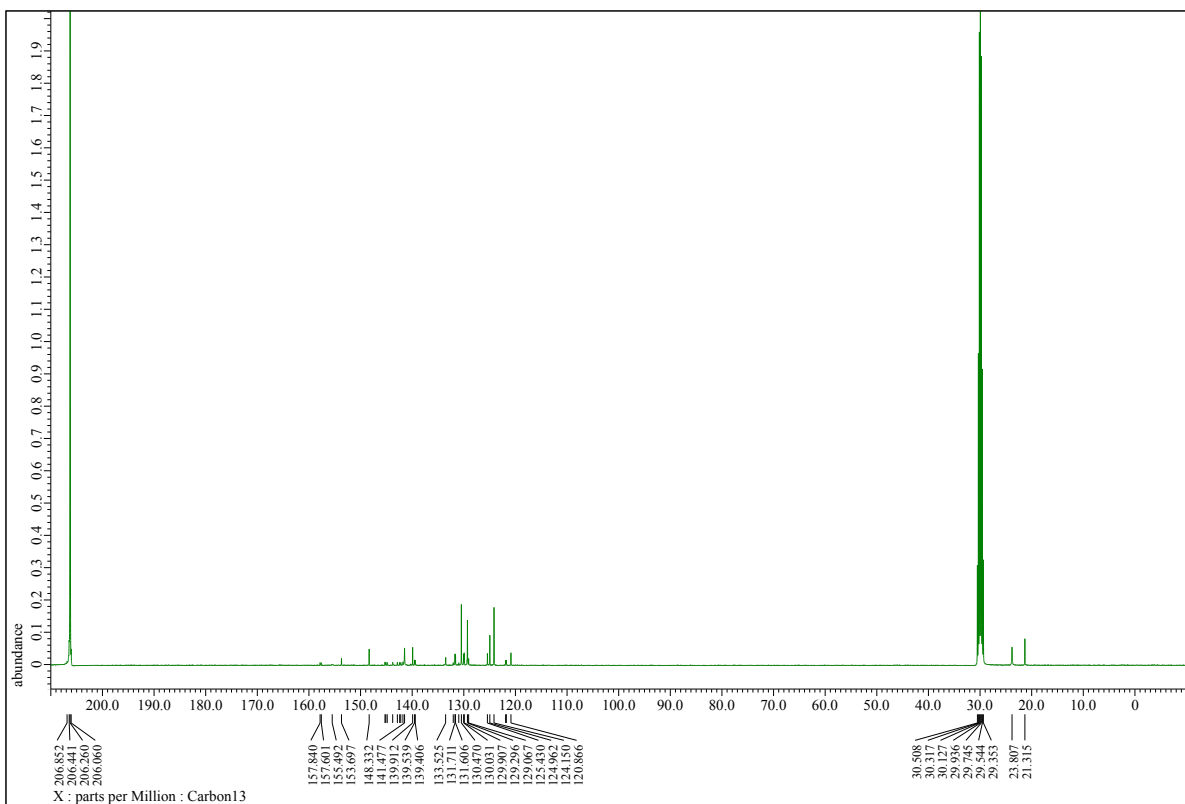


Figure S36. ^{13}C NMR spectrum of **1c** (100 MHz, acetone- d_6).

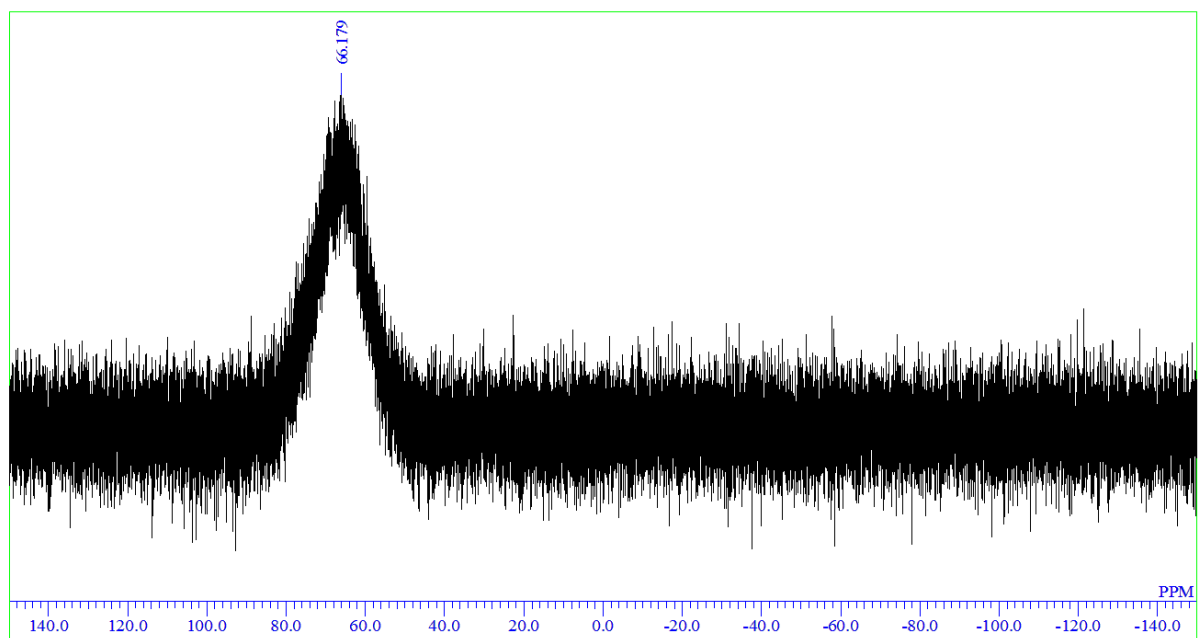


Figure S37. ^{11}B NMR spectrum of **1c** (128 MHz, acetone- d_6).

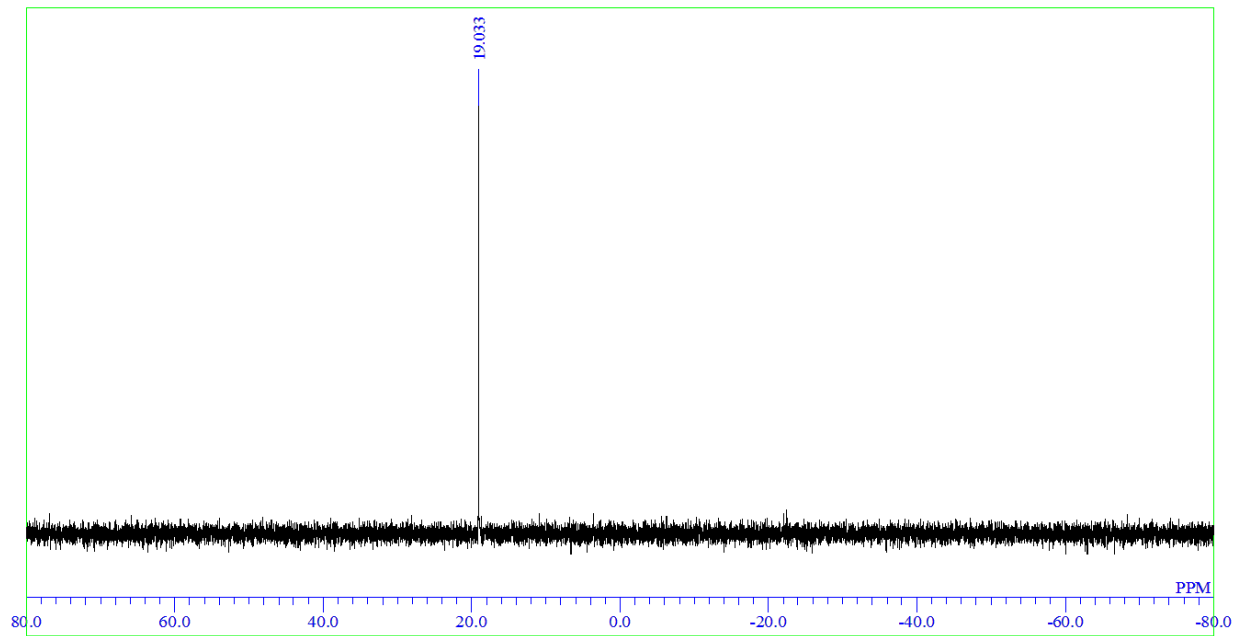


Figure S38. ^{31}P NMR spectrum of **1c** (162 MHz, CDCl_3).

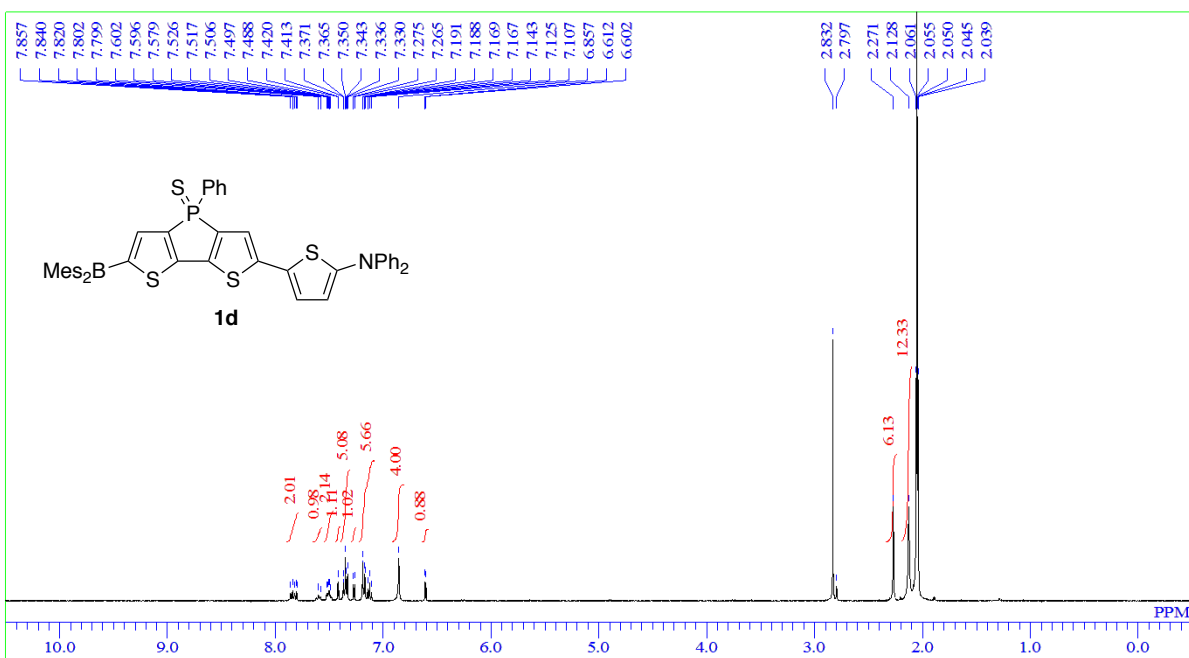


Figure S39. ^1H NMR spectrum of **1d** (400 MHz, acetone- d_6).

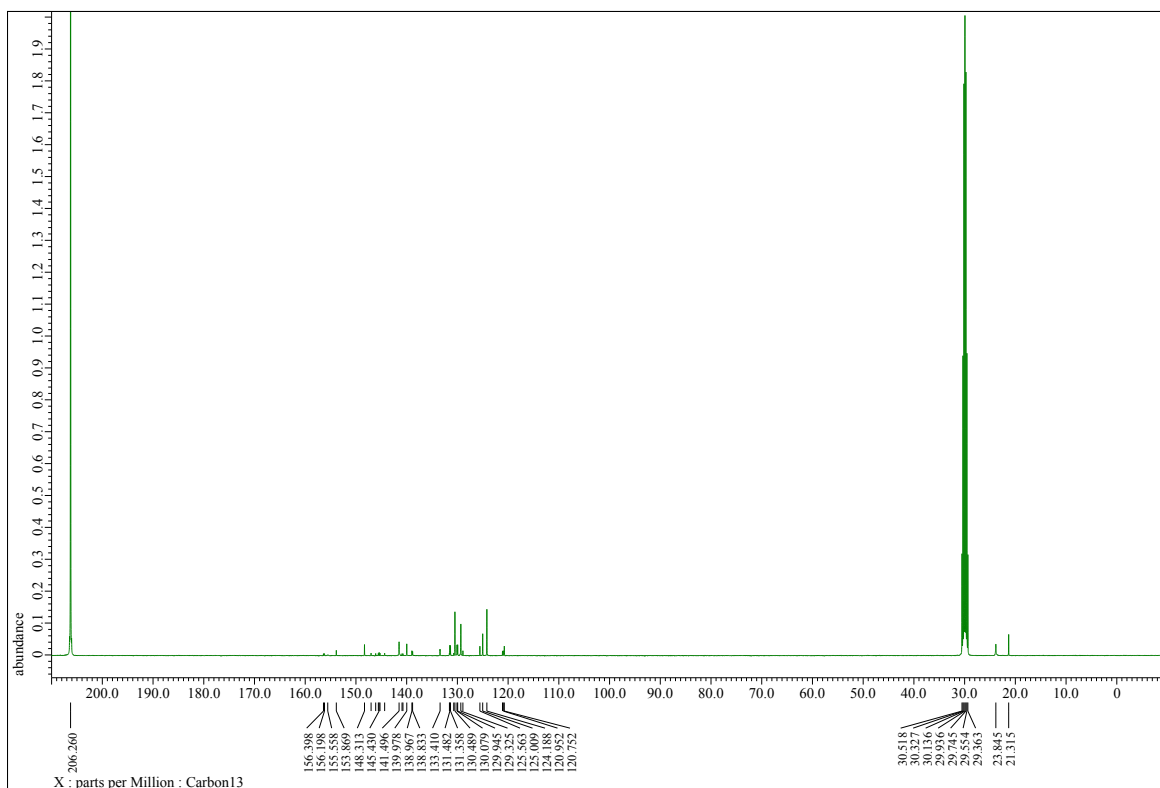


Figure S40. ^{13}C NMR spectrum of **1d** (100 MHz, acetone- d_6).

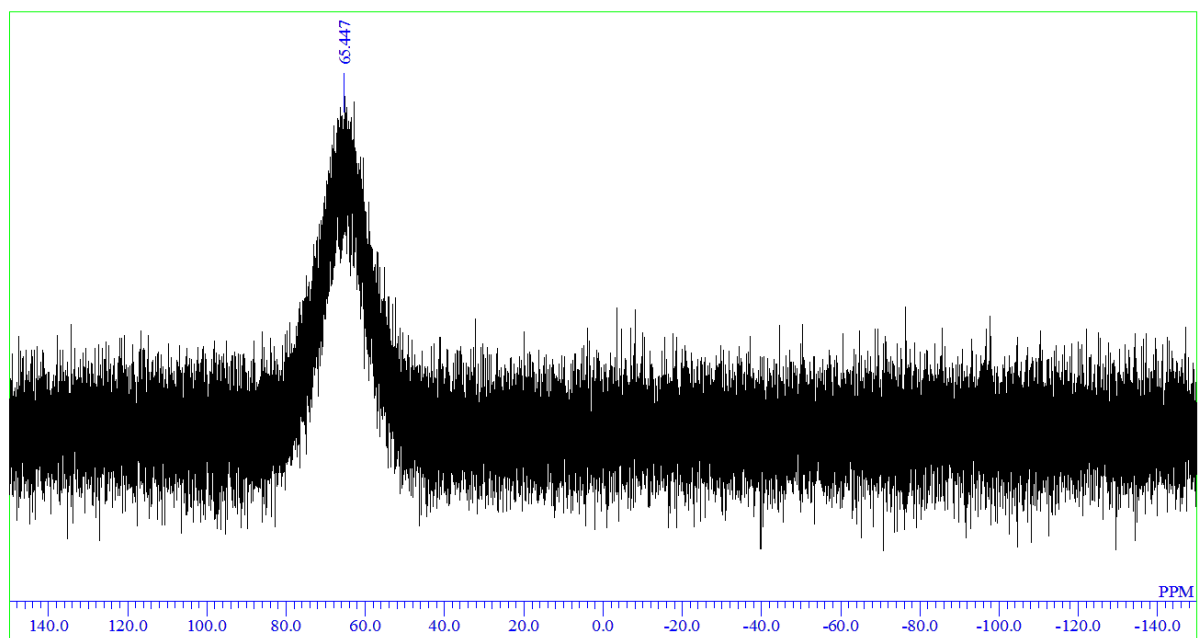


Figure S41. ^{11}B NMR spectrum of **1d** (128 MHz, acetone- d_6).

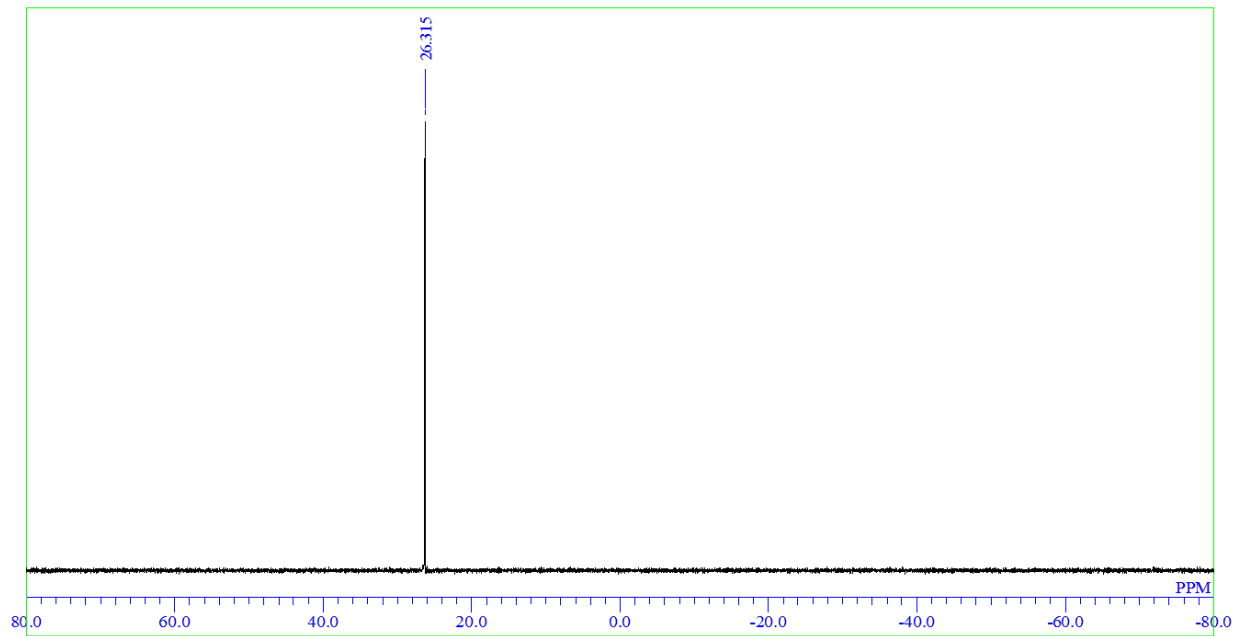


Figure S42. ^{31}P NMR spectrum of **1d** (162 MHz, CDCl_3).

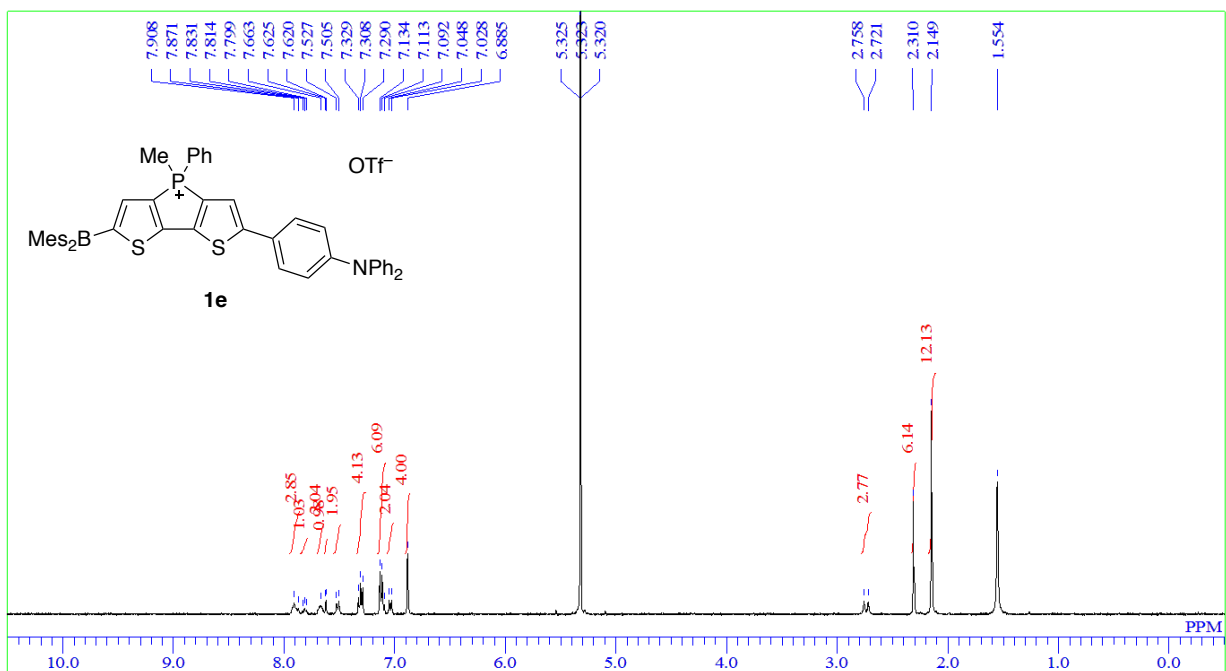


Figure S43. ^1H NMR spectrum of **1e** (400 MHz, CD_2Cl_2).

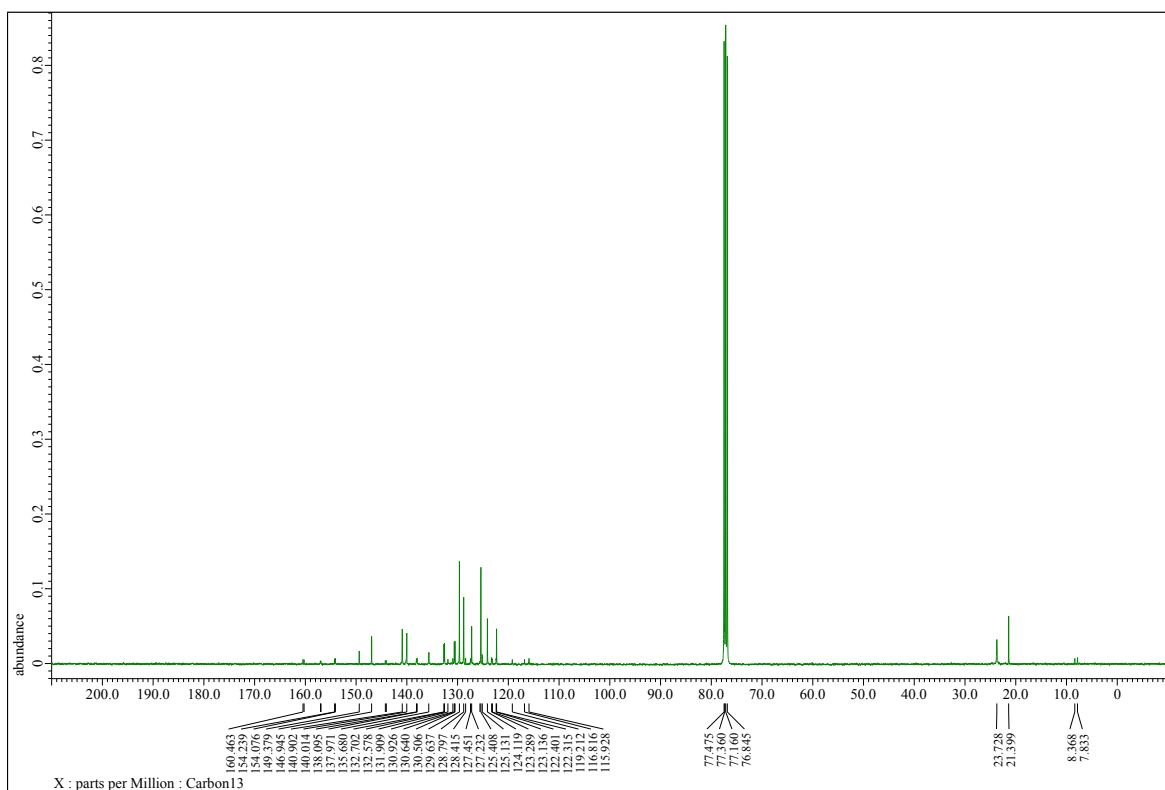


Figure S44. ^{13}C NMR spectrum of **1e** (100 MHz, CDCl_3).

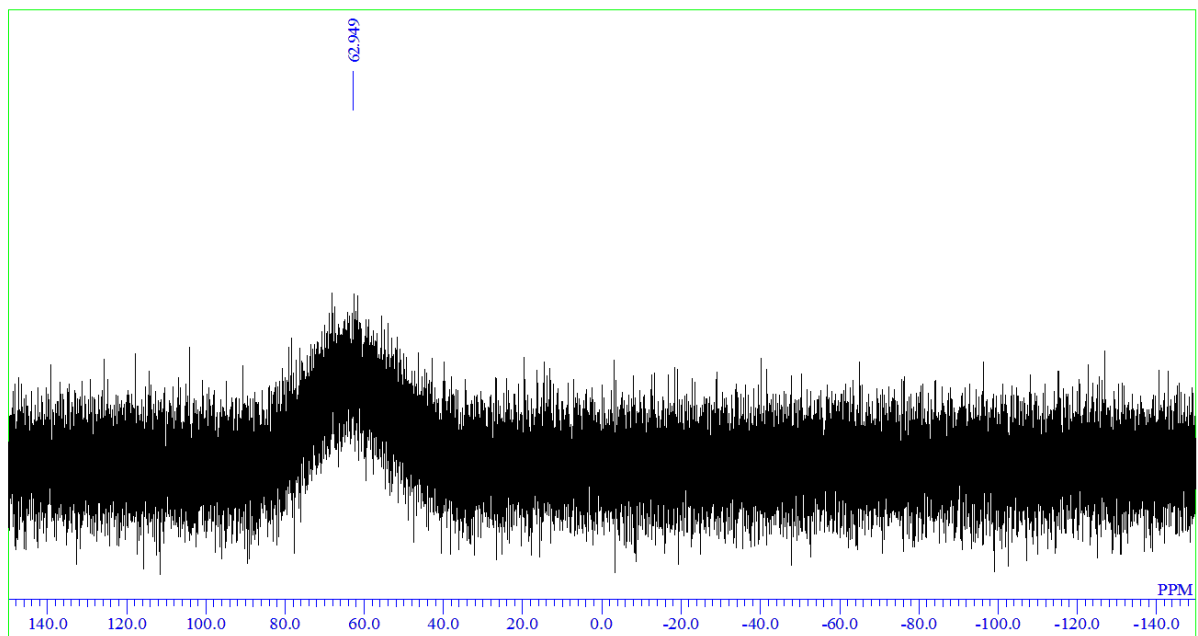


Figure S45. ^{11}B NMR spectrum of **1e** (128 MHz, CDCl_3).

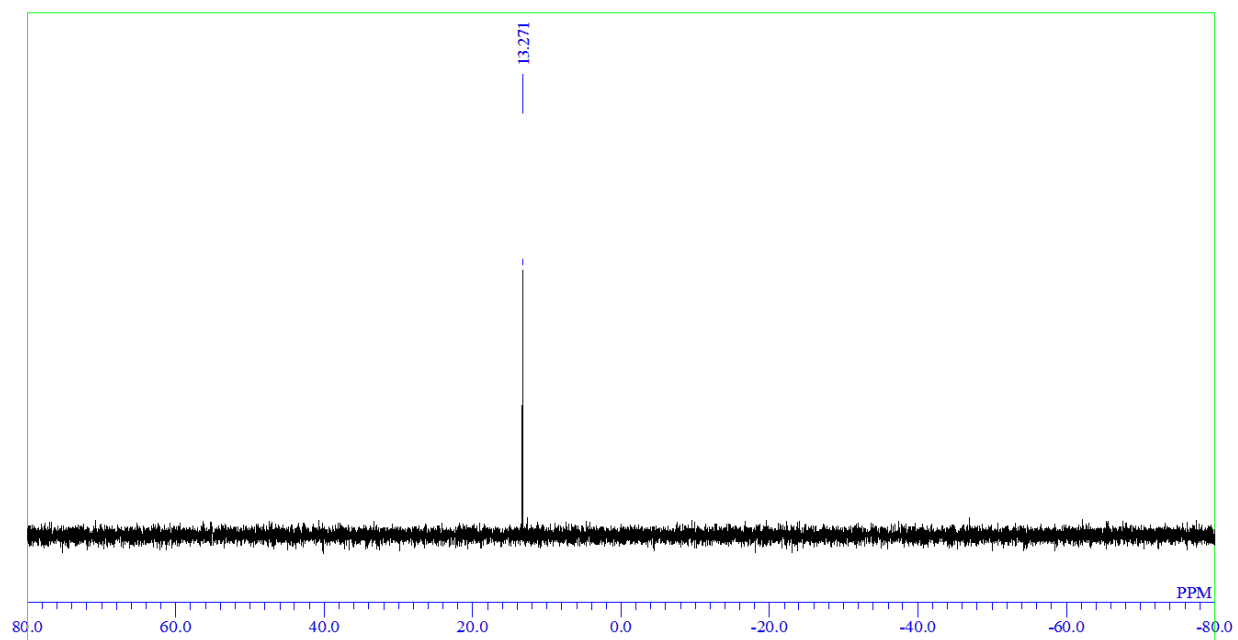


Figure S46. ^{31}P NMR spectrum of **1e** (162 MHz, CDCl_3).

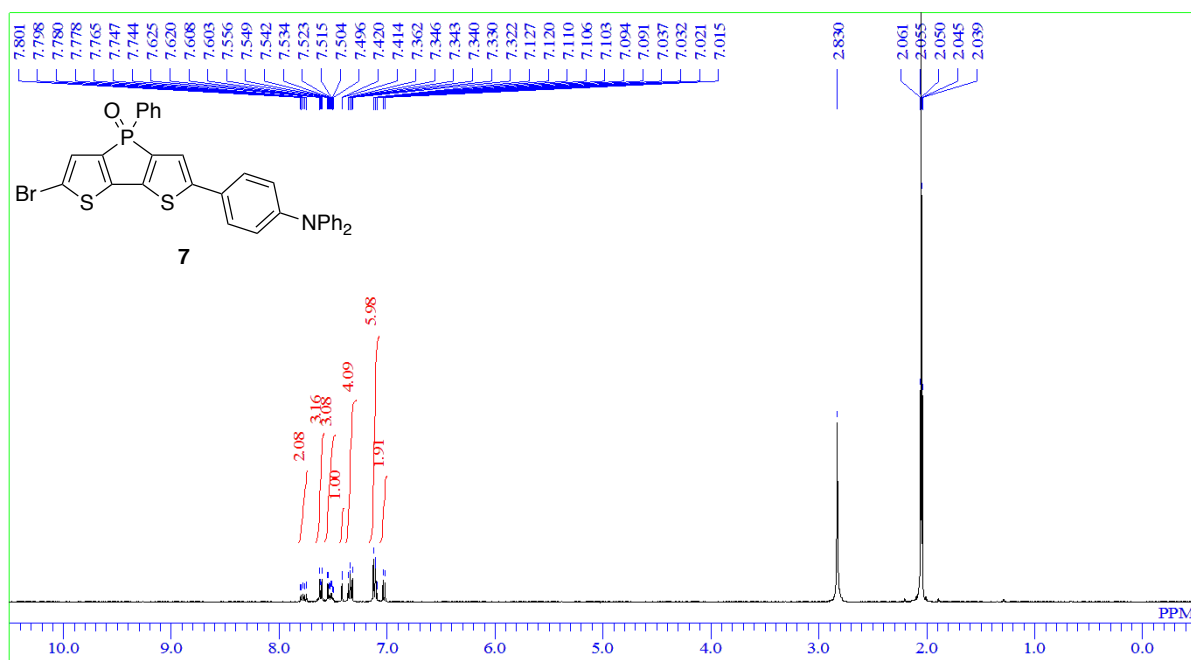


Figure S47. ^1H NMR spectrum of **7** (400 MHz, acetone- d_6).

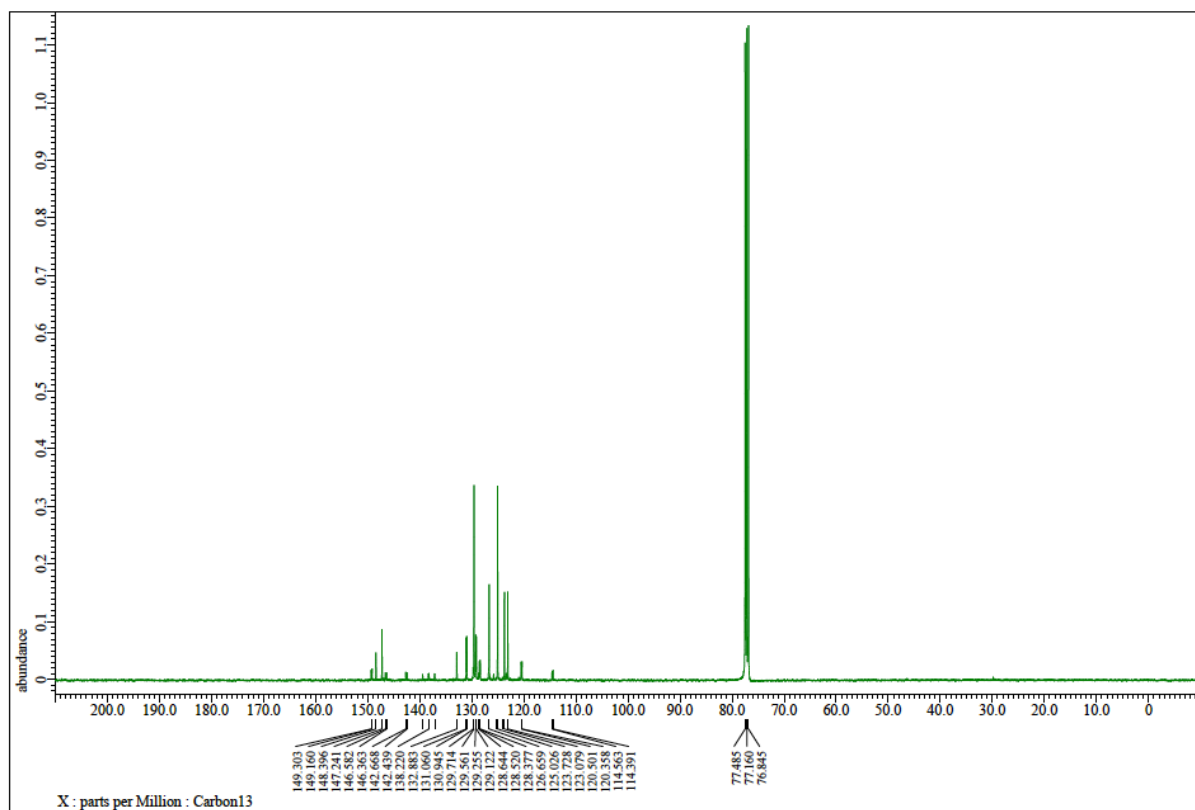


Figure S48. ^{13}C NMR spectrum of **7** (100 MHz, CDCl_3).

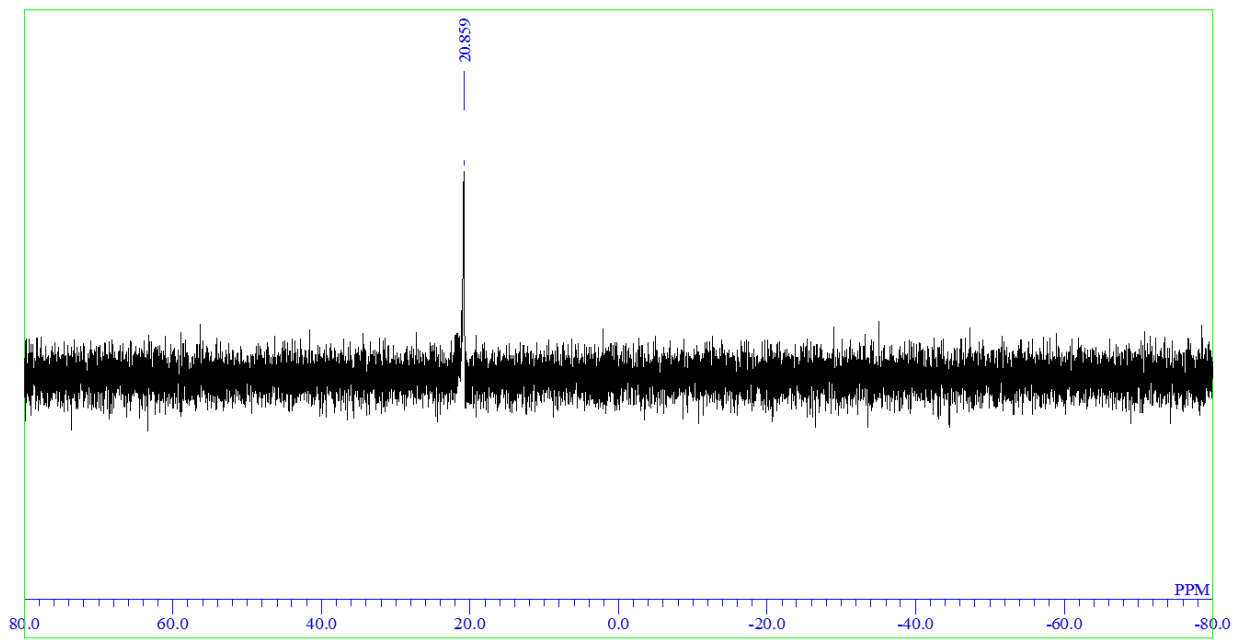


Figure S49. ^{31}P NMR spectrum of **7** (162 MHz, CDCl_3).

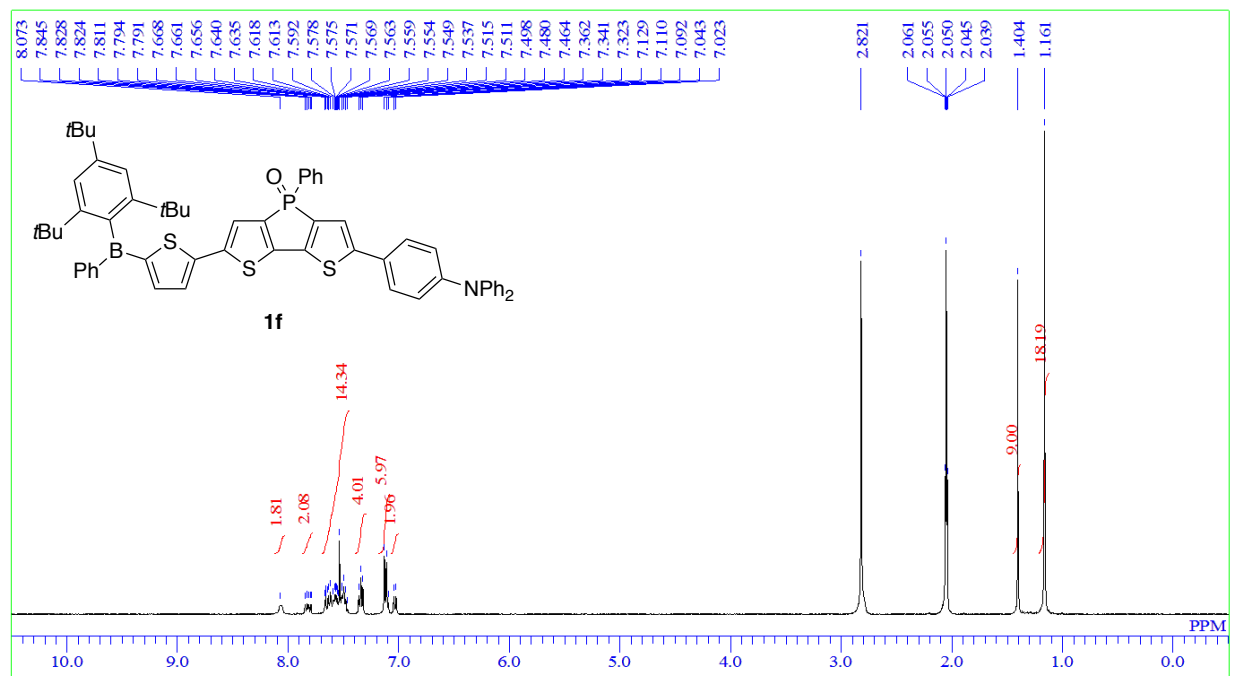


Figure S50. ^1H NMR spectrum of **1f** (400 MHz, acetone- d_6).

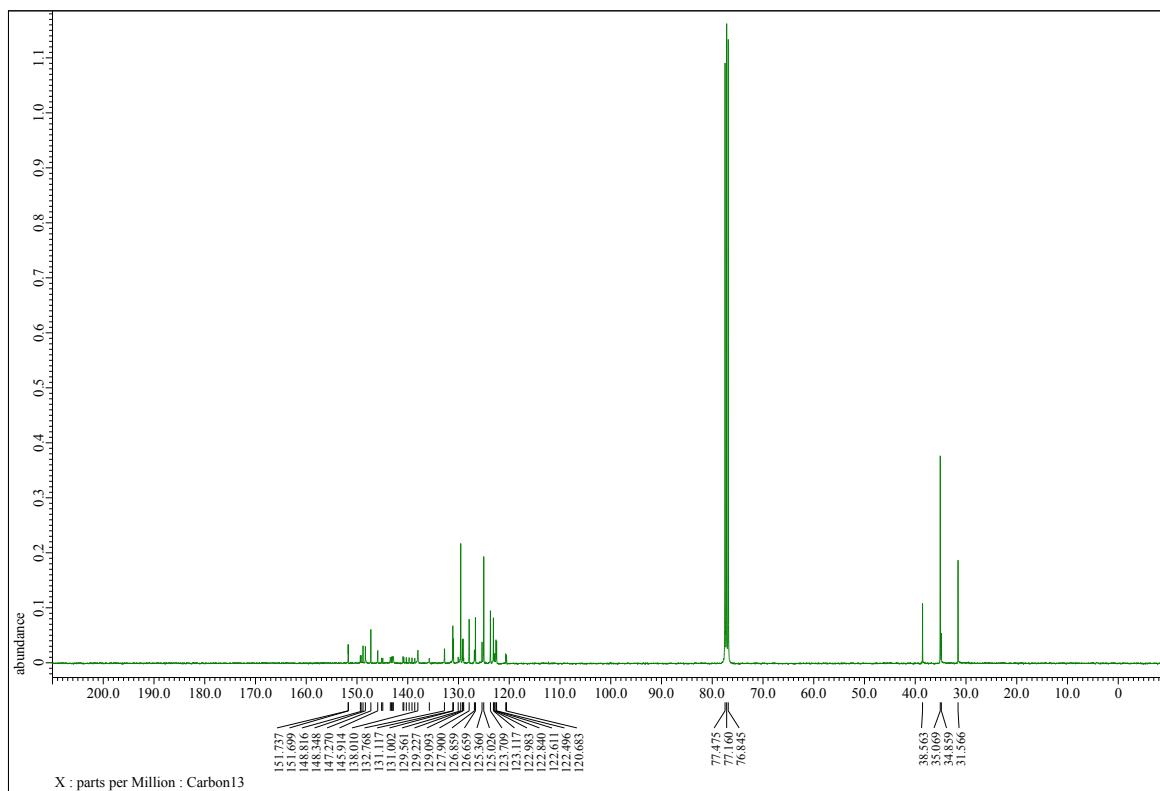


Figure S51. ^{13}C NMR spectrum of **1f** (100 MHz, CDCl_3).

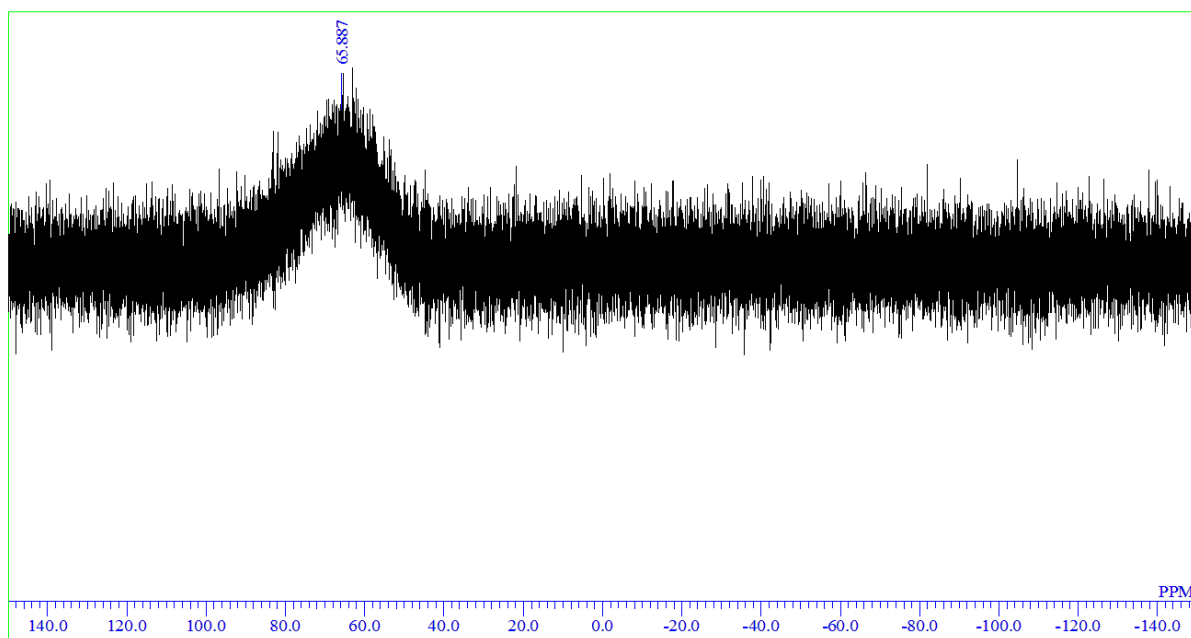


Figure S52. ^{11}B NMR spectrum of **1f** (128 MHz, CDCl_3).

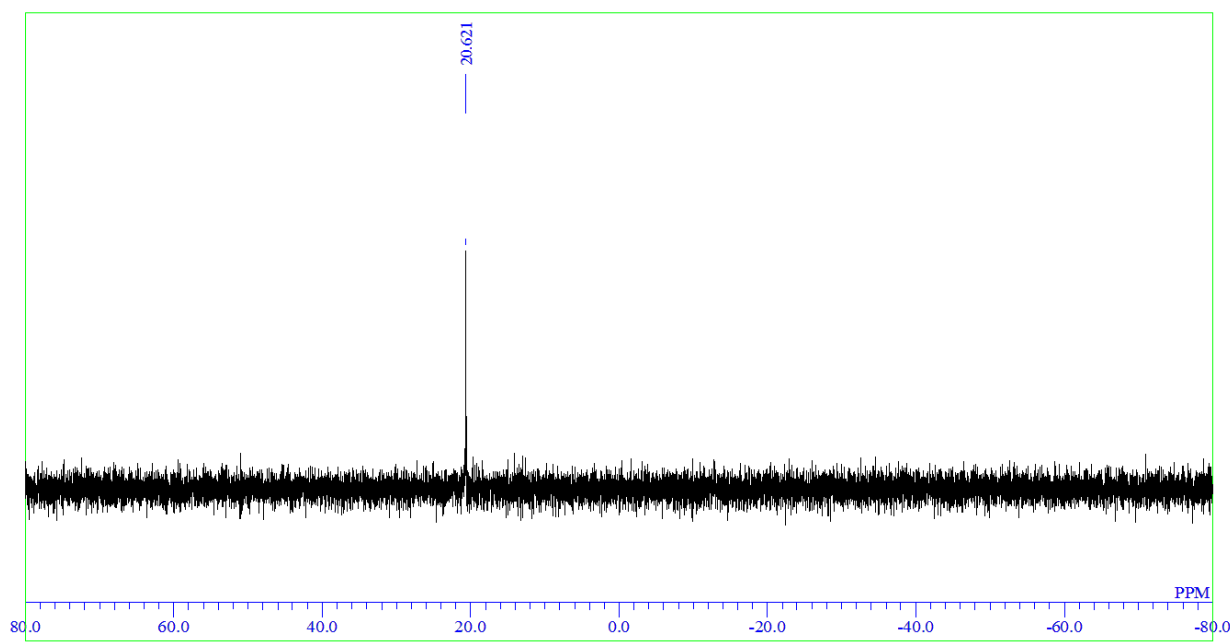


Figure S53. ^{31}P NMR spectrum of **1f** (162 MHz, CDCl_3).

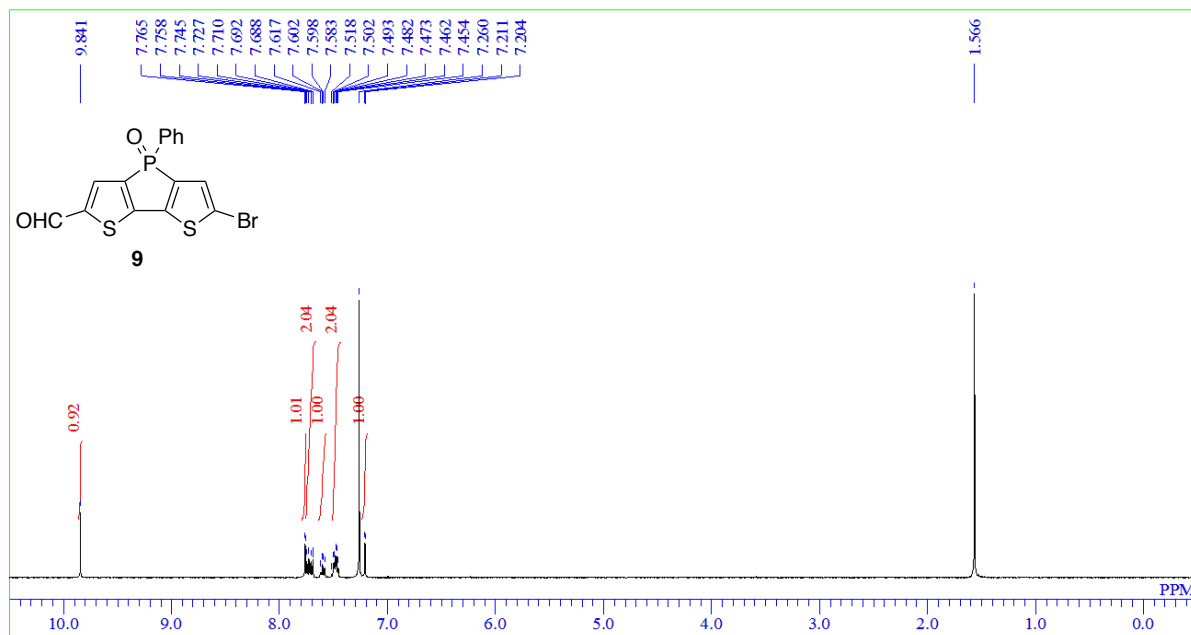


Figure S54. ^1H NMR spectrum of **9** (400 MHz, CDCl_3).

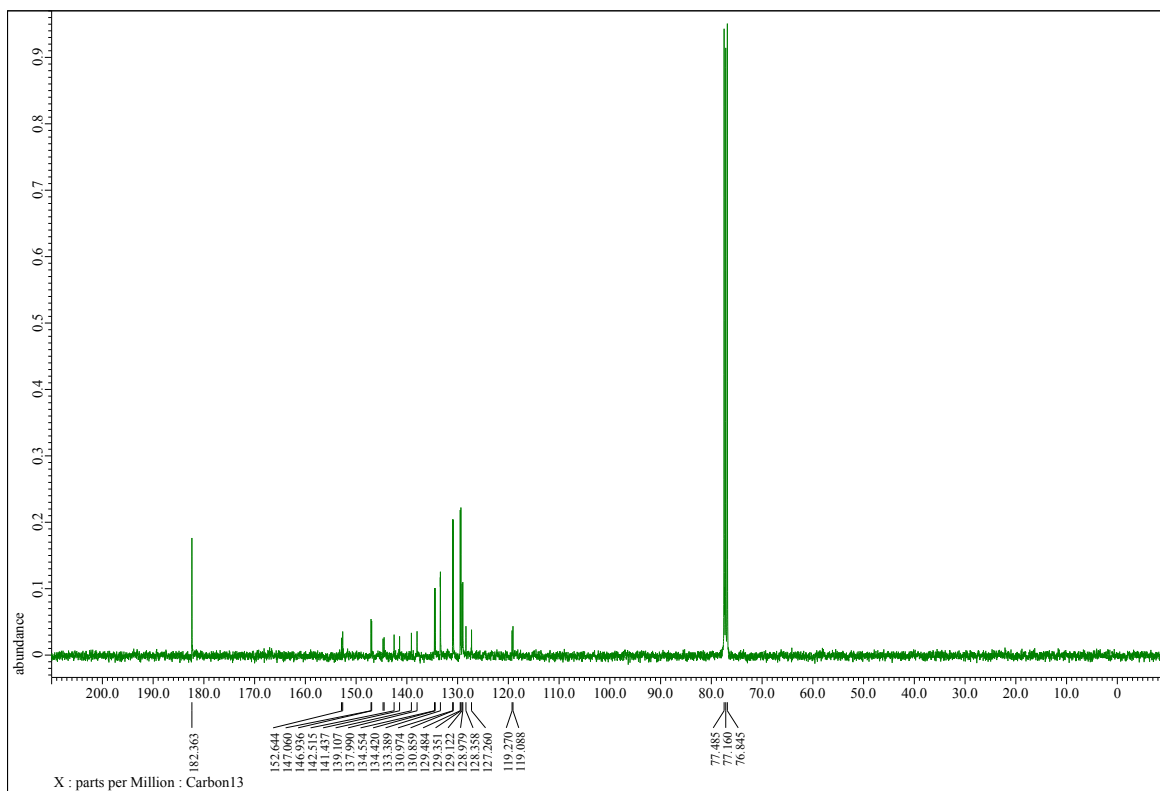


Figure S55. ^{13}C NMR spectrum of **9** (100 MHz, CDCl_3).

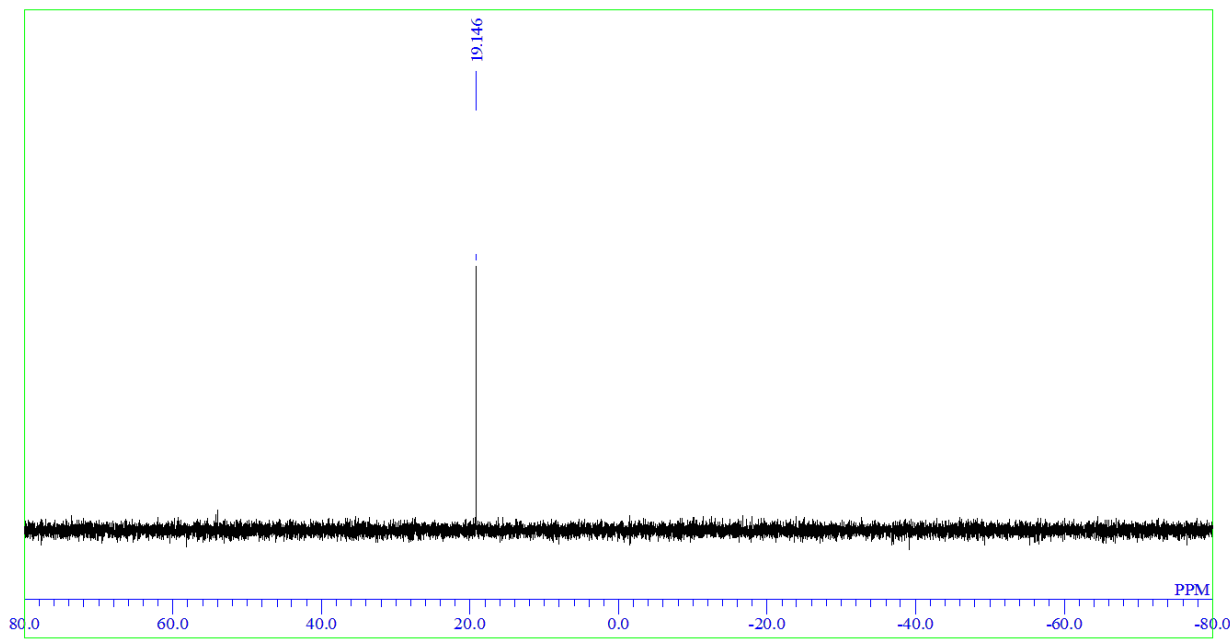


Figure S56. ^{31}P NMR spectrum of **9** (162 MHz, CDCl_3).

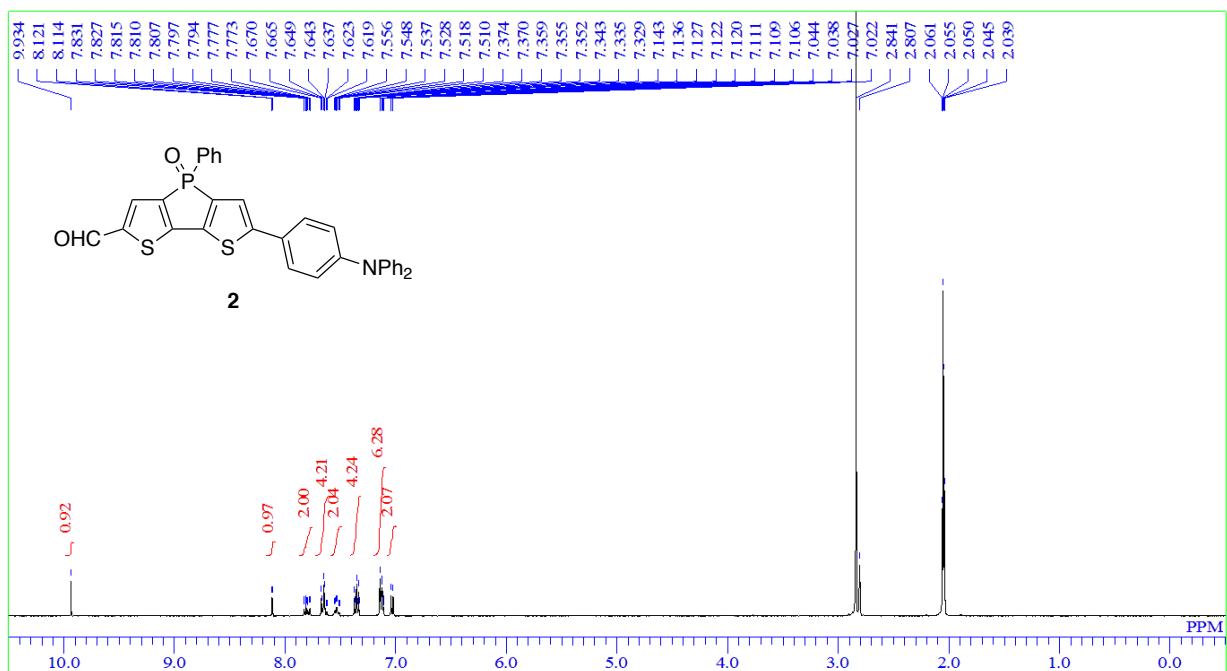


Figure S57. ^1H NMR spectrum of **2** (400 MHz, acetone- d_6).

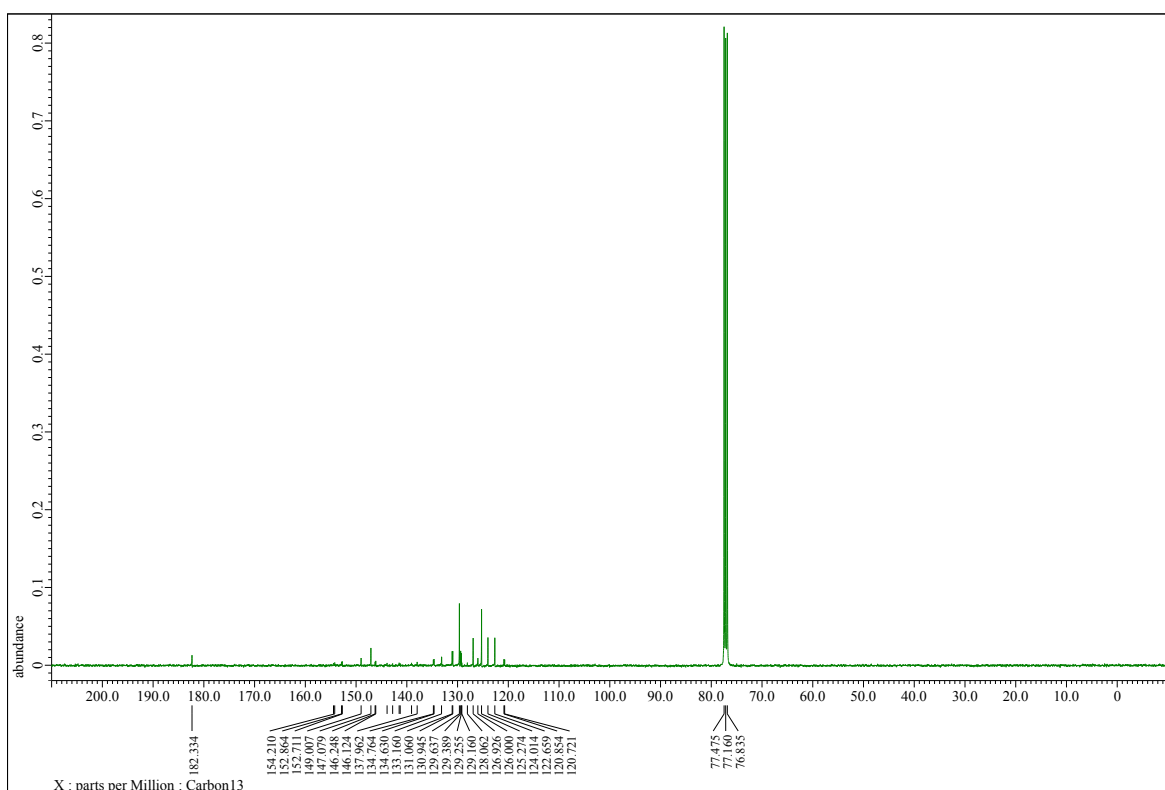


Figure S58. ^{13}C NMR spectrum of **2** (100 MHz, CDCl_3).

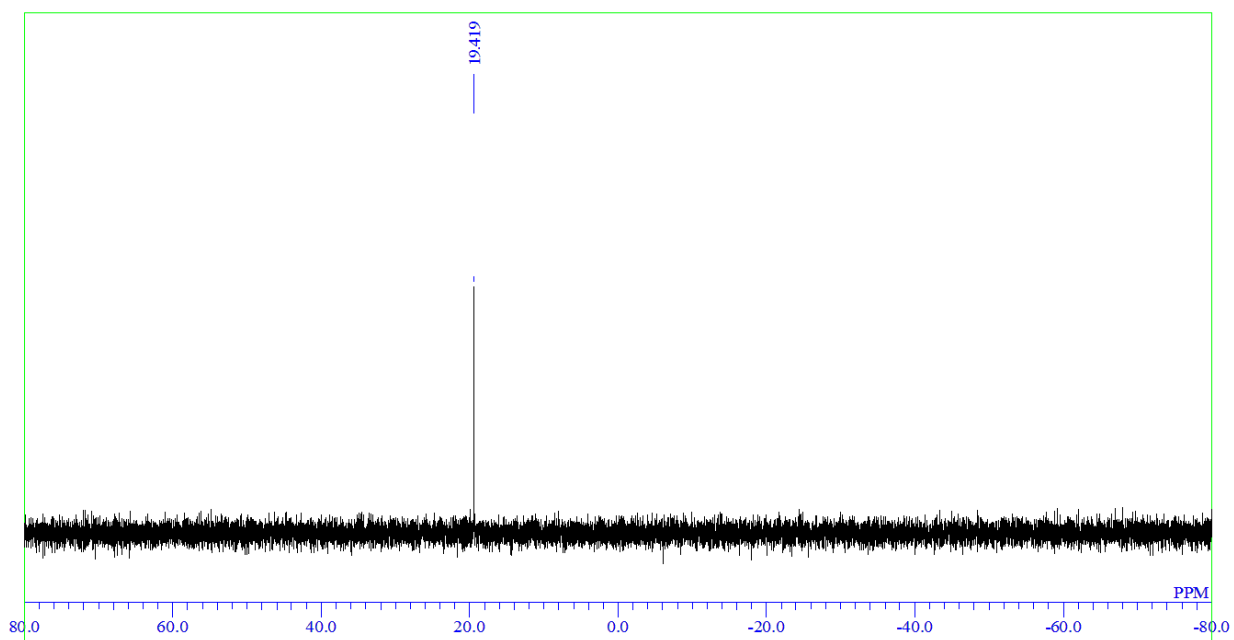


Figure S59. ^{31}P NMR spectrum of **2** (162 MHz, CDCl_3).

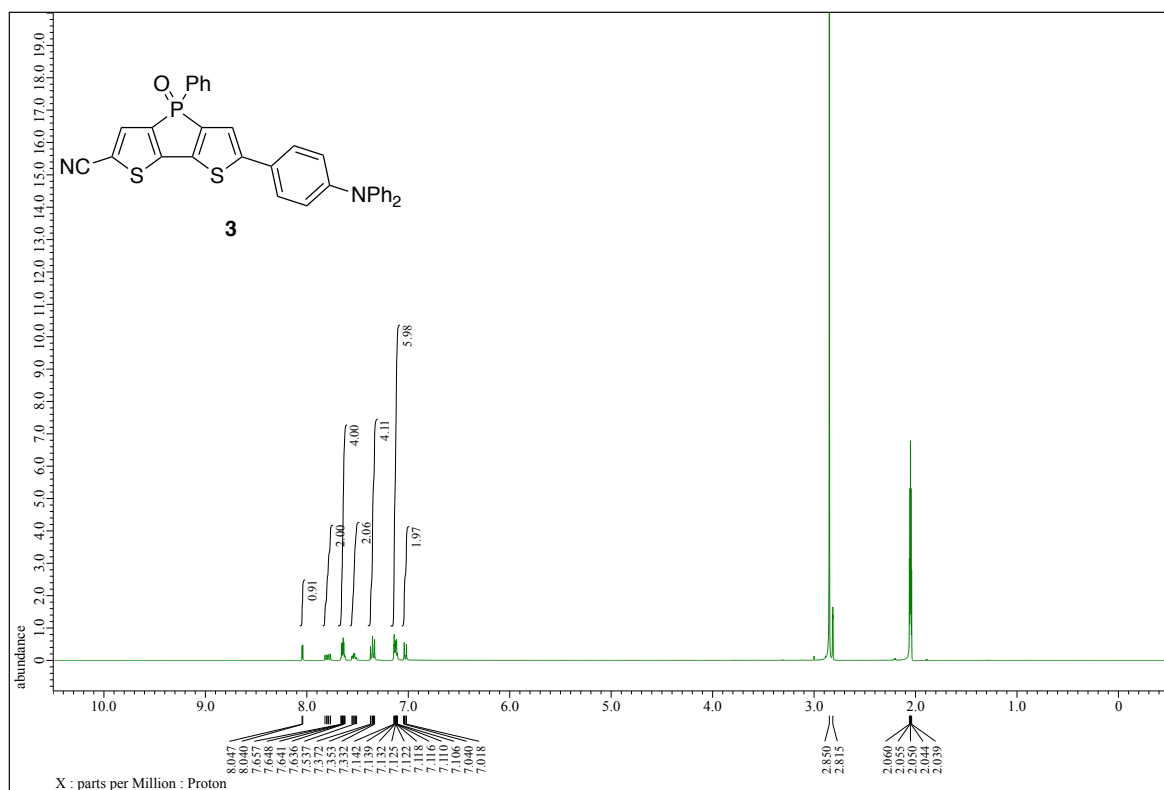


Figure S60. ^1H NMR spectrum of **3** (400 MHz, acetone- d_6).

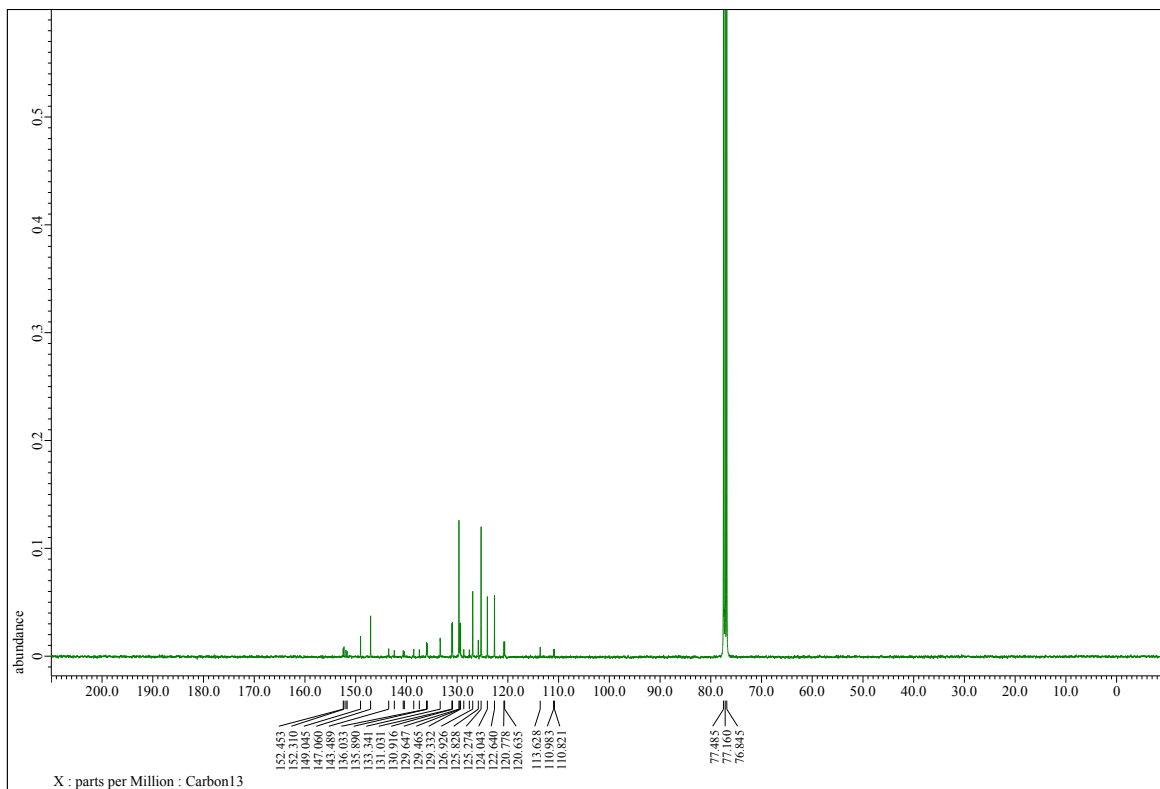


Figure S61. ^{13}C NMR spectrum of **3** (100 MHz, CDCl_3).

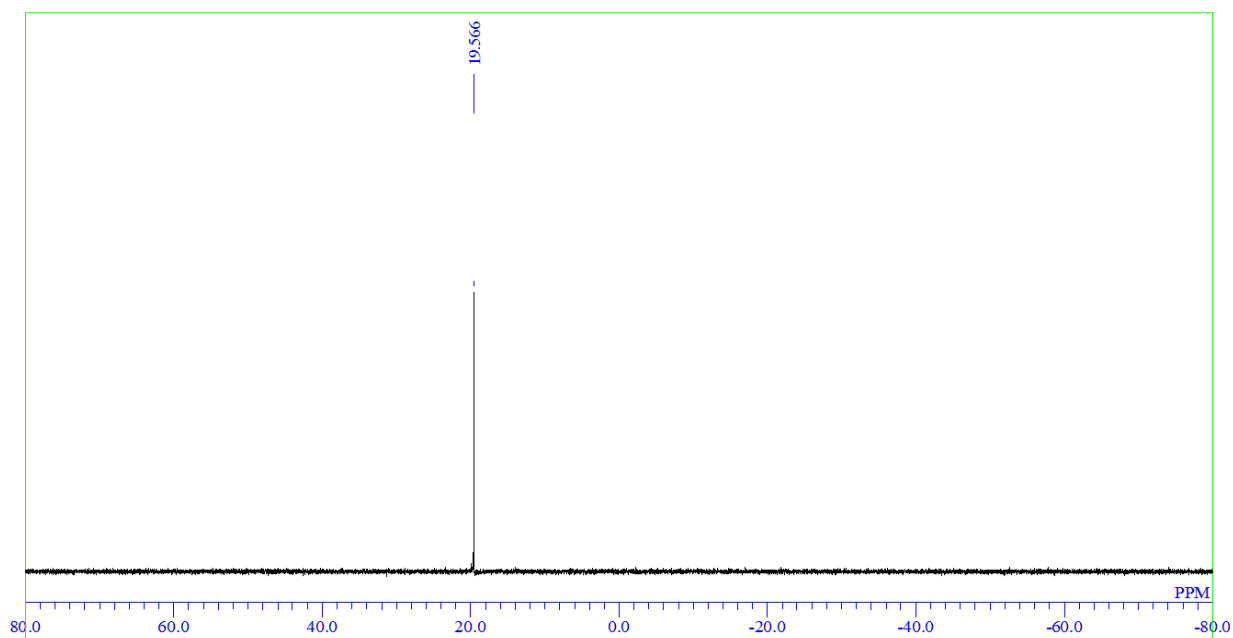


Figure S62. ^{31}P NMR spectrum of **3** (162 MHz, CDCl_3).